FUNCTIONAL STUDIES OF THREE GENES INVOLVED IN DIPHTHAMIDE BIOSYNTHESIS

A Dissertation

Presented to the Faculty of the Graduate School

of Cornell University

In Partial Fulfillment of the Requirements for the Degree of

Doctor of Philosophy

by

Zhewang Lin

August 2016

© 2016 Zhewang Lin

FUNCTIONAL STUDIES OF THREE GENES INVOLVED IN DIPHTHAMIDE BIOSYNTHESIS

Zhewang Lin, Ph. D.

Cornell University 2016

Diphthamide is a post-translationally modified histidine residue uniquely found in eukaryotic and archaeal elongation factor 2 (eEF2), a protein involved in the elongation step of protein synthesis. It is the target of the bacterial toxins, Diphtheria toxin (DT) and Pseudomonas exotoxin A (ETA), which catalyze the ADP-ribosylation reaction on the diphthamide residue of eEF2. ADP-ribosylation on eEF2 inactivates eEF2, which in turn stops protein translation, leading to cell death. The diphthamide biosynthesis pathway in eukaryotes was initially proposed to involve three steps, requiring seven proteins, Dph1-Dph7. While the functional assignments of Dph1-Dph6 were well established, the role of Dph7 in the pathway was unclear.

I started my graduate study research working on the function of Dph7 in the diphthamide biosynthesis pathway. I identified a previously unknown intermediate, methylated diphthine, from yeast *DPH7* deletion strain. My results showed that Dph7 catalyzes an additional step in the diphthamide biosynthesis pathway. This step is between the Dph5-catalyzed and Dph6-catalyzed reactions. This allowed us to propose a revisited diphthamide biosynthesis pathway.

Then, I worked on addressing the question whether diphthamide formation is regulated. We speculated that the reduction process of Dph3 in the first step of the biosynthesis is the potential regulatory point because the first step is the rate limiting step and the reduction of Dph3 is the key for the catalytic activity of Dph1-Dph2 in this step. Using a

proteomic approach, I identified cytochrome B5 reductase (Cbr1) as a NADH-dependent reductase for Dph3. I showed that Cbr1 is the physiological reductase of Dph3 and it is important for the tRNA wobble uridine modifications that are also implicated in translation. Thus, I found a potential regulatory linkage between the metabolic state of the cells (NADH level) and protein translation via the diphthamide and tRNA wobble uridine modifications.

In chapter 4, I summarize my recent work on functional characterization of Kti13, the newly reported protein to be involved in diphthamide biosynthesis. Kti13 likely plays a subsidiary role in both diphthamide and tRNA wobble uridine modifications by reducing the reduction potential of Dph3, allowing more efficient electron transfer to Dph3's electron acceptors.

The final part of my thesis describes my effort in elucidating the poorly understood biological function of diphthamide. Using ribosome profiling, I attempted to identify the potential "frameshifted proteome" using ribosomal profiling. I also showed that diphthamide deficient cells are hypersensitive to rapamycin treatment, implicating a role of diphthamide in stress response.

BIOGRAPHICAL SKETCH

Zhewang was born in Guangdong province, China in 1988. He graduated from University of Cambridge UK in 2010, majored in chemistry. He worked as a research assistant at Institute of Biotechnology and Nanotechnology Singapore with Dr. Yugen Zhang from 2010-2011. He joined the Department of Chemistry and Chemical Biology at Cornell University in 2011 working in Prof. Hening Lin's group. Both his undergraduate and graduate studies were generously supported by the National Science Scholarship from Singapore. He won the Tunis Wentink Prize for Outstanding Graduate Students in 2016. His thesis entitled "Functional studies of three genes involved in the diphthamide biosynthesis" was supervised by Dr. Hening Lin.

ACKNOWLEDGMENTS

I would like to express my sincere gratitude to my thesis advisor, Prof. Hening Lin. My entire thesis research was only made possible by his guidance, advice, support and encouragement along the way. The lessons and insights from him are invaluable and essential for me in this process of becoming an academic researcher. I would also like to thank my committee members, Prof. Richard Cerione and Prof. Ailong Ke, for their suggestions and help.

Dr. Xiaoyang Su has helped and taught me immensely in my first year. When I first started in the lab, I had very little, if any, biochemical research experiences. He was both patient and attentive in providing the initial training for me. Dr. Min Dong showed me how to perform the *in vitro* reconstitution of the first step of diphthamide biosynthesis using ^{14}C-S-adenosylmethionine. Min has also provided very helpful discussion on our diphthamide projects.

I would also like to thank the undergraduate students who have worked with me. Ray Jhun helped me purified the eEF2 protein from *dph6*Δ and *dph7*Δ cells. Alisa Eunyoung Lee helped me purify the eEF2 protein from *dph2*Δ cells for *in vitro* reconstitution of the first step of diphthamide biosynthesis, generate Dph7 mutants and screened for Dph7's catalytic mutants. It has been a great pleasure working with all the Lin lab members who are friendly and supportive to each other.

Finally, I would like to thank my wife, Yan Zhu, for her selfless support throughout this long and challenging journey of graduate study.

TABLE OF CONTENTS

LIST OF FIGURES

CHAPTER 1

THE DIPHTHAMIDE BIOSYNTHESIS PATHWAY – AN OVERVIEW[a]

Introduction

Post-translational modifications (PTM) on proteins are nature's escape from genetic imprisonment. PTMs such as phosphorylation, glycosylation, ubiquitination, nitrosylation, methylation, acetylation and lipidation influence almost every aspect of cell biology and pathogenesis via dynamic control over protein function. Diphthamide represents one of the most intriguing PTMs since its discovery almost four decades ago.[1] Diphthamide is a post-translationally modified histidine residue only found in eukaryotic and archaeal elongation factor 2 (eEF2), a protein involved in the elongation step of protein synthesis. During certain bacterial infections, it is the target of bacterial toxins, Diphtheria toxin (DT), Pseudomonas exotoxin A (ETA) and Cholix toxin, which catalyze the ADP-ribosylation reaction on the diphthamide residue of eEF2 using NAD as the ADP-ribosyl donor.[2] ADP-ribosylation on eEF2 inactivates eEF2, which in turn stops protein translation, leading to cell death.[3] Although the pathological relevance of diphthamide is well studied, the physiological function of diphthamide is still poorly understood. Interestingly, diphthamide is not present in EFG, the bacterial ortholog of eEF2 but it is highly conserved among archaea and eukaryotes. This evolutionary conservation of diphthamide modification suggests a fundamental role of diphthamide in cells.

Structural determination of diphthamide

The study of diphthamide started with the elucidation of the DT modification site. It was first discovered that the target residue of diphtheria toxin is not an ordinary amino acid residue.[4] It was further revealed that diphthamide exists only on eEF2 and there is one diphthamide residue per eEF2 protein.[1] The modification sites were determined in both rat and yeast. The surrounding

[a] This is a revised version of our published review article: Su, X., Lin, Z. & Lin, H. The biosynthesis and biological function of diphthamide. *Crit Rev Biochem Mol Biol* **48**, 515-521, (2013)

residues were found to be highly conserved.[1] The structure of ADP-ribosyl diphthamide was determined using NMR and later confirmed by fast atom bombardment mass spectrometry.[5,6] The structure of diphthamide was proposed as 2-[3-carboxyamido-3-(trimethylammonio)propyl] histidine (Figure 1.1). The structure determination has also been confirmed by X-ray crystallography[7,8]. However, there is a noteworthy discrepancy on the stereochemistry of diphthamide. The reported crystal structure suggests that the chiral center of the third carbon atom (marked by an asterisk in Figure 1.1) to be an R-enantiomer[7] instead of an S-enantiomer in the previously proposed structure. This assignment of carbon chirality is surprising because this carbon derives from a methionine molecule and the S-configuration of methionine should therefore be retained in diphthamide unless there is an inversion of chirality during diphthamide biosynthesis. The validity and implication of this change in chiral center during diphthamide biosynthesis awaits further study.

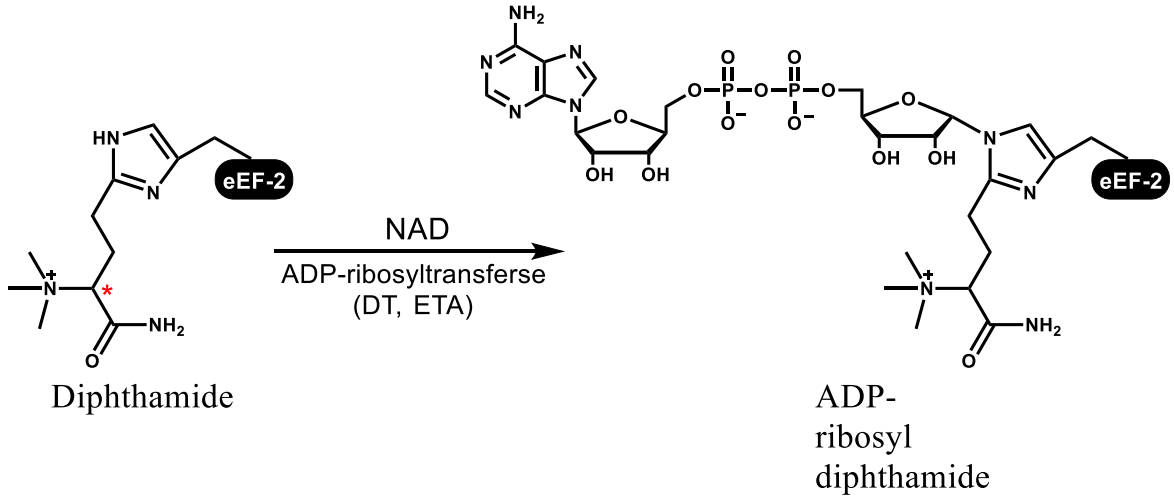

Figure 1.1 The structure of diphthamide and ADP-ribosylation reaction. The asterisk marks the carbon with ambiguous chiral centre.

Elucidation of diphthamide biosynthesis pathway

The structure determination facilitated the elucidation of diphthamide biosynthesis pathway. By

using biosynthetic labeling technique, it became clear that the backbone and the three methyl groups of diphthamide come from S-adenosyl methionine (SAM).[9] Classic genetic screens based on the resistance of diphthamide deficient mutants to diphtheria toxin has led to identification of five diphthamide synthesis genes (Dph1-Dph5) in eukaryotes.[10-12] It was then found that Dph1-4 are responsible for the first step[13] (Figure 1.2a), which involves the transfer of the 3-amino-3-carboxypropyl (ACP) group from SAM to the C2 carbon of the imidazole ring of the to-be-modified histidine residue in eEF2. Dph5 is a methyltransferase responsible for the second step, carrying out a trimethylation reaction on the amino group (Figure 1.2a).[13] For three decades, the diphthamide biosynthesis pathway was thought to have three steps. The last step is the amidation of diphthine to give diphthamide, but the proteins required remained unknown until 2012 (Figure 1.2a).

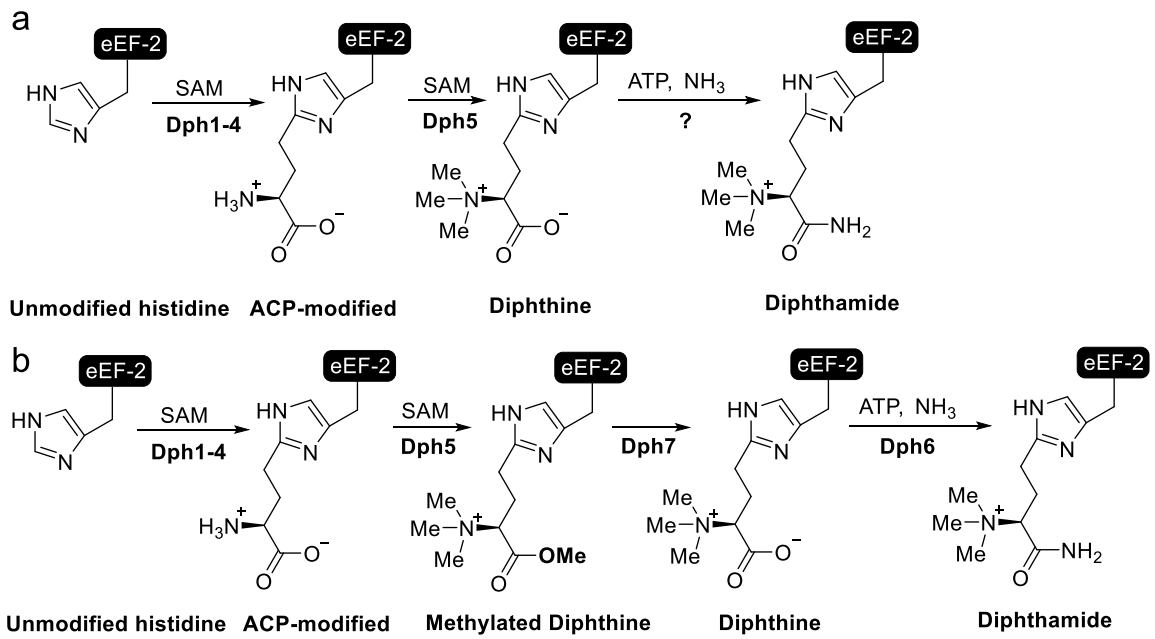

Figure 1.2 The diphthamide biosynthesis pathway in eukaryotes. (A) The initially proposed diphthamide biosynthesis pathway. (B) The revisited diphthamide biosynthesis pathway.

It was speculated that the genetic screening did not identify mutants deficient in the last amidation step because diphthine can be ADP-ribosylated by DT at a slower rate. Hence, diphthine containing strains are also sensitive to DT.[13] A breakthrough came when Carette et al. identified human gene *WDR85*, which is the ortholog of yeast gene *YBR246W*, as a diphthamide biosynthetic gene (hence later named *DPH7*) using haploid genetic screening.[14] However, Dph7 is not the diphthamide synthetase catalyzing the last step because Dph7 has no ATP binding domain required for the last amidation reaction. The actual diphthamide synthetase was identified independently by three groups, making use of large scale functional genomic data.[15-17] Using purified protein for in vitro reconstitution, yeast gene *YLR143W* was firmly established to be the final diphthamide synthetase and given the common name Dph6.[15] Subsequent investigation of the functional role of Dph7 in diphthamide biosynthesis has led to discovery of a new intermediate and a previously unknown step in the diphthamide biosynthesis pathway.[18] Dph7 is a methylesterase that hydrolyzes the second step product, methylated diphthine, to produce diphthine and allows Dph6-catalyzed amidation reaction to occur (Figure 1.2b).[18] These recent studies allowed proposal of a revisited diphthamide biosynthesis pathway in eukaryotes (figure 1.2b).

Although these recent findings have greatly improved our understanding, the complexity of the diphthamide biosynthesis pathway never ceases to amaze researchers in the field. Only very recently, yet another new player in the biosynthesis pathway was reported.[19] Yeast cells with deletion of the *Kluveromyces lactis* Toxin Insensitive 13 (*KTI13*) gene was showed to have partial resistance to DT, suggesting that diphthamide formation is impaired in this strain.[19] Kti13 is found to form a heterodimer with Dph3 and this complex formation is important for the diphthamide biosynthesis.[19,20] Surprisingly, the structure of the Kti13/Dph3 heterodimer suggests that Kti13 in complex with Dph3 blocks the redox active iron atom in Dph3 and also inhibits it's electron acceptor/transfer activity.[20] This finding is seemingly contradictory to Kti13's subsidiary

role in helping to form the diphthamide modification. The impact of this inhibition by Kti13 *in vivo* and the exact role of Kti13 in diphthamide biosynthesis await further investigation.

Diphthamide is present in both achaea and eukaryotes. The eukaryotic diphthamide biosynthesis pathway appears to be more sophisticated than the archaeal one, involving more genes. Evolutionarily, the diphthamide biosynthetic pathway developed in two phases. P. horikoshii and most other sequenced archaeal species have the orthologs of Dph2, Dph5 and Dph6.[16] However, in one species of the deep-branching phylum Korarchaeota, these three dph genes are absent. In fact, this organism lacks only five genes that are represented in all sequenced archaeal genomes, namely, orthologs of Dph2, Dph5 and Dph6, predicted Zn-ribbon RNA-binding protein, and small-conductance mechanosensitive channel.[21] This strongly suggests that the most essential part of this pathway emerged all at once. Other DPH genes that emerged later are conserved in eukaryotes but are absent in archaea. The added complexity of the diphthamide biosynthesis in eukaryotes suggests a possible regulation on the formation of diphthamide emerged later through evolution.

Enzymology of diphthamide biosynthesis: a step-by-step dissection

Step 1- formation of the ACP intermediate

The first step of diphthamide biosynthesis is the transfer of the ACP group from SAM to the C2 position of the imidazole ring of the histidine residue being modified in eEF-2. This reaction has been reconstituted *in vitro* and studied in great detail using the enzyme from an archaeal species *Pyrococcus horikoshii* (Zhang et al., 2010). Unlike eukaryotes which need Dph1-Dph4 for the first step, P. horikoshii has only one protein, Dph2, identified for the first step. The *P. horikoshii* Dph2 (PhDph2) is homologous to eukaryotic Dph1 and Dph2. Crystal structure of PhDhp2 revealed that PhDph2 forms a homodimer and each monomer consists of three domains with similar folding patterns (Figure 1.3).

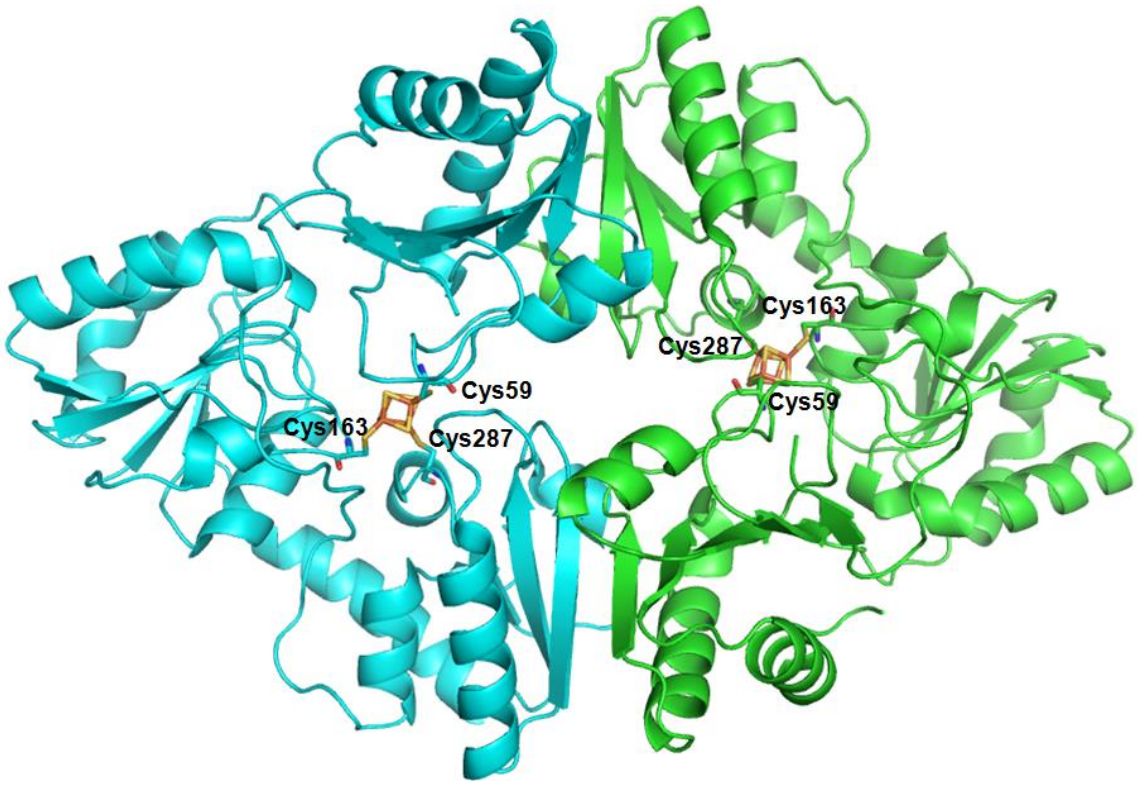

Figure 1.3. Structure of PhDph2 homodimer (PDB 3LZD) showing the [4Fe-4S] cluster coordinated by three cysteine residues.

The basic domain folding pattern is a four-stranded parallel β-sheet with three flanking α-helices.[22] Although PhDph2 lacks the CX3CX2C motif which is present in most radical SAM enzymes,[23] it contains three cysteine residues (Cys59, Cys163 and Cys287) that are spatially closed (Figure 3). This observation led to the discovery that PhDph2 coordinates a [4Fe-4S] clusters and is an unusual radical SAM enzyme. Unlike most other radical SAM enzymes, PhDph2 does not generate a 5'-deoxyadenosyl radical (Figure 4). Instead, PhDph2 cleaves the $C_{\gamma,Met}$–S bond of SAM to form 5'-deoxy-5'-methylthioadenosine (MTA) and an ACP radical.[24] The ACP radical then likely adds to the imidazole ring of the histidine residue to give the product (Figure 4). PhDph2 is the first enzyme known to generate an ACP radical from SAM and this may help to understand how radical SAM enzymes work in general.

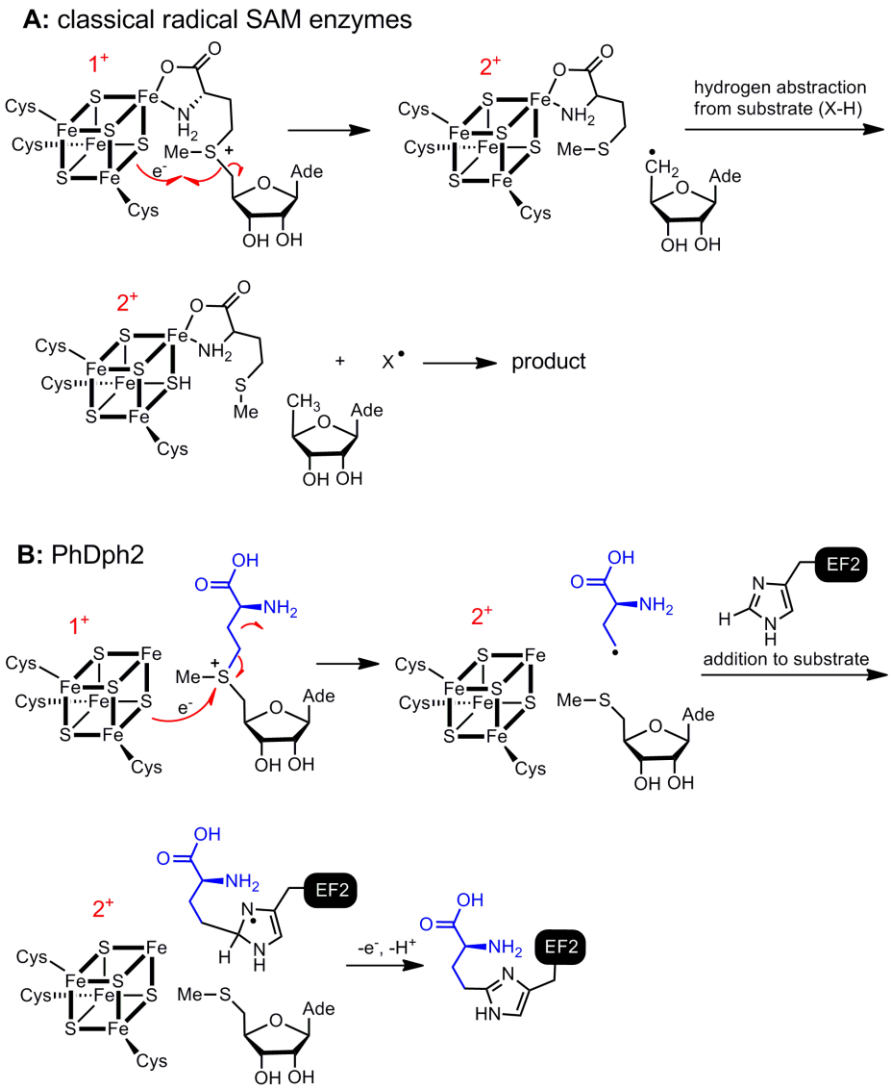

Figure 1.4. The reaction catalyzed by classical radical SAM enzymes (A) and by PhDph2 (B). Classical radical SAM enzymes generate a 5'-deoxyadenosyl radical, while PhDph2 generates an ACP radical. The 5'-deoxyadenosyl radical normally undergoes hydrogen abstraction reactions, while the ACP radical generated by PhDph2 likely undergoes an addition reaction to give the enzymatic product.

In eukaryotes, the first step is considerably more complicated than in *P. horikoshii*. There are 4 genes known to be required for this step, Dph1-Dph4. Dph1 and Dph2 are both homologous to PhDph2 and presumably form a heterodimer that is functionally similar to the PhDph2 homodimer. Therefore, it is conceivable that Dph1-Dph2 complex is the catalytic unit among the four proteins required in eukaryotic first step reaction.

Dph3 from *Saccharomyces cerevisiae* is as small as 82 amino acids. However, there are two domains, a N-terminal cystathionine β-synthase (CBS) domain and a C-terminal Zn ribbon domain.[25] The C-terminal Zn ribbon domain has 4 conserved cysteine residues arranged in Cys-X-Cys-X19-Cys-X2-Cys motif. The Zn ribbon domain was found to bind both zinc and iron. It was found that Dph3 can be reduced by E. coli rubredoxin reductase NorW, suggesting its role as a rubredoxin-like electron carrier.[25] Since the catalytic Dph1-Dph2 complex needs to be reduced by an electron to initiate the reaction, it is conceivable that Dph3 delivers the electron to Dph1-Dph2. In line with this, Dph3 has been found to co-purify with Dph1-Dph2 complex.[26,27] Direct evidence for Dph3 serving as an electron donor for Dph1-Dph2 came from *in vitro* reconstitution of the first step diphthamide biosynthesis using Dph1-Dph2, Dph3, NADH and NorW.[28] In this system, NorW acts as a non-physiological reductase to reduce Dph3 which then channels the electron to reduce the Dph1-Dph2 complex.[28] This finding that Dph3 is an electron donor for the radical SAM enzyme Dph1-Dph2 is the first report for reduction activation of radical SAM enzymes in eukaryotes.

While the functional roles of Dph1-Dph3 in the first step of eukaryotic diphthamide biosynthesis are well established, Dph4's role remains elusive. Dph4 has an N-terminal J domain which is commonly found in co-chaperones of 70 kilodalton heat shock proteins (Hsp70) proteins. J domain is responsible for the stimulation of the ATPase activity of their partner Hsp70s which is crucial for the interaction of these chaperone machineries with their client proteins. The C-terminal of Dph4 is the CSL zinc finger, and the J domain is required for the activity of Dph4

in diphthamide biosynthesis.[29] However, a chimeric version of Dph4 with the J domain from Ydj1 is also active. The cysteine residue in the CSL sequence is also important for the activity of Dph4, and it was shown to bind Fe more tightly than Zn. Interesting, the iron containing Dph4 is also redox-active.[30] Based on the domain organization, Dph4 may have either electron transfer activity or co-chaperone activity or both. However, unlike Dph3, Dph4 does not co-localize with Dph1 and Dph2.[31] These findings suggest that the likely role of Dph4 is to support the iron-sulfur cluster assembly on Dph1 and Dph2 by the co-chaperone activity of Dph4. Further studies are needed to test this idea.

Step 2- formation of methylated diphthine, a newly discovered intermediate

Dph5 was first reported as diphthine synthase which catalyzes the trimethylation of the amino group in the second step of the diphthamide biosynthesis (Figure 1.2a).[13,32,33] It was proposed after the fact that acid hydrolysis of eEF2 with *in vitro* reconstitution of the second step yields diphthine.[13] However, a new intermediate in diphthamide biosynthesis with mass 15 Dalton larger than that of diphthamide was recently identified in a lymphoma cell line with a deletion of the *DPH7* gene.[34] This new intermediate was later characterized as methylated diphthine using mass spectrometry (MS).[18] It was also demonstrated to be the actual product of the Dph5 reaction by MS study on trypsin digested eEF2 following the *in vitro* reconstitution (Figure 1.2b).[18] This newly identified intermediate was overlooked because previously the reconstituted eEF2 was hydrolyzed in acidic conditions to single amino acid for HPLC analysis. Under such condition, the methylated diphthine, a methyl ester, was hydrolyzed to diphthine and was not detected. Thus, the eukaryotic Dph5 is a promiscuous methyltransferase performing both N- and O-methylation to form the methylated diphthine intermediate in the second step of diphthamide biosynthesis pathway.

Step 3- formation of diphthine, a novel demethylation step

The introduction of an extra methyl group on the carboxylate group by Dph5 necessitates an additional step to convert the methylated diphthine to diphthine, the substrate of the last amidation step (Figure 1.2b). In eukaryotic cells, Dph7 is the demethylase catalyzing this conversion.[18] This functional assignment of Dph7 in the diphthamide biosynthesis pathway has been a subject of debate since its discovery by a haploid genetic screening.[14] The human homolog of Dph7, *WDR85*, was first reported to be involved in the first step of diphthamide biosynthesis.[14] Later mass spectrometry studies on eEF2 purified from yeast *DPH7* deletion strain showed that the diphthamide biosynthesis proceed beyond the first step in *DPH7* deletion strain.[17,35] It was then proposed that Dph7 is involved in the last amidation step because diphthine was detected.[17,35] However, a human lymphoma cell line with *DPH7* deletion was reported to contain a previously overlook intermediate with mass 15 Dalton larger than that of diphthamide.[34] Using purified eEF2 from yeast *DPH7* deletion cells, it was demonstrated that this new intermediate is actually methylated diphthine and that recombinant Dph7 converts the methylated diphthine to diphthine *in vitro*.[18] The reason that diphthine is also observed in MS studies of eEF2 purified from *DPH7* deletion cells is because the extra methyl group on the carboxylate group is prone to hydrolysis during the sample preparation for MS.

Step 4- formation of diphthamide, the amidation step

The final step involves conversion of the diphthine intermediate to form the final product, diphthamide. Using total cell lysate, it was first shown that this is an ATP dependent reaction[13] but the actual enzyme(s) for this step remained elusive for more than three decades. Interestingly, the genetic screening on the basis of DT resistance never identify mutants deficient in the last amidation step because diphthine can be ADP-ribosylated by DT at a slower rate.[13] Hence, diphthine containing strains are also sensitive to DT and no mutants can be identified. Only recently, the actual diphthamide synthetase, Dph6, was identified independently by three groups using comparative genomic analysis[16], yeast co-fitness analysis[15], and yeast gene interaction

databases[17]. Mass spectrometry analysis on *DPH6* deletion strain confirmed that it contains diphthine intermediate.[15,17] More importantly, using purified protein for *in vitro* reconstitution of the last amidation step, yeast Dph6 protein was firmly established to be the final diphthamide synthetase.[15] Dph6 belongs to the adenine nucleotide alpha hydrolases superfamily. *In vitro* assay also suggested that Dph6 consumes ATP and generates AMP.[15] The direct nitrogen donor in the diphthine amidation reaction is ammonia.[15] Yeast Dph6 has two distinctive functional domains. At the N-terminal is an alpha_ANH_like_IV domain and at the C-terminal is an Yjg-YER057c-UK114 domain. Both domains are reported to be important for the function of yeast Dph6.[15] Human gene ATP-binding-domain containing protein 4 (*ATPBD4*), the ortholog of yeast Dph6, is able to rescue diphthamide biosynthesis in yeast with *DPH6* deletion.[15]

The biological function of diphthamide

Unlike the well-defined pathological relevance of diphthamide, the biological function of diphthamide is still enigmatic. Diphthamide modification makes cells susceptible to bacterial toxins, yet it is highly conserved among archaea and eukaryotes. Moreover, the formation of diphthamide involves a sophisticated network of proteins performing multiple reaction steps. It is hard to believe that such a system exists only to be exploited by bacterial toxins. The evolutionary conservation and complexity of diphthamide modification suggest a fundamental role of diphthamide.

Diphthamide has been suggested to be important in maintaining translational fidelity. Using an artificial luciferase reporter system with a "slippery sequence" prone to translational frameshift, the lack of diphthamide was shown to result in elevated -1 frameshift in protein synthesis.[36,37] Diphthamide resides in the tip of domain IV of eEF2 which is in close proximity with the tRNA in the P-site.[38] It was proposed that the positive charge brought incurred by diphthamide modification helps eEF2 to maintain conformational integrity.[37] However, it is unclear if the

observation of elevated translational -1 frameshift in diphthamide deficient cells using an artificial reporter system is physiologically relevant.

Despite of the presumed role of diphthamide in maintaining translation fidelity, in yeast none of the DPH genes is essential. In contrast, DPH genes have much more important functions in mammals. Dph1 gene has been found to be frequently deleted in ovarian and breast cancer, hence the alias *OVCA1* (ovarian cancer gene).[39-41] Overexpression of *OVCA1* suppresses the colony formation of ovarian cancer cells, presumably by cell cycle arrest at G1 phase.[42] It was further demonstrated that *OVCA1* overexpression in ovarian cancer cells A2780 leads to down-regulation of cyclin D1, and up-regulation of cyclin-dependent kinase inhibitor p16.[43] *OVCA1* homozygous mutant mice die at birth due to developmental delay and multiple organ defects. *OVCA1* heterozygous mice develop cancer spontaneously.[44] Similar to *DPH1*, *DPH3* homozygous deletion leads to embryonic death[45] and *DPH4* homozygous mutants were retarded in growth and development.[31] These developmental defects have been attributed to the deficiency of diphthamide.[37] However, it is not clear whether these phenotypes are due to decreased translation fidelity or due to the loss of other unknown functions of diphthamide.

It has long been speculated that diphthamide is the target of endogenous ADP-ribosyltransferases. Bacterial toxin induced ADP-ribosylation shuts down ribosomal protein synthesis and kills host cells. It has been reported that diphthamide can also be ADP-ribosylated by endogenous ADP-ribosyltransferase and this may serve as a regulatory mechanism for cellular protein synthesis.[46] The endogenous ADP-ribosyltransferase activity was found from both polyoma virus-transformed baby hamster kidney (pyBHK) cells[47] and beef liver.[46] However, later studies showed that the eEF-2 ADP-ribosylation activity from pyBHK cells was independent of diphthamide modification.[48,49] It has also been reported that interleukin-1β may act as an activator of the endogenous ADP-ribosylation.[50] To our best knowledge, there has not been any endogenous diphthamide ADP-ribosyltransferase cloned and characterized.

Most recently, using electron cryomicroscopy (cryo-EM), the binding of the Cricket Paralysis Virus Internal Ribosomal Entry Site (CrPV-IRES) of viral mRNA to the small ribosomal subunit (40S) and eEF2 during translation translocation was captured.[51] The structure revealed direct interaction of diphthamide on eEF2 with the pseudoknot I (PKI) of the CrPV-IRES. It was further demonstrated that this interaction was important for CrPV-IRES translation *in vitro*.[51] This finding provides a structural basis for an important role of diphthamide in cap-independent IRES translation. In line with this, it has been reported that diphthamide is critical for the translation of two IRES-dependent protein targets, XIAP and FGF2, under oxidative stress conditions.[52] Further studies are needed to check the physiological implication of this potential function of diphthamide.

Dissertation statement

My thesis research focused on the functional studies of several genes involved in the diphthamide biosynthesis pathway. I started my graduate study research on elucidating the function of Dph7 in the diphthamide biosynthesis pathway. In chapter 2, I describe how I identified a previously unknown intermediate, methylated diphthine, from the yeast *DPH*7 deletion strain. My results showed that Dph7 catalyzes an additional step in the diphthamide biosynthesis pathway. This step is between the Dph5-catalyzed and Dph6-catalyzed reactions. This allowed us to propose a revisited diphthamide biosynthesis pathway.

Then, I worked on addressing the question whether diphthamide formation is regulated. I speculated that the reduction process of Dph3 in the first step is the potential regulatory point because the first step is the rate limiting step and the reduction of Dph3 is the key for the catalytic activity of Dph1-Dph2 in this step. In chapter 3, I describe how I used a proteomic approach to identify cytochrome B5 reductase (Cbr1) as a NADH-dependent reductase for Dph3. I showed that Cbr1 is the physiological reductase of Dph3 and it is important for the tRNA wobble uridine modifications that are also implicated in translation. Thus, I found a potential regulatory linkage

between the metabolic state of the cells (NADH level) and protein translation via the diphthamide and tRNA wobble uridine modifications.

In chapter 4, I summarize my recent work on functional characterization of Kti13, the newly reported protein to be involved in diphthamide biosynthesis. Kti13 likely plays a subsidiary role in both diphthamide and tRNA wobble uridine modifications by reducing the reduction potential of Dph3, allowing more efficient electron transfer to Dph3's electron acceptors.

The final part of my thesis describes my effort in elucidating the poorly understood biological function of diphthamide. Using ribosome profiling, I attempted to identify the potential "frameshifted proteome" using ribosomal profiling. I also showed that diphthamide deficient cells are hypersensitive to rapamycin treatment, implicating a role of diphthamide in stress response.

REFERENCES

1 Van Ness, B. G., Howard, J. B. & Bodley, J. W. Isolation and properties of the trypsin-derived ADP-ribosyl peptide from diphtheria toxin-modified yeast elongation factor 2. *J Biol Chem* **253**, 8687-8690 (1978).

2 Collier, R. J. Understanding the mode of action of diphtheria toxin: a perspective on progress during the 20th century. *Toxicon* **39**, 1793-1803 (2001).

3 Honjo, T., Nishizuka, Y. & Hayaishi, O. Diphtheria toxin-dependent adenosine diphosphate ribosylation of aminoacyl transferase II and inhibition of protein synthesis. *J Biol Chem* **243**, 3553-3555 (1968).

4 Robinson, E. A., Henriksen, O. & Maxwell, E. S. Elongation factor 2. amino acid sequence at the site of adenosine diphosphate ribosylation. *J. Biol. Chem.* **249**, 5088-5093 (1974).

5 Van Ness, B. G., Howard, J. B. & Bodley, J. W. ADP-ribosylation of elongation factor 2 by diphtheria toxin. NMR spectra and proposed structures of ribosyl-diphthamide and its hydrolysis products. *J. Biol. Chem.* **255**, 10710-10716 (1980).

6 Van Ness, B. G., Howard, J. B. & Bodley, J. W. ADP-ribosylation of elongation factor 2 by diphtheria toxin. Isolation and properties of the novel ribosyl-amino acid and its hydrolysis products. *J. Biol. Chem.* **255**, 10717-10720 (1980).

7 Jorgensen, R., Merrill, A. R. & Andersen, G. R. The life and death of translation elongation factor 2. *Biochem Soc Trans* **34**, 1-6, doi:10.1042/BST20060001 (2006).

8 Jorgensen, R. *et al.* Crystal structure of ADP-ribosylated ribosomal translocase from *Saccharomyces cerevisiae*. *J. Biol. Chem.* **279**, 45919-45925 (2004).

9 Dunlop, P. C. & Bodley, J. W. Biosynthetic labeling of diphthamide in *Saccharomyces cerevisiae*. *J. Biol. Chem.* **258**, 4754-4758 (1983).

10 Chen, J. Y., Bodley, J. W. & Livingston, D. M. Diphtheria toxin-resistant mutants of

Saccharomyces cerevisiae. *Mol Cell Biol* **5**, 3357-3360 (1985).

11 Moehring, T. J., Danley, D. E. & Moehring, J. M. In vitro biosynthesis of diphthamide, studied with mutant Chinese hamster ovary cells resistant to diphtheria toxin. *Mol Cell Biol* **4**, 642-650 (1984).

12 Liu, S., Milne, G. T., Kuremsky, J. G., Fink, G. R. & Leppla, S. H. Identification of the proteins required for biosynthesis of diphthamide, the target of bacterial ADP-ribosylating toxins on translation elongation factor 2. *Mol Cell Biol* **24**, 9487-9497, doi:10.1128/MCB.24.21.9487-9497.2004 (2004).

13 Chen, J. Y. & Bodley, J. W. Biosynthesis of diphthamide in Saccharomyces cerevisiae. Partial purification and characterization of a specific S-adenosylmethionine:elongation factor 2 methyltransferase. *J Biol Chem* **263**, 11692-11696 (1988).

14 Carette, J. E. *et al.* Haploid genetic screens in human cells identify host factors used by pathogens. *Science* **326**, 1231-1235, doi:10.1126/science.1178955 (2009).

15 Su, X. *et al.* Chemogenomic approach identified yeast YLR143W as diphthamide synthetase. *Proc Natl Acad Sci U S A* **109**, 19983-19987, doi:10.1073/pnas.1214346109 (2012).

16 de Crecy-Lagard, V., Forouhar, F., Brochier-Armanet, C., Tong, L. & Hunt, J. F. Comparative genomic analysis of the DUF71/COG2102 family predicts roles in diphthamide biosynthesis and B12 salvage. *Biol Direct* **7**, 32, doi:10.1186/1745-6150-7-32 (2012).

17 Uthman, S. *et al.* The amidation step of diphthamide biosynthesis in yeast requires DPH6, a gene identified through mining the DPH1-DPH5 interaction network. *PLoS Genet* **9**, e1003334, doi:10.1371/journal.pgen.1003334 (2013).

18 Lin, Z. *et al.* Dph7 catalyzes a previously unknown demethylation step in diphthamide biosynthesis. *J Am Chem Soc* **136**, 6179-6182, doi:10.1021/ja5009272 (2014).

19 Glatt, S. *et al.* Structure of the Kti11/Kti13 heterodimer and its double role in

modifications of tRNA and eukaryotic elongation factor 2. *Structure* **23**, 149-160, doi:10.1016/j.str.2014.11.008 (2015).

20 Kolaj-Robin, O., McEwen, A. G., Cavarelli, J. & Seraphin, B. Structure of the Elongator cofactor complex Kti11/Kti13 provides insight into the role of Kti13 in Elongator-dependent tRNA modification. *FEBS J* **282**, 819-833, doi:10.1111/febs.13199 (2015).

21 Elkins, J. G. *et al.* A korarchaeal genome reveals insights into the evolution of the Archaea. *Proc Natl Acad Sci U S A* **105**, 8102-8107, doi:10.1073/pnas.0801980105 (2008).

22 Zhang, Y. *et al.* Diphthamide biosynthesis requires an organic radical generated by an iron-sulphur enzyme. *Nature* **465**, 891-896, doi:10.1038/nature09138 (2010).

23 Frey, P. A., Hegeman, A. D. & Ruzicka, F. J. The Radical SAM Superfamily. *Crit Rev Biochem Mol Biol* **43**, 63-88, doi:10.1080/10409230701829169 (2008).

24 Zhu, X. *et al.* Mechanistic understanding of Pyrococcus horikoshii Dph2, a [4Fe-4S] enzyme required for diphthamide biosynthesis. *Mol Biosyst* **7**, 74-81, doi:10.1039/c0mb00076k (2011).

25 Proudfoot, M. *et al.* Biochemical and structural characterization of a novel family of cystathionine beta-synthase domain proteins fused to a Zn ribbon-like domain. *J Mol Biol* **375**, 301-315, doi:10.1016/j.jmb.2007.10.060 (2008).

26 Fichtner, L. *et al.* Elongator's toxin-target (TOT) function is nuclear localization sequence dependent and suppressed by post-translational modification. *Mol Microbiol* **49**, 1297-1307 (2003).

27 Bar, C., Zabel, R., Liu, S., Stark, M. J. & Schaffrath, R. A versatile partner of eukaryotic protein complexes that is involved in multiple biological processes: Kti11/Dph3. *Mol Microbiol* **69**, 1221-1233, doi:10.1111/j.1365-2958.2008.06350.x (2008).

28 Dong, M. *et al.* Dph3 is an electron donor for Dph1-Dph2 in the first step of eukaryotic

diphthamide biosynthesis. *J Am Chem Soc* **136**, 1754-1757, doi:10.1021/ja4118957 (2014).

29 Sahi, C. & Craig, E. A. Network of general and specialty J protein chaperones of the yeast cytosol. *Proc Natl Acad Sci U S A* **104**, 7163-7168, doi:10.1073/pnas.0702357104 (2007).

30 Thakur, A. *et al.* Structure and mechanistic insights into novel iron-mediated moonlighting functions of human J-protein cochaperone, Dph4. *J Biol Chem* **287**, 13194-13205, doi:10.1074/jbc.M112.339655 (2012).

31 Webb, T. R. *et al.* Diphthamide modification of eEF2 requires a J-domain protein and is essential for normal development. *J Cell Sci* **121**, 3140-3145, doi:10.1242/jcs.035550 (2008).

32 Moehring, J. M. & Moehring, T. J. Diphthamide: in vitro biosynthesis. *Methods Enzymol* **106**, 388-395 (1984).

33 Mattheakis, L. C., Shen, W. H. & Collier, R. J. DPH5, a methyltransferase gene required for diphthamide biosynthesis in Saccharomyces cerevisiae. *Mol Cell Biol* **12**, 4026-4037 (1992).

34 Wei, H. *et al.* A modified form of diphthamide causes immunotoxin resistance in a lymphoma cell line with a deletion of the WDR85 gene. *J Biol Chem* **288**, 12305-12312, doi:10.1074/jbc.M113.461343 (2013).

35 Su, X. *et al.* YBR246W is required for the third step of diphthamide biosynthesis. *J Am Chem Soc* **134**, 773-776, doi:10.1021/ja208870a (2012).

36 Ortiz, P. A., Ulloque, R., Kihara, G. K., Zheng, H. & Kinzy, T. G. Translation elongation factor 2 anticodon mimicry domain mutants affect fidelity and diphtheria toxin resistance. *J. Biol. Chem.* **281**, 32639-32648 (2006).

37 Liu, S. *et al.* Diphthamide modification on eukaryotic elongation factor 2 is needed to assure fidelity of mRNA translation and mouse development. *Proc Natl Acad Sci U S A*

109, 13817-13822, doi:10.1073/pnas.1206933109 (2012).

38 Spahn, C. M. *et al.* Domain movements of elongation factor eEF2 and the eukaryotic 80S ribosome facilitate tRNA translocation. *EMBO J* **23**, 1008-1019, doi:10.1038/sj.emboj.76001027600102 [pii] (2004).

39 Chen, C. M. & Behringer, R. R. Cloning, structure, and expression of the mouse Ovca1 gene. *Biochem Biophys Res Commun* **286**, 1019-1026, doi:10.1006/bbrc.2001.5488 S0006-291X(01)95488-9 [pii] (2001).

40 Phillips, N. J., Ziegler, M. R. & Deaven, L. L. A cDNA from the ovarian cancer critical region of deletion on chromosome 17p13.3. *Cancer Letters* **102**, 85 (1996).

41 Phillips, N. J. *et al.* Allelic deletion on chromosome 17p13.3 in early ovarian cancer. *Cancer Res.* **56**, 606-611 (1996).

42 Bruening, W. *et al.* Expression of OVCA1, a candidate tumor suppressor, is reduced in tumors and inhibits growth of ovarian cancer cells. *Cancer Res* **59**, 4973-4983 (1999).

43 Kong, F. *et al.* OVCA1 inhibits the proliferation of epithelial ovarian cancer cells by decreasing cyclin D1 and increasing p16. *Mol Cell Biochem* **354**, 199-205, doi:10.1007/s11010-011-0819-0 (2011).

44 Chen, C.-M. & Behringer, R. R. Ovca1 regulates cell proliferation, embryonic development, and tumorigenesis. *Genes Dev.* **18**, 320-332 (2004).

45 Liu, S. *et al.* Dph3, a small protein required for diphthamide biosynthesis, is essential in mouse development. *Mol Cell Biol* **26**, 3835-3841, doi:10.1128/MCB.26.10.3835-3841.2006 (2006).

46 Iglewski, W. J., Lee, H. & Muller, P. ADP-ribosyltransferase from beef liver which ADP-ribosylates elongation factor-2. *FEBS Lett* **173**, 113-118, doi:0014-5793(84)81028-5 [pii] (1984).

47 Lee, H. & Iglewski, W. J. Cellular ADP-ribosyltransferase with the same mechanism of action as diphtheria toxin and Pseudomonas toxin A. *Proc. Natl. Acad. Sci. USA* **81**,

2703-2707 (1984).

48 Fendrick, J. L., Iglewski, W. J., Moehring, J. M. & Moehring, T. J. Characterization of the endogenous ADP-ribosylation of wild-type and mutant elongation factor-II in eukaryotic cells. *Eur. J. Biochem.* **205**, 25-31 (1992).

49 Muhammet, B., scedil, K., R. N., inodot & van ç Ergen, E. B. Endogenous ADP-ribosylation for eukaryotic elongation factor 2: evidence of two different sites and reactions. *Cell Biochemistry and Function* **24**, 369-380 (2006).

50 Jager, D., Werdan, K. & Muller-Werdan, U. Endogenous ADP-ribosylation of elongation factor-2 by interleukin-1beta. *Mol Cell Biochem* **348**, 125-128, doi:10.1007/s11010-010-0646-8 (2011).

51 Murray, J. *et al.* Structural characterization of ribosome recruitment and translocation by type IV IRES. *Elife* **5**, doi:10.7554/eLife.13567 (2016).

52 Arguelles, S., Camandola, S., Cutler, R. G., Ayala, A. & Mattson, M. P. Elongation factor 2 diphthamide is critical for translation of two IRES-dependent protein targets, XIAP and FGF2, under oxidative stress conditions. *Free Radic Biol Med* **67**, 131-138, doi:10.1016/j.freeradbiomed.2013.10.015 (2014).

CHAPTER 2

DPH7 CATALYZES A PREVIOUSLY UNKNOWN DEMETHYLATION STEP IN DIPHTHAMIDE BIOSYNTHESIS[a]

Abstract

Present on archaeal and eukaryotic translation elongation factor 2, diphthamide represents one of the most intriguing post-translational modifications on proteins. The biosynthesis of diphthamide was proposed to occur in three steps requiring seven genes, Dph1-7, in eukaryotes. The functional assignments of Dph1-5 in the first and second step have been well established. Recent studies suggest that Dph6 (yeast *YLR143W* or human *ATPBD4*) and Dph7 (yeast *YBR246W* or human *WDR85*) are involved in the last amidation step, with Dph6 being the actual diphthamide synthetase catalyzing the ATP-dependent amidation reaction. However, the exact molecular role of Dph7 is unclear. Here we demonstrate that Dph7 is an enzyme catalyzing a previously unknown step in the diphthamide biosynthesis pathway. This step is between the Dph5-catalyzed and Dph6-catalyzed reactions. We demonstrate that Dph5-catalyzed reaction generates methylated diphthine, a previously overlooked intermediate, and Dph7 is a methylesterase that hydrolyzes methylated diphthine to produce diphthine and allows Dph6-catalyzed amidation reaction to occur. Thus, our study characterizes the molecular function of Dph7 for the first time and provides a revised diphthamide biosynthesis pathway.

[a] This is a revised version of our published paper: Lin, Z. et al. Dph7 catalyzes a previously unknown demethylation step in diphthamide biosynthesis. J Am Chem Soc 136, 6179-6182, (2014).

Introduction

Diphthamide is a post-translationally modified histidine residue present on archaeal and eukaryotic elongation factor 2 (eEF-2), a GTPase involved in the translocation of mRNA and tRNA on the ribosome during translation elongation.[1-3] This exceptional modification is targeted by the pathogenic bacterium, Corynebacterium Diphtheria, which causes the infectious disease diphtheria in humans. Diphtheria toxin (DT) produced by this bacterium catalyzes the ADP-ribosylation of the diphthamide residue of eEF2 using nicotinamide adenine dinucleotide (NAD) as the ADP-ribosyl donor.[4] Irreversible ADP-ribosylation inactivates eEF2, which in turn stops translation, leading to cell death.[5] Diphthamide is reported to be important for preventing -1 translational frame shift in yeast and mammalian cells.[6,7] Intriguingly, this modification is not present in EF-G, the bacterial ortholog of eEF-2.

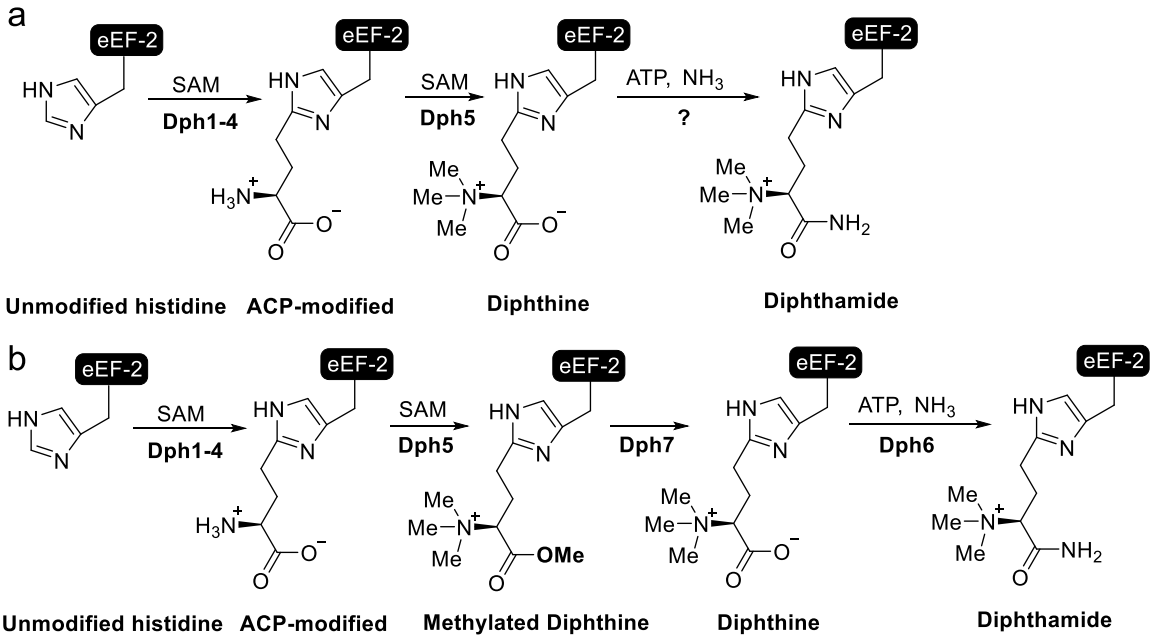

Figure 2.1 The diphthamide biosynthesis pathway in eukaryotes. (A) The initially proposed diphthamide biosynthesis pathway. (B) The revisited diphthamide biosynthesis pathway.

Genetic and biochemical studies in the budding yeast *Saccharomyces cerevisiae* allowed dissection of the diphthamide biosynthesis pathway. It was initially proposed that the biosynthesis

involves three steps (Figure 2.1).[8-10] Four proteins, Dph1-Dph4, are required for the first step, which involves the transfer of the 3-amino-3-carboxypropyl (ACP) group from S-adenosyl methionine (SAM) to the C2 carbon of the imidazole ring of His699 of yeast eEF2 (His715 of mammalian eEF-2). Recent evidence suggests that this step uses a unique [4Fe-4S]-containing enzyme and a radical reaction mechanism.[11,12] The second step involves a single methyltransferase, Dph5, which catalyzes the trimethylation of the amino group to form the diphthine intermediate (Figure 2.1A). The last step is the amidation of the carboxyl group of diphthine to form diphthamide, but the proteins required for this step evaded the initial genetic screening[10] and remained elusive for a long time. A breakthrough came when Carette et al. identified human gene *WDR85* (yeast gene *YBR246W*) as a new diphthamide biosynthetic gene (later named *DPH7*) through haploid genetic screening.[13] It was initially proposed that Dph7 is involved in the first step of diphthamide biosynthesis, but later study by our laboratory showed that deletion of Dph7 led to accumulation of diphthine, suggesting that Dph7 is involved in the last step of diphthamide biosynthesis.[14] However, Dph7 is not the diphthamide synthetase as it lacks the ATP-binding domain required.[15] The actual diphthamide synthetase, Dph6, was identified independently by three groups using comparative genomic analysis[16], yeast co-fitness analysis[15], and yeast gene interaction databases[17].

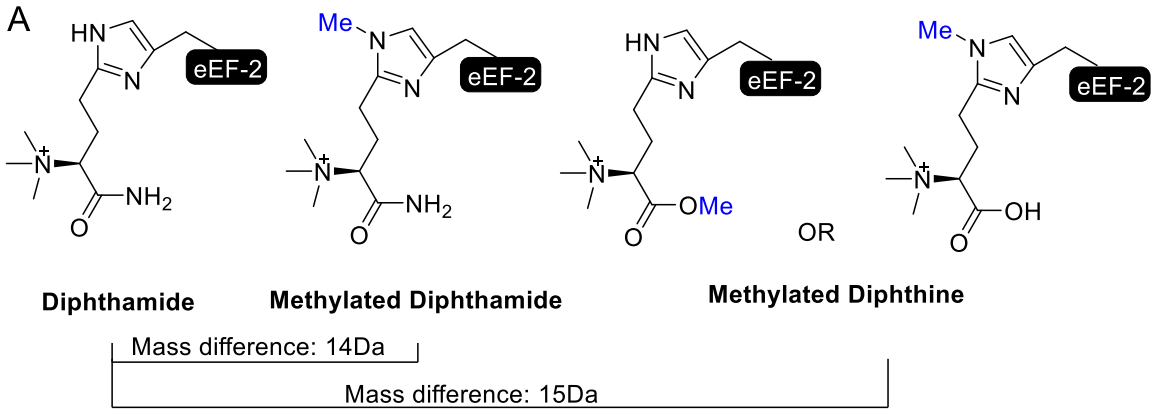

Figure 2.2. Proposed structures of methylated diphthamide and methylated diphthine.

What is the exact role of Dph7 in the pathway then? Initially, we thought that Dph7 could be a scaffold protein for the amidation reaction as it contains WD40 domains that are known to mediate protein-protein interactions.[14] Contrary to this notion, Dph6 and Dph7 were not found to interact with each other by co-immunoprecipitation.[17] It was also suggested that Dph7 is required to displace Dph5 after the second step to allow amidation catalyzed by Dph6 to occur as eEF2 binds more Dph5 in the absence of Dph7.[17] Interestingly, a novel methylated diphthamide (Figure 2.2) was recently reported in a lymphoma cell line with Dph7 gene deletion.[18] This methylation was thought to occur on one of the nitrogen atoms of the imidazole ring of the histidine residue (Figure 2.2).[18] Here we demonstrate that this modification is actually methylated diphthine with the methyl group on the carboxylate of diphthine (Figure 2.2) and Dph7 is a methylesterase responsible for the hydrolysis of the methylated diphthine to generate diphthine, which can then be used by Dph6 in the last amidation step (Figure 2.1B). The methylated diphthine is produced by the enzymatic function of Dph5. The present work thus uncovers the molecular function of Dph7 and provides a revised diphthamide biosynthesis pathway (Figure 2.1B).

Results and discussion

Dph7 has enzymatic function

To determine if Dph7 had an enzymatic role or merely mediated the interaction of Dph6 with eEF2 *in vivo*, we purified eEF2 proteins from a yeast strain with *DPH6* deletion (*dph6Δ*) and a yeast strain with *DPH7* deletion (*dph7*Δ) for *in vitro* reconstitution of the amidation reaction. The purified eEF2 proteins were incubated with Dph6, ATP and ammonium chloride for amidation. Diphthamide formation was detected with fluorescently labeled rhodamine-NAD (Rh-NAD) and a low concentration of DT, as previously described.[14] Under this condition, only diphthamide, but not other intermediate forms, can be labeled by Rh-NAD. Hence, the fluorescence labeling indicates the formation of diphthamide. We found that purified eEF2 from *dph7*Δ was not the

immediate substrate for the *in vitro* amidation by Dph6 (Figure 2.3A, lane 2). In contrast, eEF2 from *dph6*Δ was a substrate for the *in vitro* reaction (Figure 2.3A, lane 1). Diphthamide was formed on *dph7*Δ eEF2 only in the presence of both Dph6 and Dph7 (Figure 2.3A, lane 3). These results support the notion that Dph7 converts *dph7*Δ eEF2 into *dph6*Δ eEF-2, a form of eEF2 that can be amidated by Dph6 to generate diphthamide.

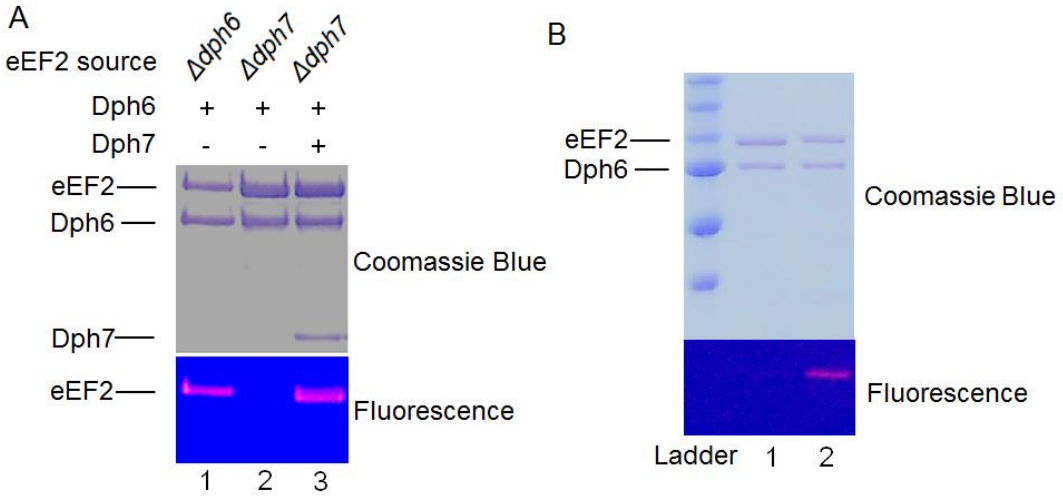

Figure 2.3. Dph7 converts *dph7*Δ eEF2 to a substrate for amidation by Dph6. (A) Dph6 and Dph7 are both required for *in vitro* amidation of *dph7*Δ eEF2. The fluorescence labels indicate formation of diphthamide by the amidation reaction catalyzed by Dph6. (B) Stepwise *in vitro* reconstitution of diphthamide formation on *dph7*Δ eEF2. Lane 1: flag-tagged *dph7*Δ *eEF2* incubated without Dph7. Lane 2: flag-tagged *dph7*Δ eEF2 incubated with Dph7 and then purified to remove Dph7. Both *dph7*Δ eEF2 samples were then incubated with Dph6 and labeled with DT and Rh-NAD.

To further demonstrate that Dph7 catalyzes an additional step, we incubated flag-tagged *dph7*Δ eEF2 with Dph7 and re-purified the *dph7*Δ eEF2 to remove Dph7. We found that the re-purified *dph7*Δ eEF2 was a substrate for the amidation by Dph6 alone (Figure 2.3B, lane 2). In contrast, flag-tagged *dph7*Δ eEF2 incubated without Dph7 did not form diphthamide (Figure 2.3B, lane 1). Taken together, these findings indicate that there is an additional step before the last amidation step in the diphthamide biosynthesis and Dph7 is the enzyme catalyzing this step.

Methylated diphthine is present in *Dph6*Δ strain

The conclusion of Dph7 having enzymatic function is seemingly contradictory to previous reports showing that *dph6*Δ eEF2 and *dph7*Δ eEF2 both contain diphthine.[14,15,17] Based on these observations, there is no room for any apparent chemical transformation for Dph7's enzymatic activity. Interestingly, a species with a mass of 15 Da larger than diphthamide was reported in a lymphoma cell line with Dph7 gene deletion.[18] The proposed structure for this species was methylated diphthamide (Figure 2.2). However, the expected mass difference of methylated diphthamide and diphthamide is 14 Da.

Therefore, we speculated that the observed species was methylated diphthine instead (Figure 2.2). In light of this report, we investigated the presence of methylated diphthine in *dph7*Δ eEF2 and *DPH6*Δ eEF2 via liquid chromatography mass spectrometry (LC-MS) studies. Consistent with previous studies, we found diphthine containing tryptic peptide (686-VNILDVTLHADAIHR-700) from both *dph7*Δ and *dph6*Δ eEF2 samples (Figure 2.4A). Likewise, we observed a small amount of unmodified peptides but no diphthamide containing peptides were detected in either eEF2 sample.[14,17] We also found the presence of methylated diphthine containing peptide in *dph7*Δ eEF2 (Figure 2.4B). Most strikingly, this methylated diphthine containing peptide was not detected in *dph6*Δ eEF-2. This unexpected form of modification had an *m/z* larger than all the previously known intermediates of diphthamide biosynthesis or diphthamide. The results of this investigation suggested a possible enzymatic role for Dph7 as a demethylase. We hypothesized that Dph7 functions to remove the extra methyl group on methylated diphthine to form diphthine. Furthermore, the fact that diphthine was also observed in MS studies of *dph7*Δ eEF2 suggested that this methyl group was relatively labile during the sample preparation for MS. Therefore, we proposed that methylated diphthine is a methyl ester which is prone to hydrolysis (Figure 2.1B).

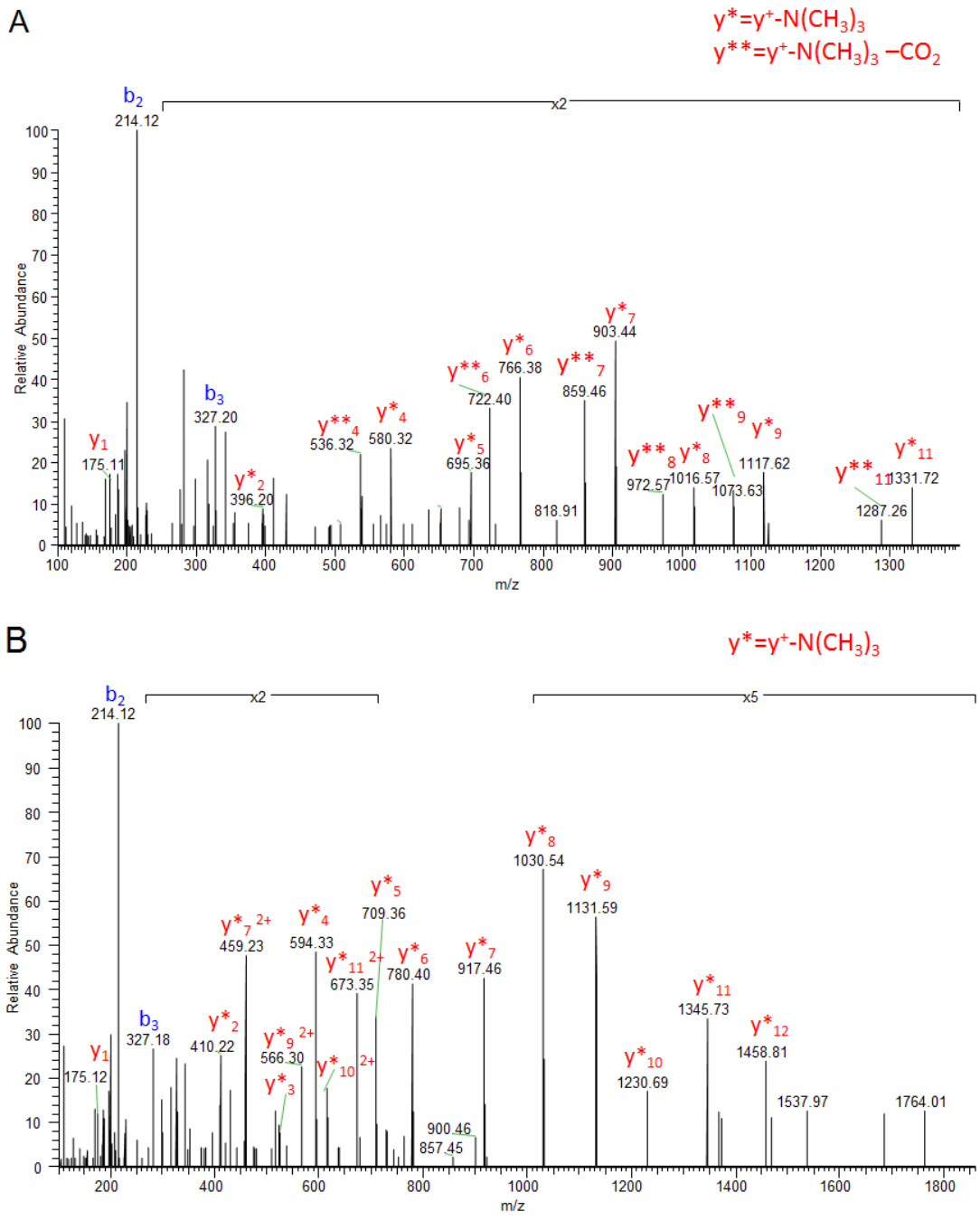

Figure 2.4. MS/MS spectra of diphthine (A, observed parental ion *m/z* 610.6793, Calculated *m/z* 610.6792) and methylated diphthine (B, observed parental ion *m/z* 615.3514, Calculated *m/z* 615.3518) containing peptides from *dph7*Δ eEF-2. A neutral loss of the trimethyl amino group on each of y ion series was observed and labeled as y*. Neutral loss of both the trimethyl amino group and carbon dioxide was observed and labeled as y**.

Methylated diphthine is a methylester

To test the hypothesis that methylated diphthine is a methyl ester, we examined the non-enzymatic hydrolysis of the methyl ester under mild basic condition. Purified *dph7*Δ eEF2 in Tris-HCl pH 9.0 buffer was incubated at 30 ℃ for various time intervals. The conversion of methylated diphthine to diphthine was monitored by the amidation reaction as Dph6 selectively amidates diphthine, but not methylated diphthine, to form diphthamide. Formation of diphthamide is then detected by fluorescence labeling using Rh-NAD and DT. As shown in Figure 2.5A, increased incubation time for *dph7*Δ eEF2 leads to increased fluorescence labeling, indicating the time-dependent conversion of methylated diphthine to diphthine. In contrast, extending the incubation time for diphthine containing *dph6*Δ eEF2 has no effect on the fluorescence intensity (Figure 2.5B). Moreover, the labeling intensities of *dph7*Δ eEF2 after incubation at pH 9.0 are considerably lower than those of *dph6*Δ eEF-2, suggesting incomplete conversion even after four hours of incubation (Figure 2.5A). This non-enzymatic reaction demonstrated that the extra methylation site is susceptible to hydrolysis. Thus, the most likely configuration of the methylated diphthine is a methyl ester.

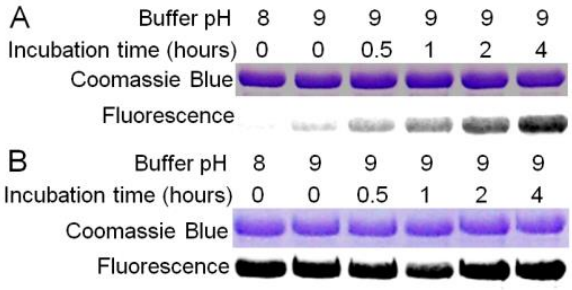

Figure 2.5. Non-enzymatic hydrolysis of methylated diphthine to diphthine. (A) *dph7*Δ eEF2 or (B) *dph6*Δ eEF2 were buffer-exchanged into a buffer containing 25 mM Tris-HCl pH 9.0 and 150 mM NaCl and incubated at 30 ℃ for various time intervals before the amidation reaction by Dph6. Formation of diphthamide was detected by fluorescence label generated by DT and Rh-NAD.

Dph7 convert methylated diphthine to diphthine *in vitro*

To further show that Dph7 catalyzes the hydrolysis reaction to form diphthine, we incubated *dph7*Δ eEF2 with Dph7 protein in Tris-HCl pH 8.0 buffer and examined the levels of methylated diphthine and diphthine. *dph7*Δ eEF2 incubated with or without Dph7 was subjected to in-solution trypsin digestion and subsequently LC-MS analysis. A tryptic peptide (815-AGEIVLAAR-823) without any post-translational modifications from eEF2 was used as an internal reference peak for both samples (Figure 2.6A and 2.6B). The level of methylated diphthine containing peptide decreases drastically after incubation with Dph7 (Figure 2.6C-2.6F). Correspondingly, the level of diphthine containing peptide increases after treatment with Dph7 (Figure 2.6G-2.6J)). Consistent with previous MS analysis, a significant amount of diphthine containing peptide is present in *dph7*Δ eEF2 sample without Dph7, possibly due to non-enzymatic hydrolysis of the methyl ester during incubation in pH 8.0 buffer and during the sample preparation process for MS analysis.

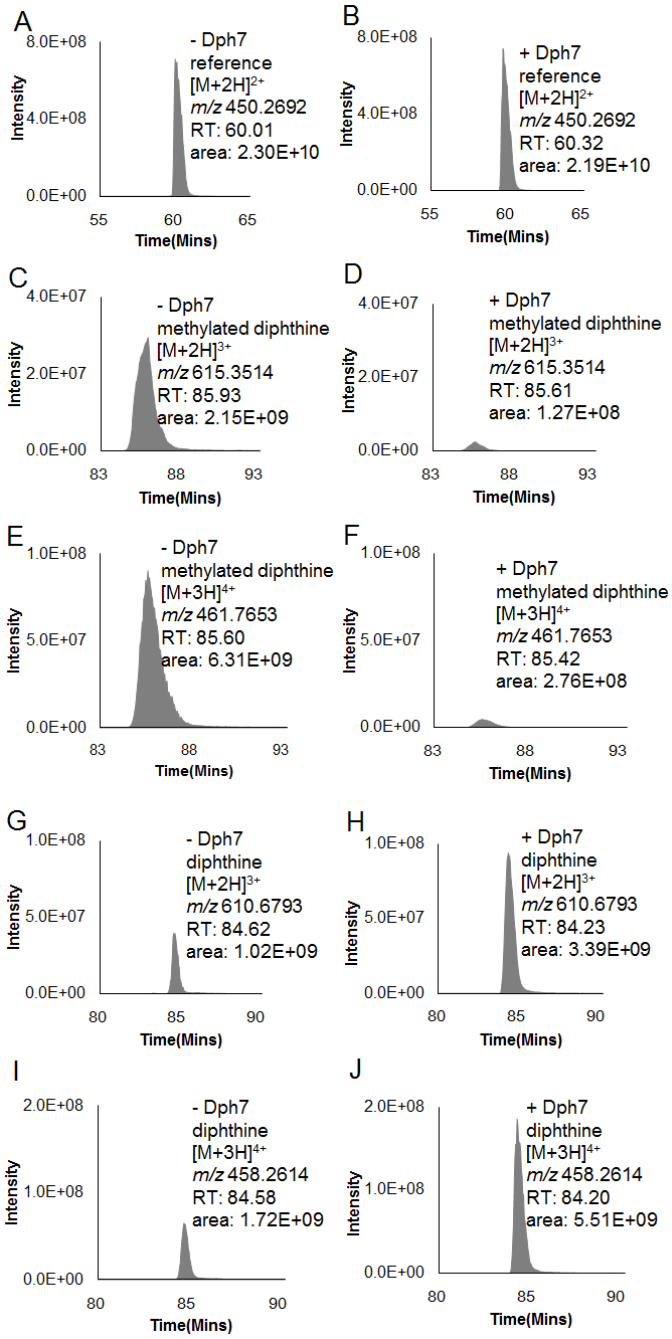

Figure 2.6. Dph7 hydrolyzes methylated diphthine to form diphthine. Relative quantification of tryptic peptides from *dph7*Δ eEF2 with or without Dph7 treatment is shown by extracted ion chromatograms of the target ions. Peaks correspond to reference peptide^{2+} (A and B, observed *m/z* 450.2692, calculated *m/z* 450.2691); methylated diphthine^{3+} (C and D, observed *m/z* 615.3514, calculated *m/z* 615.3518); methylated diphthine^{4+} (E and F, observed *m/z* 461.7653, calculated *m/z* 461.7658); diphthine^{3+} (G and H, observed *m/z* 610.6793, calculated *m/z* 610.6792); diphthine^{4+} (I and J, observed *m/z* 458.2614, calculated *m/z* 458.2619). "-Dph7" indicates peptides from *dph7*Δ eEF2 without Dph7 treatment. "+Dph7" indicates peptides from *dph7*Δ eEF2 with Dph7 treatment.

Dph5 forms methylated diphthine *in vitro*

Our finding that Dph7 is a methylesterase converting methylated diphthine to diphthine suggests that the diphthamide biosynthesis pathway needs to be revised. In the current literature, diphthine is proposed as the product of the second step catalyzed by the methyltransferase, Dph5. It was proposed after the fact that acid hydrolysis of eEF2 with *in vitro* reconstitution of the second step yields diphthine.[19] However, under such conditions, it was likely that the methylated diphthine, a methyl ester, was hydrolyzed to diphthine and was not detected. To investigate if methylated diphthine is produced by Dph5 in the second step, we reconstituted the reaction *in vitro* using purified eEF2 from *dph5*Δ yeast strain, SAM, and purified Dph5 protein. *dph5*Δ eEF2 incubated with SAM but without Dph5 was used as a control. The *dph5*Δ strain is deficient in the second step of diphthamide biosynthesis and therefore the eEF2 contains 3-amino-3-carboxypropyl (ACP) modified His_{699}, the product of the first step. Both experimental and control eEF2 samples were trypsin-digested and subjected to LC-MS analysis. In agreement with previous MS reports, we found ACP-modified peptide and unmodified peptide, but not other intermediates in the *dph5*Δ eEF2 sample without Dph5.[19] For the *dph5*Δ eEF2 sample treated with Dph5 and SAM, the level of ACP-modified peptide was considerably lower than that of the control, indicating that the ACP-modified eEF2 was consumed (Figure 2.7C and 2.7D). In addition, we found three other types of modifications on His_{699} of the tryptic peptide (686-VNILDVTLHADAIHR-700): monomethylated ACP (Figure 2.7F), diphthine (Figure 2.7H), and methylated diphthine (Figure 2.7J). These three modified forms of the tryptic peptide were not present in the control sample without Dph5 (Figure 2.7E and 2.7G, Figure 2.7I). The monomethylated ACP-modified eEF2 was likely an intermediate for the formation of methylated diphthine. Diphthine containing peptide was again observed, probably due to hydrolysis of methylated diphthine. Thus, the MS study demonstrated that methylated diphthine is the product of the second step in diphthamide biosynthesis and Dph5 is responsible for the extra methylation.

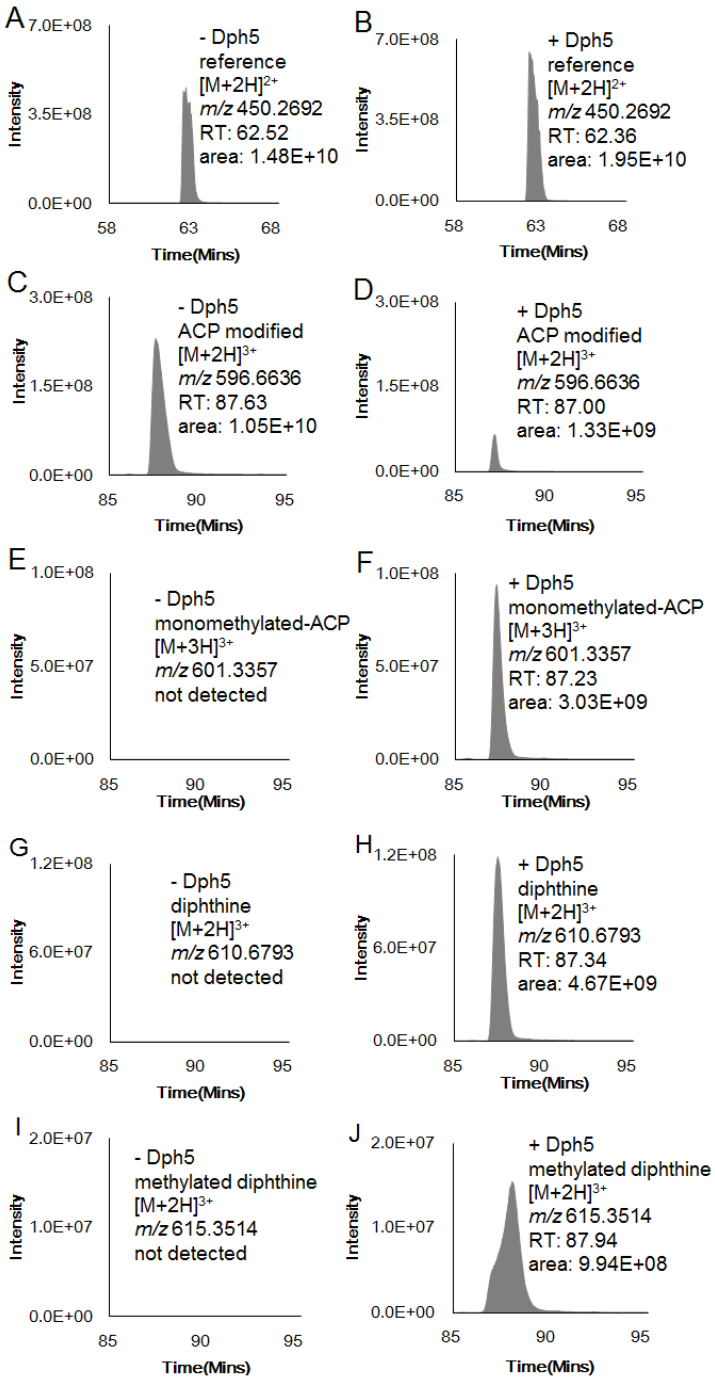

Figure 2.7. Dph5 generates methylated diphthine. Relative quantification of tryptic peptides from *dph5*Δ eEF2 with or without Dph5 treatment is shown by extracted ion chromatograms of the target ions. Peaks correspond to reference peptide^{2+} (A and B, observed *m/z* 450.2692, calculated *m/z* 450.2691); ACP-modified^{3+} (C and D, observed *m/z* 596.6636, calculated *m/z* 596.6643); monomethylated-ACP^{3+} (E and F, observed *m/z* 601.3357, calculated *m/z* 601.3361); diphthine^{3+} (G and H, observed *m/z* 610.6793, calculated *m/z* 610.6792); methylated diphthine^{3+} (I and J, observed *m/z* 615.3514, calculated *m/z* 615.3518). "–Dph5" indicates peptides from *dph5*Δ eEF2 without Dph5 treat-ment. "+Dph5" indicates peptides from *dph5*Δ eEF2 with Dph5 treatment.

In summary, our results presented here demonstrate that there is a previously unidentified step in the diphthamide biosynthesis pathway and we propose a revised scheme of the diphthamide biosynthesis pathway (Scheme 1B). Yeast Dph5 catalyzes the methylation of the amino and the carboxylate groups of ACP, generating methylated diphthine. The molecular function of Dph7 is to convert methylated diphthine to diphthine so that Dph6 can convert it to diphthamide. Although a considerable amount of diphthine containing peptide was observed in both the MS studies of *dph7*Δ eEF2 and *dph5*Δ eEF2 treated with Dph5, we believe that methylated diphthine is the predominant intermediate formed *in vivo*. This is because in the yeast Dph7 deletion strain, if both diphthine and methylated diphthine are formed by Dph5, any diphthine formed will be converted to diphthamide due to the presence of Dph6. Since diphthamide was not observed in the MS analysis of *dph7*Δ eEF2 (as we and others previously reported), we believe that only methylated diphthine is formed by yeast Dph5 *in vivo*. The observation of diphthine containing tryptic peptide in *dph7*Δ eEF2 during MS analysis is likely due to the hydrolysis of the methyl ester in the sample preparation process.

Interestingly, such promiscuous methylation activity (both N- and O-methylation) of yeast Dph5 has not been observed in other methyltransferases. Nonetheless, Dph5 belongs to the tetrapyrrole methyltransferase superfamily which methylate diverse substrates. Another superfamily member, Ribosomal RNA small subunit methyltransferase I (RsmI), catalyzes the 2-O-methylation of the ribose of cytidine 1402 in 16S rRNA.[20]

Dph7 is the first WD40 protein to have an enzymatic function. Multiple sequence alignments with Dph7 orthologs reveal conserved serine, aspartic acid and histidine residues that can potentially form a catalytic Ser-His-Asp triad, commonly found in α/β hydrolases (Figure 2.8). However, due to the presence of WD40 repeats, Dph7 is predicted to adopt a circularized beta-propeller structure,[21] lacking the usual α/β hydrolase fold. Pectin methylesterase, which also lacks the α/β hydrolase fold, was demonstrated to adopt a novel esterase active site with two

catalytic aspartic residues.[22] Thus, it is possible that the catalytic residues of Dph7 differ from the conventional catalytic triad of α/β hydrolases.

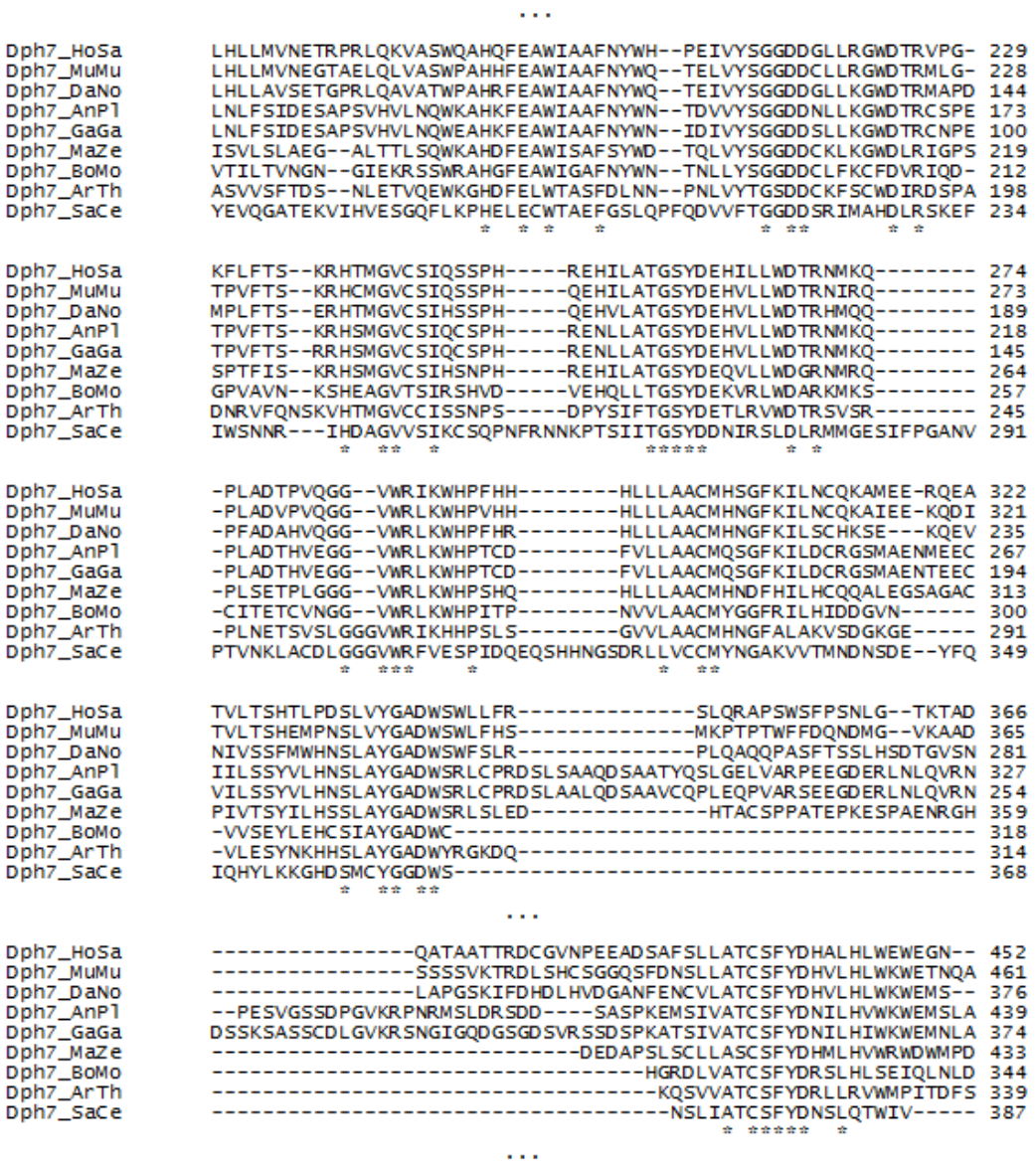

Figure 2.8. Representative sequences from an alignment of Dph7 orthologs using CLUSTAL W showing conserved residues. The protein sequences were obtained from the NCBI protein database: Dph7_HoSa, Homo sapiens Dph7 (GI:24308452); Dph7_MuMu, Mus musculus Dph7 (GI:21313066); Dph7_DaNo, Dasypus novemcinctus Dph7 (GI:488589513); Dph7_AnPl, Anas platyrhynchos Dph7 (GI:514780369); Dph7_GaGa, Gallus gallus Dph7 (GI:513212019); Dph7_MaZe, Maylandia zebra Dph7 (GI:499047390); Dph7_BoMo, Bombyx mori Dph7 (GI:512887870); Dph7_ArTh, Arabidopsis thaliana Dph7 (GI:15242588); Dph7_SaCe, Saccharomyces cerevisiae Dph7 (GI:6319723).

Mutagenesis study identify D220 as a catalytically important residue of Dph7

Unfortunately, there is no structure of Dph7 to guide the investigation of the potential novel catalytic mechanism of Dph7. Furthermore, there is no suitable known protein structure for reliable homology modeling of Dph7 structure. Hence, mutagenesis was used to identify catalytic mutants of Dph7. Sequence analysis of Dph7 from different species revealed eight conserved aspartic acids, three serines, two cysteins, three threonines and a histidine that could be important for its activity (Figure 2.8). To efficiently screen for these Dph7 catalytic mutants, we made use of an *in vivo* diphtheria toxin (DT) sensitivity assay. We generated a galactose-inducible DT mutant (N45D) which selectively ADP-ribosylates diphthamide but not methylated-diphthine or diphthine *in vivo*.[15] When expression of N45D DT is induced in *DPH7* deletion strain which contains methylated-diphthine, N45D DT mutant does not ADP-ribosylate the eEF2 and the cells can survive. However, when functional Dph7 is introduced back in *DPH7* deletion strain, diphthamide is formed and the expression of N45D DT ADP-ribosylates the eEF2 and kills the cells (Figure 2.9). Dph7 catalytic mutants can be identified though this assay as the cells will survive even after the Dph7 catalytic mutant is introduced back into the *DPH7* deletion strain.

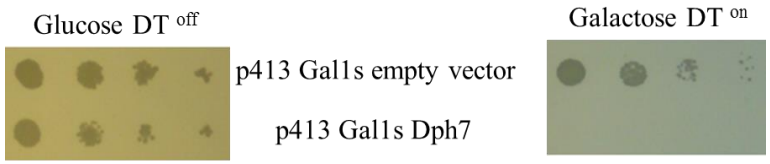

Figure 2.9. DT growth assay. *dph7*Δ were co-transformed with p416 Gals DT N45D and P413 Gals empty vector or P413 Gals Dph7 plasmid.

Using this method to screen for all the conserved aspartic acid, serine, cysteine, threonine and histidine residues, we identified a single mutation Dph7 D220N that abolishes Dph7's function *in vivo* (Figure 2.10A). We further confirmed that the D220N mutation is important for Dph7's catalytic activity by purifying the Dph7 D220N mutant protein and using this mutant Dph7 protein for *in vitro* reconstitution. We found that while WT Dph7 is able to demethylate *dph7*Δ

eEF2 for Dph6 to form diphthamide, the mutant Dph7 D220N is inactive under the same reaction condition (Figure 2.10B).

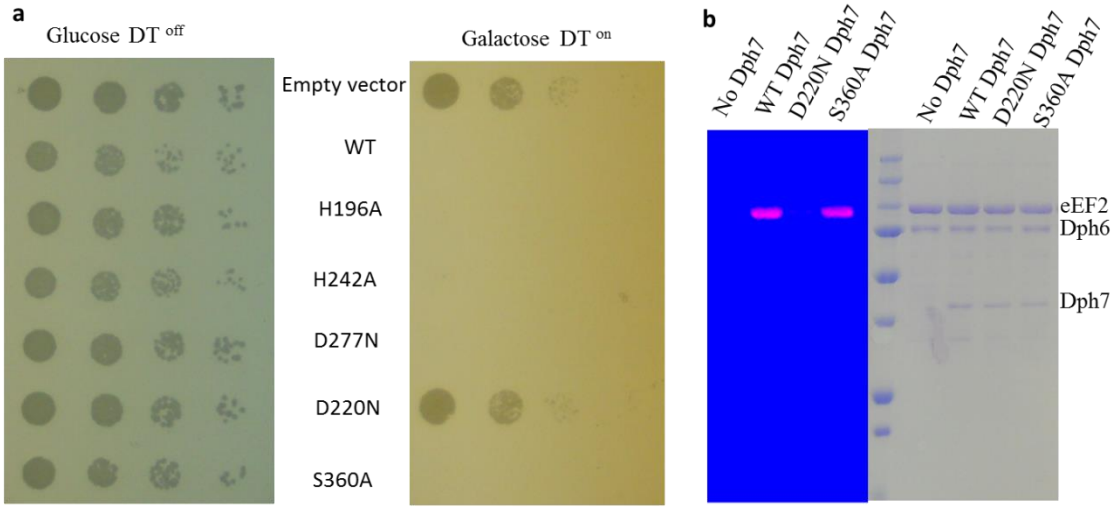

Figure 2.10. Yeast Dph7 D220N mutant reduce Dph7 activity. (A) DT growth assay. *dph7*Δ were co-transformed with p416 Gals DT N45D and P413 Gals Dph7 mutants as indicated. (B) *In vitro* diphthamide reconstitution using Dph6 and Dph7 mutants. Formation of diphthamide was detected by fluorescence.

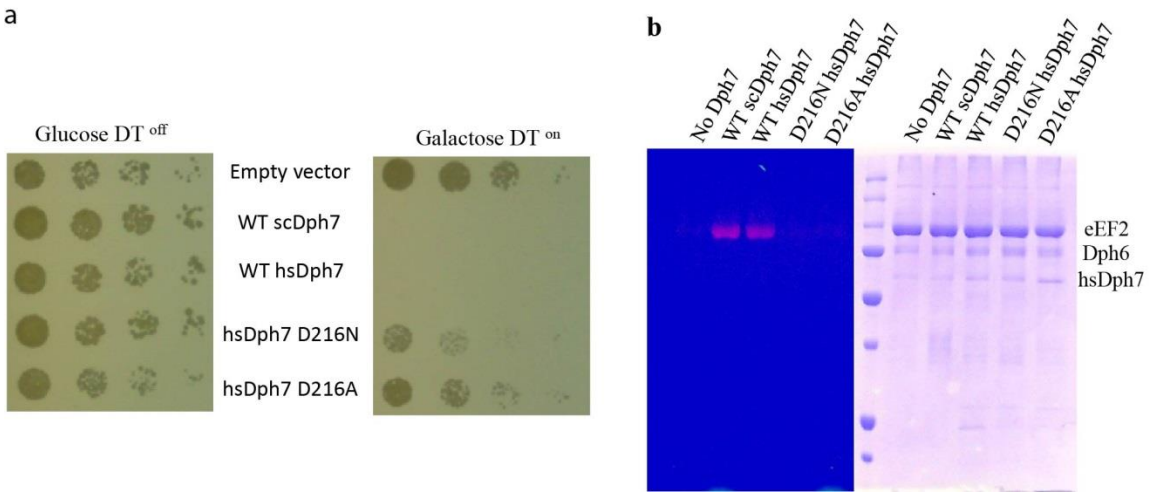

Figure 2.11. Human Dph7 D216N mutant reduce hsDph7 activity. (A) DT growth assay. Yeast *dph7*Δ were co-transformed with p416 Gals DT N45D and P413 Gals hsDph7 mutants as indicated. (B) *In vitro* diphthamide reconstitution using Dph6 and Dph7 mutants. Formation of diphthamide was detected by fluorescence.

We next test if this conserved aspartic acid residue is also important for Dph7 in other species. Interestingly, the human Dph7 ortholog is able to rescue diphthamide formation in yeast *dph7*Δ cells as indicated by complete loss of resistance to DT when human Dph7 is introduced into *dph7*Δ cells (Figure 2.11A). We found that the conserved D216 in human Dph7 is also important for the activity of human Dph7 as shown by both the DT assay and *in vitro* diphthamide reconstitution reaction (Figure 2.11A and 2.11B). These results together suggest that the conserved aspartic acid residue (D220 in scDph7 and D216 in hsDph7) is likely a catalytic residue in Dph7. However, the Pectin methylesterase which was reported to have a novel active site contains two catalytic aspartate residues. It is unclear if Dph7 only needs one aspartate to catalyze the hydrolysis or other catalytic residues only modestly decrease Dph7's activity such that multiple mutations at the same time are needed to see the phenotype. Structural information of Dph7 in the future, if any, would be most valuable in guiding the mechanistic study of Dph7's catalytic mechanism.

Conclusion

The functional implication of the additional methylation-demethylation step catalyzed by Dph7 is still unclear at this point. It is hard to believe that this extra methylation is merely a side reaction due to eukaryotic Dph5's lack of specificity. Interestingly, the recently reported crystal structure of eEF2 suggests the chiral center of the third carbon atom being an R-enantiomer[23] instead of an S-enantiomer in the previously proposed structure. This assignment of carbon chirality is surprising because this carbon derives from a methionine molecule and the S-configuration of methionine. If this chirality assignment is reliable, it implies that there is a change in chirality during the diphthamide biosynthesis. Therefore, it is possible that the extra methylation on methylated diphthine is to neutralize the negative charged on the carboxylate group which helps the subsequent inversion of chirality. The verification of the change in chirality and the potential role of the extra methylation in this process await further study.

Methods

Expression and purification of yeast eEF-2

The eEF2 proteins from *dph5*Δ, *dph6*Δ and *dph7*Δ strains were expressed and purified as previously described,[14] with a minor modification on the method for lysing cells. Cells were lysed using a beadbeater (BioSpec Products, Inc., USA) instead of the Emulsi Flex-C3 cell disruptor.

Cloning and expression of Dph7

Yeast *YBR246W* (*DPH7*) was amplified from yeast genomic DNA, which was extracted from BY4741 using Pierce Yeast DNA Extraction Kit. The primers used were ZL001 (5'-agtcagACTAGTATGcatcatcatcatcatcatGACTCTATTCAAGAATCAG ATG -3') and ZL002 (5'-agtcagGTCGACCTAAACTATCCATGTTTGCAAG -3'). The amplified gene was inserted into the p423GAL1 vector for protein production. The p423GAL1-Dph7 plasmid was transformed into BY4741 strain. Cells were grown in 2 liters of synthetic complete galactose media lacking histidine at 30 ℃ and 200 rpm for 24 hours or till the OD600 reached 2.0. Subsequent cell harvesting and purification were the same as those for eEF2 protein purification described above. Protein concentrations were determined by Bradford assay.

Cloning of eEF2 with $(His)_6$ and flag tags

DNA encoding eEF2 with C-terminal $(His)_6$ and flag tags was amplified from plasmid p423MET25-EFT1His (from strain HL610E). The primers used were ZL010 (5'-agtcagGGATCCATGGTTGCTTTCACTGTTGACCA-3') and ZL011 (5'-agtcagCTCGAGTTActtgtcatcgtcgtccttgtagtcgggatgatgatgatgatgatgCAATTTGTCGTAATAT TCTTGCC -3'). The amplified fragment was inserted into the p423 MET25 vector. The plasmid p423MET25-ETF1His&Flag was transformed into *dph7*Δ strain. Expression and purification of

the double tagged eEF2 were the same as the procedures described above for purification of yeast eEF-2.

In vitro diphthine amidation and ADP-ribosylation using Rh-NAD

The reconstitution of the amidation reaction on *dph6*Δ eEF2 was same as previously described.[15] Dph7 (50 nM) was used for the reconstitution of diphthamide formation on *dph7*Δ eEF-2. Detection of diphthamide formation was done by ADP-ribosylation reaction using Rh-NAD labeling as described.[15] The fluorescence signals were visualized using a Fisher Scientific Ultraviolet Transilluminators (Figure 2) or a Typhoon 9400 Imager (Figure 3).

Dph7 treatment of Dph7Δ eEF2 and repurification of treated eEF-2

Flag-tagged *dph7*Δ eEF2 (2 μM) was incubated with 50 nM of Dph7 at 30℃ for 1 hour. The reaction mixture was then incubated with the anti-flag M2 affinity gel (SIGMA-ALDRICH, USA) for 1 hour at 4℃ with gentle shaking on a platform shaker. The anti-flag resins were collected by centrifugation at 1000xg for 5 minutes and washed with TBS (50 mM Tris-HCl pH 7.4, 150 mM NaCl) three times. The flag tagged *dph7*Δ eEF2 was eluted by 100 μg/mL of FLAG peptides (SIGMA-ALDRICH, USA) in TBS.

Non-enzymatic hydrolysis of methylated diphthine to diphthine

*dph7*Δ eEF2 and *dph6*Δ eEF2 were buffer exchanged into a buffer containing 25 mM Tris-HCl pH 9.0 and 150 mM NaCl using Amicon Ultra Centrifugal Filters (EMD Millipore, USA). Buffer exchanged eEF2 proteins were incubated at 30℃ for various time intervals. *In vitro* diphthine amidation and detection of diphthamide formation were carried out as described above using DT and Rh-NAD.

Dph7-catalyzed hydrolysis of methylated diphthine

*dph7*Δ eEF2 (2 μM) was incubated with Dph7 (50 nM) in buffer containing Tris-HCl pH 8.0 and 150 mM NaCl at 30℃ for 1 hour. As a control, *dph7*Δ eEF2 (2 μM) in buffer containing Tris-HCl pH 8.0 and 150 mM NaCl was incubated at 30°C for 1 hour without Dph7. Then 10 μg of both Dph7-treated and untreated *dph7*Δ eEF2 samples were used for subsequent in-solution trypsin digestion and MS analysis.

Cloning and purification of Dph5

Yeast *YLR172C* (*DPH5*) was amplified from yeast genomic DNA, which was extracted from BY4741 using Pierce Yeast DNA Extraction Kit. The primers used were XS220 (5'-agtcagGTCGACTTACTCGTCGCTGTCGTCTTCT-3') and XS221 (5'-agtcagG GATCCATGCTTTATTTGATCGGACTTG-3'). The amplified gene was inserted into pET28a vector for protein production. The pET28a YLR172C plasmid was transformed into BL21 pRARE2 strain. Cells were grown in 2 liters of LB medium at 37℃ and 200 rpm. It took 4-5 hours for the OD600 to reach 0.8 after inoculation with the overnight culture. Then the culturing temperature was changed to 16℃, and the protein expression was induced by 0.4 mM isopropyl-D-thiogalactoside (IPTG). Cells were harvested after incubation at 16℃ for 18 hours. The purification using HisTrap column (GE Healthcare) was the same as eEF2 protein described above. Protein concentrations were determined by Bradford assay.

In vitro reconstitution of Dph5 activity

*dph5*Δ eEF2 (2μM) was incubated with Dph5 (50 nM) and SAM (100 μM) in buffer containing Tris-HCl pH 8.0 and 150 mM NaCl at 30℃ for 1 hour. As a control, *dph5*Δ eEF2 (2μM) was incubated with SAM (100μM) in the same buffer at 30°C for 1 hour without Dph5. Then 10 μg of both Dph5-treated or untreated *dph5*Δ eEF2 samples were used for subsequent in-solution trypsin digestion and MS analysis.

In-solution trypsin digestion of eEF-2

The eEF2 samples (10 μg each) were denatured and reduced using 6 M urea and 10 mM dithiothreitol (DTT) in 100 μL of Tris-HCl pH 8.0 buffer at room temperature (RT) for 1 hour. Iodoacetamide (IDA, final concentration 40 mM) was added to the mixture and left at RT for 1 hour. Extra IDA was quenched by addition of 4 μL of 1 M DTT and left at RT for 1 hour. The mixture was then diluted six times by adding a solution containing 50 mM Tris-HCl pH 8.0 and 1 mM $CaCl_2$. Then 0.5 μg of trypsin (Promega, reconstituted at 100 μg/mL) was added and the digestion was allowed to proceed at 37 ℃ for 18 hours. The resulting solution was acidified with 10% trifluoroacetic acid to pH 2-3 and then desalted using a Sep-Pak C18 1 cc Vac Cartridge (Waters, USA). The eluted solution was lyophilized.

Protein Identification with nano LC/MS/MS Analysis

The nano LC/MS/MS analysis was the same as previously described.[14] Acquired MS and MS/MS raw spectra were processed using Mascot 2.3 against Swissprot database with a taxonomy filter of *Saccharomyces cerevisiae* and one missed cleavage site by trypsin was allowed. Mass tolerances for precursor ions were set at 10 ppm and for MS/MS were set at 100 mmu. A fixed carbamidomethyl modification on cysteine, variable modifications on methionine oxidation, deamindation of asparagine and glutamine, and variable substitutions on histidine including unmodified, ACP-modified, methylated diphthine, diphthine and diphthamide as well as the possible elimination products were specified. All MS/MS spectra of identified peptides were manually inspected and verified using Xcalibur 2.2 software.

DT growth assays.

For DT sensitivity assays, *dph7*Δ were co-transformed with p416 Gals DT N45D and P413 Gals empty vector or P413 Gals Dph7 mutants. Transformed cells were cultured in synthetic complete media with histidine and uracil dropout at 30 ℃ overnight, adjusted to A_{600} of 0.2 with autoclaved water, and then diluted serially in 4-fold increments. Aliquots of each dilution were

spotted on glucose-containing or galactose-containing synthetic complete with histidine and uracil dropout agar plates using a replica plater. Plates were incubated at 30 ℃. Cell growth was recorded 2-3 days after plating.

Table 2.1 Yeast strains used

Strain	Genotype	Source
HL813Y	*MAT***a** *his3Δ1 leu2Δ0 met15Δ0 ura3Δ0*	Open Biosystems (YSC1048)
HL814Y	*MAT***a** *his3Δ1 leu2Δ0 met15Δ0 ura3Δ0 ybr246wΔ*	Open Biosystems (YSC1021-552106)
HL824Y	HL814Y [p423MET25-EFT1-Histag]	[1]
HL968Y	HL941Y [p423MET25-EFT1-Histag]	[1]
HL1026Y	HL1025Y [p423MET25-EFT1-Histag]	[2]
HL1105Y	HL813Y [p423GAL1-Dph7-Histag]	This study
HL1215Y	HL814Y [p423MET25-EFT1-His&Flagtag]	This study

REFERENCE

1 Van Ness, B. G., Howard, J. B. & Bodley, J. W. ADP-ribosylation of elongation factor 2 by diphtheria toxin. NMR spectra and proposed structures of ribosyl-diphthamide and its hydrolysis products. *J Biol Chem* **255**, 10710-10716 (1980).

2 Van Ness, B. G., Howard, J. B. & Bodley, J. W. ADP-ribosylation of elongation factor 2 by diphtheria toxin. Isolation and properties of the novel ribosyl-amino acid and its hydrolysis products. *J Biol Chem* **255**, 10717-10720 (1980).

3 Robinson, E. A., Henriksen, O. & Maxwell, E. S. Elongation factor 2. Amino acid sequence at the site of adenosine diphosphate ribosylation. *J Biol Chem* **249**, 5088-5093 (1974).

4 Collier, R. J. Understanding the mode of action of diphtheria toxin: a perspective on progress during the 20th century. *Toxicon* **39**, 1793-1803 (2001).

5 Honjo, T., Nishizuka, Y. & Hayaishi, O. Diphtheria toxin-dependent adenosine diphosphate ribosylation of aminoacyl transferase II and inhibition of protein synthesis. *J Biol Chem* **243**, 3553-3555 (1968).

6 Ortiz, P. A., Ulloque, R., Kihara, G. K., Zheng, H. & Kinzy, T. G. Translation elongation factor 2 anticodon mimicry domain mutants affect fidelity and diphtheria toxin resistance. *J. Biol. Chem.* **281**, 32639-32648 (2006).

7 Liu, S. *et al.* Diphthamide modification on eukaryotic elongation factor 2 is needed to assure fidelity of mRNA translation and mouse development. *Proc Natl Acad Sci U S A* **109**, 13817-13822, doi:10.1073/pnas.1206933109 (2012).

8 Moehring, T. J., Danley, D. E. & Moehring, J. M. In vitro biosynthesis of diphthamide, studied with mutant Chinese hamster ovary cells resistant to diphtheria toxin. *Mol Cell Biol* **4**, 642-650 (1984).

9 Chen, J. Y., Bodley, J. W. & Livingston, D. M. Diphtheria toxin-resistant mutants of

Saccharomyces cerevisiae. *Mol Cell Biol* **5**, 3357-3360 (1985).

10 Liu, S., Milne, G. T., Kuremsky, J. G., Fink, G. R. & Leppla, S. H. Identification of the proteins required for biosynthesis of diphthamide, the target of bacterial ADP-ribosylating toxins on translation elongation factor 2. *Mol Cell Biol* **24**, 9487-9497, doi:10.1128/MCB.24.21.9487-9497.2004 (2004).

11 Zhang, Y. *et al.* Diphthamide biosynthesis requires an organic radical generated by an iron-sulphur enzyme. *Nature* **465**, 891-896, doi:10.1038/nature09138 (2010).

12 Dong, M. *et al.* Dph3 is an electron donor for Dph1-Dph2 in the first step of eukaryotic diphthamide biosynthesis. *J Am Chem Soc* **136**, 1754-1757, doi:10.1021/ja4118957 (2014).

13 Carette, J. E. *et al.* Haploid genetic screens in human cells identify host factors used by pathogens. *Science* **326**, 1231-1235, doi:10.1126/science.1178955 (2009).

14 Su, X. *et al.* YBR246W is required for the third step of diphthamide biosynthesis. *J Am Chem Soc* **134**, 773-776, doi:10.1021/ja208870a (2012).

15 Su, X. *et al.* Chemogenomic approach identified yeast YLR143W as diphthamide synthetase. *Proc Natl Acad Sci U S A* **109**, 19983-19987, doi:10.1073/pnas.1214346109 (2012).

16 de Crecy-Lagard, V., Forouhar, F., Brochier-Armanet, C., Tong, L. & Hunt, J. F. Comparative genomic analysis of the DUF71/COG2102 family predicts roles in diphthamide biosynthesis and B12 salvage. *Biol Direct* **7**, 32, doi:10.1186/1745-6150-7-32 (2012).

17 Uthman, S. *et al.* The amidation step of diphthamide biosynthesis in yeast requires DPH6, a gene identified through mining the DPH1-DPH5 interaction network. *PLoS Genet* **9**, e1003334, doi:10.1371/journal.pgen.1003334 (2013).

18 Wei, H. *et al.* A modified form of diphthamide causes immunotoxin resistance in a lymphoma cell line with a deletion of the WDR85 gene. *J Biol Chem* **288**, 12305-12312,

doi:10.1074/jbc.M113.461343 (2013).

19 Chen, J. Y. & Bodley, J. W. Biosynthesis of diphthamide in Saccharomyces cerevisiae. Partial purification and characterization of a specific S-adenosylmethionine:elongation factor 2 methyltransferase. *J Biol Chem* **263**, 11692-11696 (1988).

20 Kimura, S. & Suzuki, T. Fine-tuning of the ribosomal decoding center by conserved methyl-modifications in the Escherichia coli 16S rRNA. *Nucleic Acids Res* **38**, 1341-1352, doi:10.1093/nar/gkp1073 (2010).

21 Xu, C. & Min, J. Structure and function of WD40 domain proteins. *Protein Cell* **2**, 202-214, doi:10.1007/s13238-011-1018-1 (2011).

22 Fries, M., Ihrig, J., Brocklehurst, K., Shevchik, V. E. & Pickersgill, R. W. Molecular basis of the activity of the phytopathogen pectin methylesterase. *EMBO J* **26**, 3879-3887, doi:10.1038/sj.emboj.7601816 (2007).

23 Jorgensen, R., Merrill, A. R. & Andersen, G. R. The life and death of translation elongation factor 2. *Biochem Soc Trans* **34**, 1-6, doi:10.1042/BST20060001 (2006).

CHAPTER 3

CYTOCHROME B5 REDUCTASE CBR1 IS A DPH3 REDUCTASE

Abstract

In eukaryotic cells, the elongation factor 2 protein (eEF2) contains a unique post-translational modification named diphthamide and approximately 25% of cytoplasmic tRNAs have the wobble uridine (U34) modified. The two seemingly distinct modification reactions both require a small CSL-type zinc finger protein, Dph3 (DiPHthamide biosynthesis 3) as an electron donor for the iron-sulfur clusters in their biosynthetic enzymes. However, the physiological reduction process of Dph3 itself is unknown. Here, using a proteomic approach, we identified cytochrome B5 reductase (Cbr1) as a NADH-dependent reductase for Dph3. The NADH- and Cbr1-dependent reduction of Dph3 may provide a regulatory linkage between cellular metabolic state and protein translation.

Introduction

Dph3 (DiPHthamide biosynthesis 3), also known as Kti11 (*Kluveromyces lactis* Toxin Insensitive 11), is required for two highly conserved modifications in eukaryotes: diphthamide, a unique protein post-translational modification on eukaryotic elongation factor 2 (eEF2), and the tRNA wobble uridine modification, 5-carboxymethyl-2-thiouridine (mcm^5s^2U). The two distinct modifications have both been suggested to be important for translation fidelity.[1,2] Interestingly, both modifications are exploited by bacterial or fungal toxins. Diphthamide is targeted by the pathogenic bacterium, *Corynebacterium Diphtheria*, which produces diphtheria toxin (DT) to catalyze the ADP-ribosylation of diphthamide and inactivate translation.[3] The *Kluyveromyces lactis* killer toxin targets and cleaves the mcm^5s^2U-modified tRNAs by its endonuclease subunit, the γ-toxin.[4]

Studies of the diphthamide biosynthesis pathway have elucidated the molecular function of Dph3. Formation of diphthamide in eukaryotes takes four steps (Figure 3.1a), requiring seven proteins (Dph1-Dph7).[5-7] The first step requires a unconventional radical SAM enzyme, the Dph1-Dph2 heterodimer. Dph1-Dph2 contains [4Fe-4S] clusters and relies on Dph3 as an electron donor to keep the [4Fe-4S] clusters in the active and reduced state.[8,9] The functions of Dph5, Dph7 and Dph6 in the subsequent steps of the biosynthesis pathway are well characterized[6,7,10] while the role of Dph4 is still unknown.

In eukaryotes, approximately 25% of cytoplasmic tRNA have the wobble uridine modified to 5-methoxycarbonylmethyluridine (mcm^5U), 5-carbamoylmethyl-2'-O-methyluridine (ncm^5U) or mcm^5s^2U. Synthesis of a common intermediate, 5-carboxymethyluridine (cm^5U), requires the eukaryotic elongator complex consisting of six subunits (Elp1-Elp6) and seven other associated proteins (Kti11-Kti14, Sit4, Sap185 and Sap190) in eukaryotes (Figure 3.1b).[11,12] Elp3, a radical SAM enzyme, is the catalytic subunit for this step. Recombinant archaeal Elp3 from *Methanocaldococcus infernus* catalyzes the formation of cm^5U in the presence of SAM and

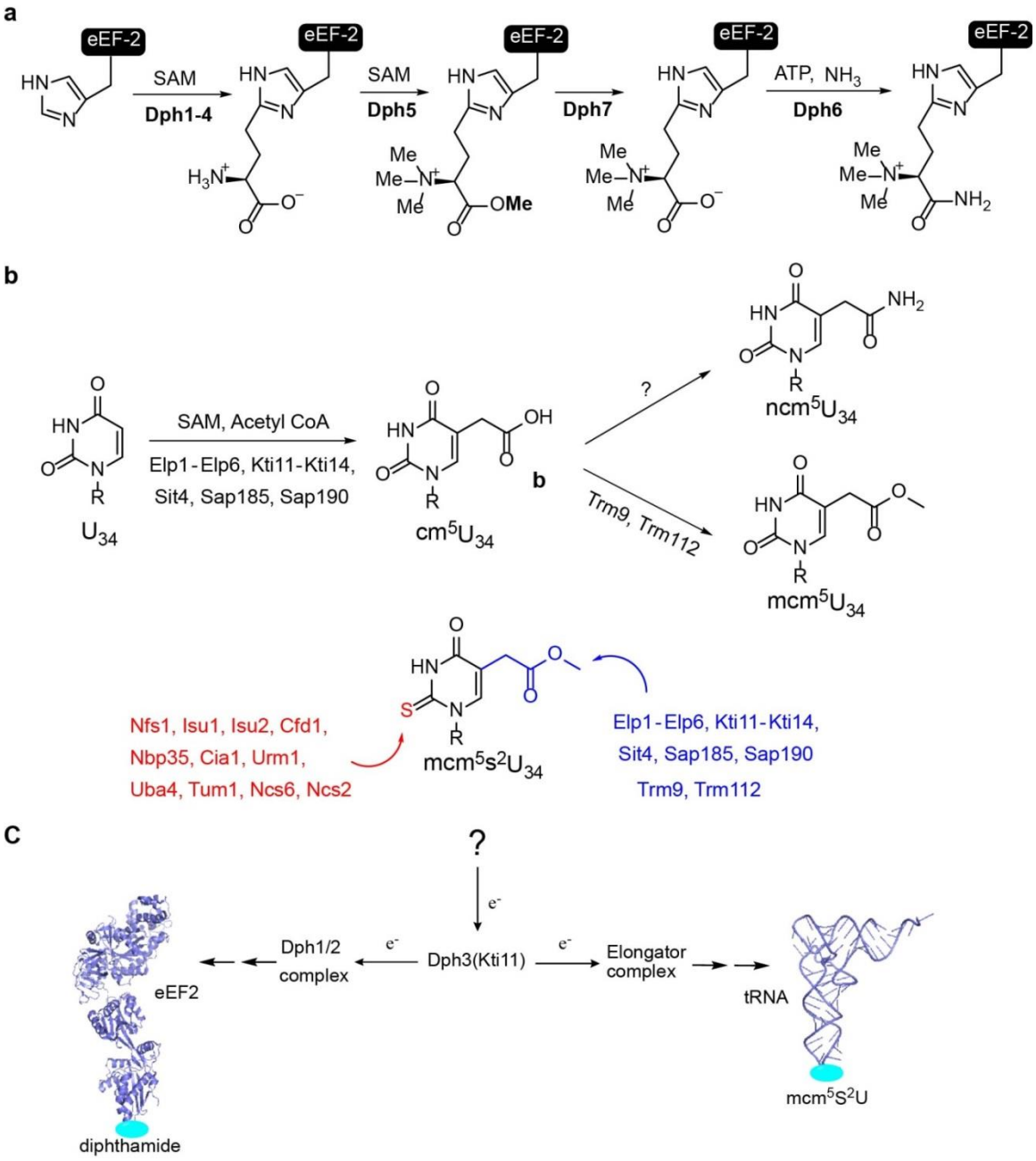

Figure 3.1. Reaction schemes for diphthamide and tRNA wobble uridine modification. (A) Diphthamide biosynthesis pathway in eukaryotes. (B) tRNA wobble uridine modifications in eukaryotes.(C) Dph3 is an electron donor essential for the two modifications.

sodium dithionite *in vitro* via a radical mechanism.[13] Given that Dph3 (also known as Kti11) is an electron donor for the radical SAM enzyme Dph1-Dph2 in diphthamide biosynthesis, it is believed that Dph3 also acts as an electron carrier for Elp3 in the tRNA modification reaction.[14] Thus, Dph3 connects the two modifications that are important for translation elongation (Figure 3.1c). However, the physiological reductase(s) that ultimately provides electrons to Dph3 is not known. While flavodoxin is known to be the biological reductant for radical SAM enzymes in bacteria,[15] the eukaryotic reduction system has not been reported. Thus, identifying the physiological reductase for Dph3 may shed light into the poorly understood reductive activation process for eukaryotic radical SAM enzymes.

Results and discussion

SILAC interactome study identified Cbr1 as a Dph3 interacting partner

To identify candidate reductase(s) for Dph3, we performed a protein interactome study on Dph3 in *Saccharomyces cerevisiae* (Figure 3.2a) using stable isotope labeling by amino acids in cell culture (SILAC). We generated a yeast BY4741 strain expressing endogenous level of FLAG-tagged Dph3 by inserting a C-terminal triple flag tag on the endogenous *dph3* gene and cultured this strain in heavy media. A BY4741 strain expressing untagged Dph3 was cultured in light media. The cell lysates were immunoprecipitated with anti-FLAG resins. The eluted fractions from both immunopreicipitation were mixed, precipitated, digested with trypsin, and analyzed by mass spectrometry to identify proteins with high heavy to light (H/L) ratios, which will be potential interacting partners of Dph3. Among the list of proteins with high H/L ratios (Figure 3.2b), we found known interactors of Dph3, such as Dph1-Dph2 and the elongator complex subunits Elp1-Elp3.[16] Our SILAC also identified Kti13. This is consistent with the recent findings reporting that Kti13 forms a stable heterodimer with Dph3.[17,18] The identification of known Dph3 interacting partners suggested that our SILAC results were reliable.

a

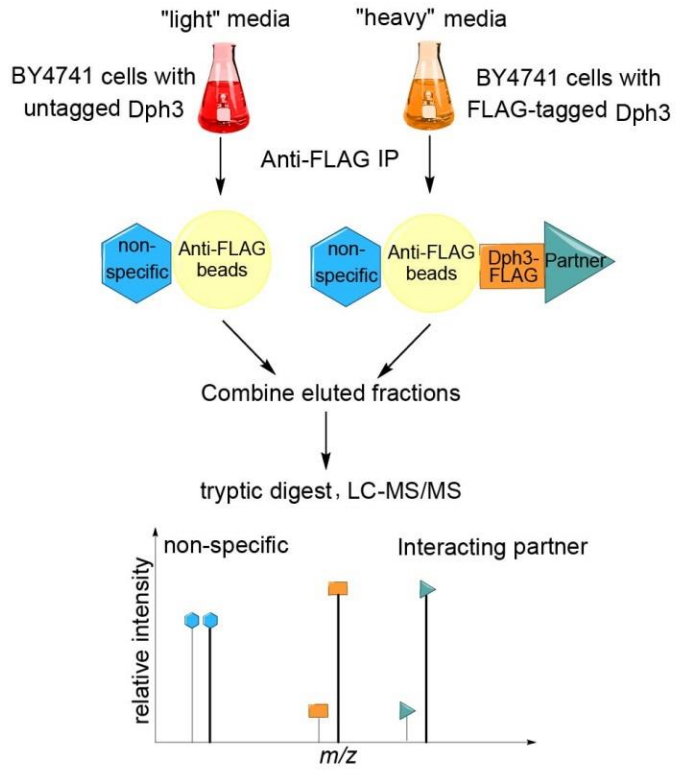

b

Protein	Heavy to light ratio
Elongator subunit Elp1	500.00
Dph2	500.00
Dph1	500.00
Elongator subunit Elp2	500.00
Elongator subunit Elp3	500.00
Serine/threonine protein kinase Hrr25	500.00
Deoxyhypusine hydroxylase	500.00
Cytochrome b_5 reductase Cbr1	500.00
F1F0 ATP synthase subunit 4	452.37
H(+)-transporting V1 sector ATPase subunit H	32.00
Mitochondrial import receptor subunit TOM40	25.06
Kti13	13.75
Regulator of ribosome biosynthesis Rrs1	11.20

c

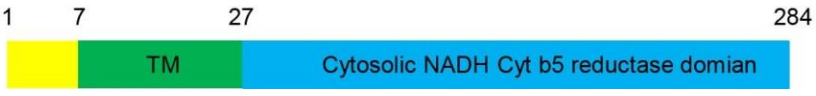

Figure 3.2. Dph3 interactome study identifies Cbr1 as a potential Dph3 reductase. (A) Schematic workflow of the Dph3 SILAC interactome study. (B) A list of proteins with high H/L ratios from Dph3 SILAC interactome study. 500 was set as the maximum H/L ratio to make it mathematically meaningful for peptides not detected in the light sample. The table lists protein with H/L ratio greater than 10. (C) Schematic view of the domain structure of yeast Cbr1.

We then looked for potential Dph3 reductases based on the SILAC results. We suspected that the reductase is likely a flavin-containing protein because electron transfer in cells from the common two-electron donors (NADH or NADPH) to Fe-containing one-electron acceptors typically require flavin cofactors, which are capable of both two-electron and one-electron transfers. Thus, to our delight, we found an NADH dependent flavoprotein, cytochrome b_5 reductase (Cbr1), among the proteins with high heavy to light ratio (Figure 3.2a). Cbr1 is a transmembrane protein embedded in the endoplasmic reticulum (ER) membrane and mitochondrion outer membrane with the catalytic domain residing on the cytosolic side (Figure 3.2c).[19] Therefore, it is plausible that Cbr1 reduces the cytosolic Dph3 which is the electron carrier for the radical SAM enzymes, Dph1-Dph2 and Elp3.

Cbr1 reduces Dph3 *in vitro*

To test if Cbr1 could reduce Dph3 *in vitro*, we cloned, expressed and purified the recombinant Cbr1 without the N-terminal transmembrane sequence. We first monitored the reduction of Dph3 by detecting the 488 nm absorption of oxidized Dph3 as previously described.[9] Upon addition of NADH to initiate the reaction, Dph3 was rapidly reduced by Cbr1 (Figure 3.3a). After the slow oxidation by air, addition of more NADH reduced Dph3 again. In contrast, addition of NADPH did not lead to reduction of Dph3, suggesting that Cbr1 is an NADH-specific enzyme (Figure 3.3b). To confirm Cbr1's role as a Dph3 reductase, we tested if this reduction system can be used to reduce Dph1-Dph2 and reconstitute the first step of diphthamide biosynthesis *in vitro*. Using ^{14}C-SAM, the substrate eEF2 was radioactively labeled in the presence of Dph1-Dph2, Dph3, Cbr1 and NADH (Figure 3.3c, lane3). The Cbr1/NADH/Dph3 reduction system was able to reduce Dph1-Dph2 similarly to dithionite, a chemical reductant for Fe-S clusters (Figure 3.3c, lane 1). When we omitted either Cbr1 or NADH, eEF2 was not labeled (Figure 3.3c, lane 4 and 5). These results demonstrated that Cbr1 can reduce Dph3 using NADH as the electron source *in vitro*.

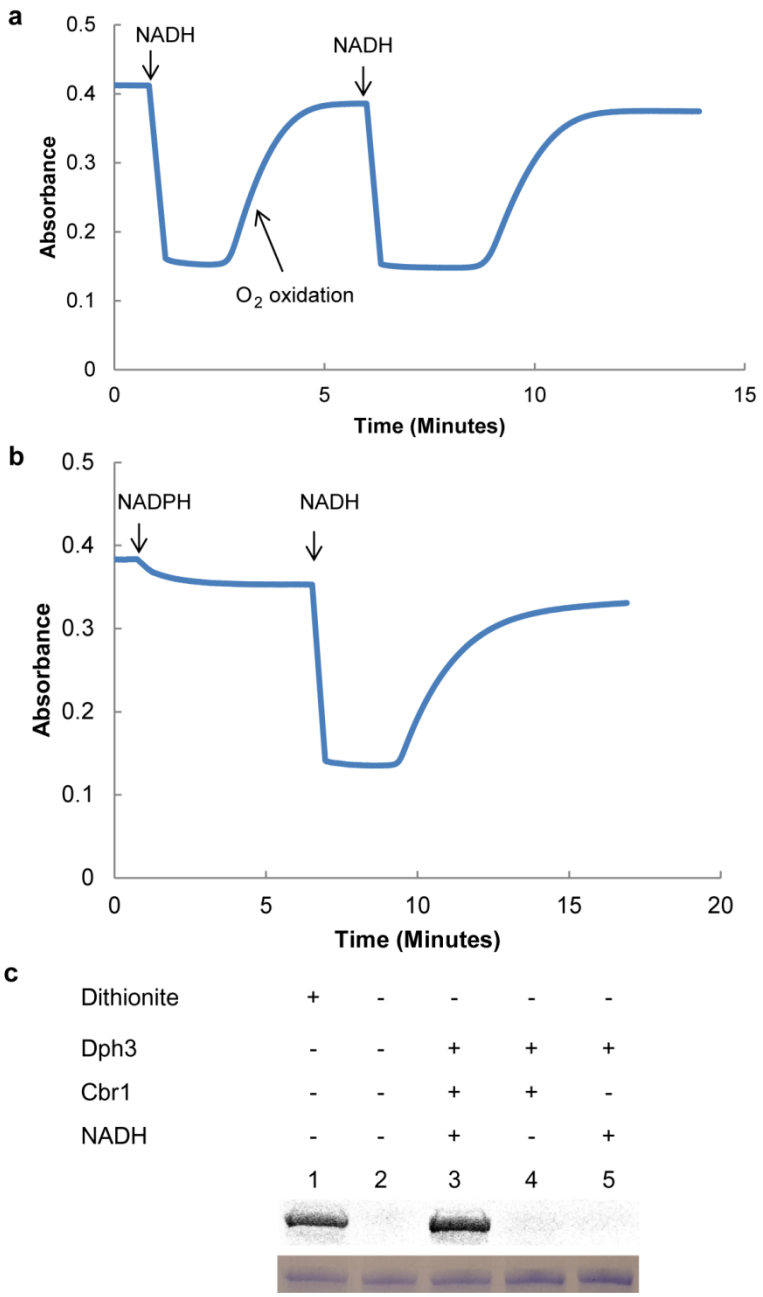

Figure 3.3. Cbr1 reduces Dph3 *in vitro.* (A) Reduction of Dph3 by addition of NADH monitored using the 488 nm absorption of oxidized Dph3. (B) Reduction of Dph3 by addition of NADPH followed by addition of NADH. (C) *In vitro* reconstitution of first step of diphthamide biosynthesis on eEF2 using Dph1-2, Dph3, Cbr1, NADH and carboxy-^{14}C-SAM. Autoradiography shows labeled eEF2. Bottom panel shows eEF2 stained with coomassie blue.

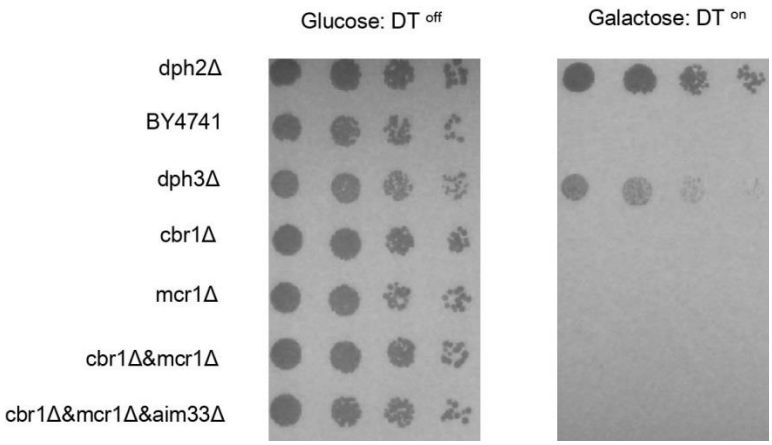

Figure 3.4. DT sensitivity assay showing that diphthamide formation is not affected in *CBR1* or *MCR1* deletion strains. The strains used are specified on the left. Each row represents a serial dilution from left to the right.

Cbr1 deletion yeast cells still form diphthamide

To confirm that Cbr1 is the reductase of Dph3 *in vivo*, we examined the formation of diphthamide in *CBR1* deletion strain (*cbr1*Δ). As diphtheria toxin targets the diphthamide modification on eEF2, yeast strains lacking diphthamide develop resistance to the toxin. We used the established diphtheria toxin sensitivity assay[20] to test if *cbr1*Δ strain abolished diphthamide formation. Interestingly, the *cbr1*Δstrain conferred no resistance to DT (Figure 3.4), suggesting that formation of diphthamide is not affected. One possibility is that multiple proteins could serve as reductases for Dph3. Thus, we used the Basic Local Alignment Search Tool (BLAST) to search for other potential reductases in *Saccharomyces cerevisiae* using the protein sequence of Cbr1. Three proteins with highly similar sequence to Cbr1 were found: Mitochondrial cytochrome b_5 reductase (Mcr1), Plasma membrane-associated coenzyme Q_6 reductase (Pga3) and Altered inheritance of mitochondria protein 33 (Aim33). Since both Cbr1 and the NADPH dependent Cytochrome P450 reductase (Ncp1) were reported to provide electrons for Cytochromes P450 involve in ergosterol biosynthesis,[21] we also tested Ncp1 for Dph3 reduction. We cloned, overexpressed and purified the recombinant Mcr1, Pga3 and Ncp1 (over-expression of the putative protein Aim33 in *E.coli* or yeast did not yield any protein) and tested their Dph3

reduction activity by monitoring the 488 nm absorption. Interestingly, we found that both Mcr1 and Ncp1 reduced Dph3 at a slower rate compared to that of Cbr1 under the similar reaction conditions (Figure 3.5a and 3.5c). However, Pga3 displayed no Dph3 reduction activity (Figure 3.5b). We found that both the Cbr1/NADH/Dph3 or Ncp1/NADPH/Dph3 reduction systems were able to reduce Dph1-Dph2 and support the first step of diphthamide (Figure 3.5d). These results suggested that Mcr1 and Ncp1 could also be reductases for Dph3.

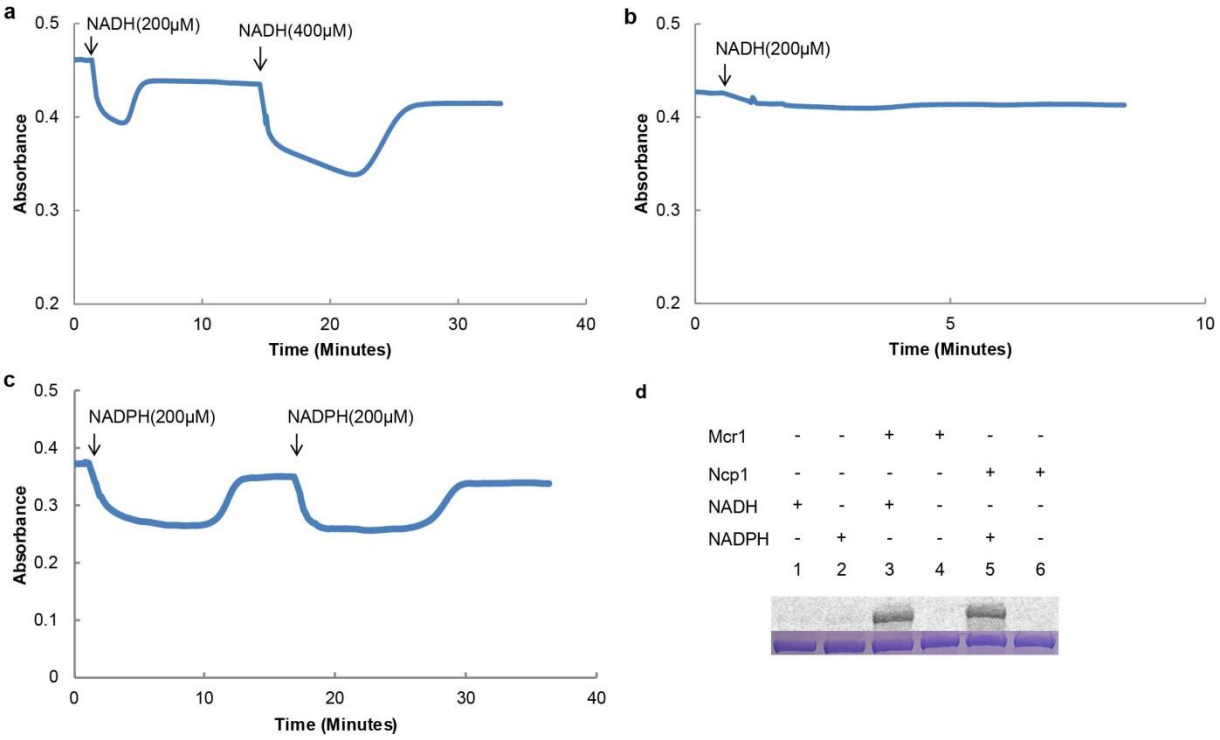

Figure 3.5. Mcr1 and Ncp1 reduce Dph3 *in vitro*. (A) Reduction of Dph3 by Mcr1 monitored using the 488 nm absorbance of oxidized Dph3. (B) Reduction of Dph3 by Pga3 monitored using the 488 nm absorbance of oxidized Dph3. (C) Reduction of Dph3 by Ncp1 monitored using the 488 nm absorbance of oxidized Dph3. (D) *In vitro* reconstitution of first step of diphthamide biosynthesis on eEF2 using Dph1-2, carboxy-^{14}C-SAM in the presence of either Mcr1/NADH or Ncp1/NADPH. Autoradiography shows labeled eEF2 substrate. Bottom panel shows eEF2 stained with coomassie blue.

We next examined diphthamide formation in multiple reductases deletion strains by DT sensitivity assay. We failed to generate a *CBR1*, *MCR1* and *NCP1* triple deletion strain as *NCP1* was found to be an essential gene by the *Saccharomyces* Genome Deletion Project (http://wwwsequence.stanford.edu/group/yeast_deletion_project/Essential_ORFs.txt).

Surprisingly, the *CBR1* and *MCR1* double deletion (*cbr1*Δ*mcr1*Δ) strain still did not confer any resistance to DT (Figure 3.4). The lack of obvious phenotype in diphthamide biosynthesis for the *cbr1*Δ*mcr1*Δ strain prompted us to investigate the tRNA modifications in these reductase(s) deletion strains. We reasoned that the synthesis of the much more abundant wobble uridine modifications (about 25% of the tRNA population)[14] is likely to depend more heavily on the efficient reduction of Dph3 compared to the formation of the irreversible diphthamide modification on the eEF2 with a slow protein turnover rate.[22] The mcm^5s^2U modified tRNAs are targeted by the *Kluyveromyces lactis* killer toxin which cleaves the modified tRNAs, leading to cell-cycle arrest. Therefore, we tested if the reductase(s) deletion strains conferred resistance to inducible expression of γ-toxin, the killer toxin catalytic subunit, using a reported assay.[23,24] As expected, BY4741 wild type and *DPH2* deletion strains which contained the mcm^5s^2U tRNA modification were unable to grow when the expression of γ-toxin was induced (Figure 3.6a). *DPH3* or *ELP3* deletion strain lacking the mcm^5s^2U tRNA modification survived under such conditions. Remarkably, we found that *CBR1* deletion alone conferred some resistance to γ-toxin, suggesting that formation of tRNA modifications was partially impaired. Furthermore, when both *CBR1* and *MCR1* were deleted, the yeast strain exhibited greater resistance to γ-toxin. *mcr1*Δ strain did not confer any resistance. To confirm that the mcm^5s^2U tRNA modification formation is impaired in *cbr1*Δ strain, we isolated total tRNA from the cells and treated the tRNA with purified γ-toxin. We found that the glu-tRNA from *cbr1*Δ strain had significantly lower cleaved glu-tRNA fragment compared to that of wild type By4741 strain (Figure 3.6b). Taken together, these results support a role for Cbr1 as the major reductase of Dph3 under normal physiological conditions.

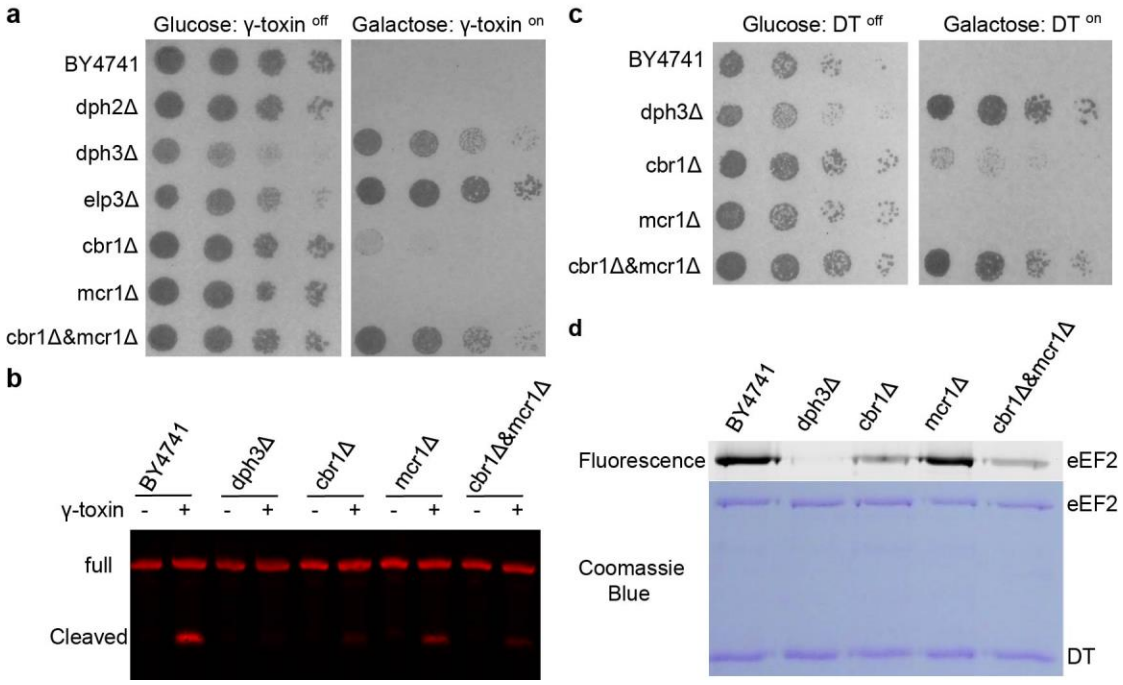

Figure 3.6. Cbr1 is the major Dph3 reductase *in vivo*. (A) *In vivo* γ-toxin sensitivity assay. The strains used are specified on the left. Each row represents a serial dilution from left to right. (B) *In vitro* γ-toxin treatment of isolated tRNA. Samples were analyzed by northern blot probing for 5' glu-tRNA. (C) *In vivo* DT sensitivity assay for cells over-expressing eEF2. The strains used are specified on the left. Each row represents a serial dilution from left to right. (D) *In vitro* ADP-ribosylation to detect diphthamide formation on purified eEF2 from cells over-expressing eEF2. Fluorescence label indicates formation of diphthamide.

Although the *cbr1*Δ*mcr1*Δ strain shows almost full resistance to the killer toxin, a small fraction of mcm^5s^2U is still formed in this strain (Figure 3.6b), indicating that there is residual reduction of Dph3 by other reductase(s), possibly by Ncp1. We hypothesized that this residual reduction of Dph3 is sufficient to support the diphthamide modification, which needs much fewer electrons compared to the more abundant tRNA wobble uridine modifications. To provide support for this hypothesis, we checked if diphthamide formation in the *cbr1*Δ*mcr1*Δ cells would be affected when eEF2 was over-expressed. While the WT BY4741 cells with over-expressed eEF2 do not confer any resistance to DT, *cbr1*Δ cells with over-expressed eEF2 is partially resistant to DT, and *CBR1* and *MCR1* double deletion render the cells nearly full resistance to DT (Figure 3.6c). Furthermore, purified eEF2 from *cbr1*Δ strain over-expressing eEF2 showed a significant

decrease in diphthamide modification level (Figure 3.6d). These results suggested that Cbr1 is required for efficient reduction of Dph3 to support the increased electron demand in diphthamide biosynthesis when eEF2 is over-expressed.

Conclusion

In summary, we identified Cbr1 as the major physiological reductase of Dph3, the electron carrier for the radical SAM enzymes required for two distinct modifications that are important for translation fidelity. In yeast, the cytochrome b_5-Cbr1 system was previously reported to be an alternative electron source, in addition to the cytochromes P450/NADPH cytochrome P450 reductase (Ncp1) system, for several sterol biosynthetic enzymes in the endoplasmic reticulum.[21] Our findings here defined a novel function of Cbr1 in reducing Dph3, an iron binding CSL-type zinc finger protein and electron carrier for the cytosolic radical SAM enzymes, Dph1-Dph2 and Elp3. The yeast Cbr1 has four homologues in human based on sequence similarity: cytochrome b_5 reductase 1-4 (CYB5R1-CYB5R4). Since both diphthamide and the wobble tRNA modifications are highly conserved in eukaryotic cells, it is conceivable that one or more of the human cytochrome b_5 reductases are Dph3 reductase(s).

Intrerestingly, our SILAC also suggested a previously unknown interaction between deoxyhypusine hydroxylase (Lia1), the dinuclear iron enzyme required for the hypusine modification on eIF5A, and Dph3. The physiological electron donor for Lia1 is still unknown. It would be plausible if Dph3 is also the electron donor for deoxyhypusine hydroxylase. However, we found that Dph3 deletion did not abolish hypusine formation. It is not clear to us whether there is any functional relationship between Dph3 and Lia1.

Because Cbr1 is a NADH dependent reductase, it is possible that the overall amount of reduced Dph3 is regulated by the redox state of the cell via the NAD^+/NADH ratio. Moreover, the abundant tRNA wobble uridine modifications are dependent on the availability of reduced Dph3.

Thus, the Cbr1 and NADH-dependent reduction of Dph3 may provide a regulatory linkage between the metabolic state of the cells and protein translation.

In bacteria, it is known that flavodoxin serves as the reductase for radical SAM enzymes.[15] However, in eukaryotes, the identity of the physiological reduction system for radical SAM enzymes is largely unknown. The Cbr1/Dph3 system is the first physiological reduction system identified for radical SAM enzymes in eukaryotes. This finding may be useful for the identification of other eukaryotic reduction systems for radical SAM enzymes.

Methods

Yeast Strains. All strains used in this study are listed in Supplementary Table 1. The HL1352Y strain expressing endogenous FLAG-tagged Dph3 was generated using PCR-based tagging method as previously described.[25] Briefly, the PCR fragment amplified from the plasmid pFA6a-6xGLY-3xFLAG-HIS3MX6 (Addgene plasmid 20753) with primers ZL210 and ZL211 (Supplementary Table 2) was transformed into BY4741 strain and plated on synthetic complete agar plates with histidine dropout for selection. The *DPH2*, *DPH3*, *CBR1* and *MCR1* single deletion strains were obtained from Open Biosystems (GE Dharmacon). The *cbr1*Δ*mcr1*Δ strain was generated from *cbr1*Δ strain by Longtine PCR-based method as previously described.[26] The PCR fragment amplified from the plasmid pFA6a-NATMX6 with primers ZL244 and ZL245 was transformed into *cbr1*Δ strain. Transformed cells were grown in YPD media for three hours to recover and plated on YPD plates with 100 μg/mL nourseothricin for selection. The *cbr1*Δ*mcr1*Δ*aim33*Δ strain was generated from *cbr1*Δ*mcr1*Δ strain transformed with PCR fragment amplified from pFA6a-His3MX6 (Addgene plasmid 41596) using primers ZL242 and Zl243 and selected with synthetic complete histidine drop out plates. The HL1352Y strain with endogenous FLAG-tagged Dph3 was verified by anti-Flag western blot. Single deletion strains obtained from Open Biosystems were verified by PCR method using strain associated barcode primers. Deletion of *MCR1* or *AIM33* by Longtine fragments were confirmed by PCR method using 5' UTR and 3' UTR primers (Supplementary Table 2).

Sample preparation of Dph3 SILAC study. *Saccharomyces cerevisiae* BY4741 strain was cultured in synthetic complete media (200 mL) with light lysine and arginine with an initial A_{600} of 0.02 untill the A_{600} reached approximately 0.5. The HL1352Y strain expressing Flag-tagged Dph3 was first cultured in synthetic complete media with heavy lysine (Sigma 608041) and arginine (Sigma 608033) for about eight generation. The overnight culture was then used to inoculate 200 mL heavy synthetic complete media with an initial A_{600} of 0.02 untill the A_{600}

reached approximately 0.5. Cells were harvested by centrifugation at 4,000 g and lysed with 600 μL of glass beads (OPS Diagnostics BAWG400-200-04) and 1 mL lysis buffer containing 50 mM Tris pH 8.0, 0.2% NP-40, 150 mM sodium chloride, 5 mM EDTA and 1 mM phenylmethanesulfonyl fluoride. Cells were lysed by 5 intervals of vortexing for 2 minutes with 2 minutes cooling on ice between intervals. Total cell lysates were cleared by centrifuging for 10 min at 13,000 g and 4 ℃. The supernatants containing 2.5 mg of proteins were incubated with 25 μL anti-flag resins (Sigma A2220) for 4 hours at 4 ℃. The resins were washed with 1 mL of lysis buffer five times and eluted with 90 μL of elution buffer (50 mM Tris pH 8.0 and 1% SDS) and heated at 95 ℃ for 5 minutes. The eluted fractions were reduced by DTT (10 mM) for 30 minutes at room temperature and then alkylated by iodoacetamide (40 mM) for 30 minutes at room temperature. The heavy (HL1352Y) and light (BY4741) eluates from equal amounts of beads loaded with equivalent amounts of total lysate (2.5 mg) from the two cultures were mixed. Proteins were precipitated by adding 600 μL of precipitation buffer containing 50% Acetone, 49.9% ethanol and 0.1% acetic acid and cooling on ice for 30 minutes. The protein pellet was washed with 400 μL of ice-cold precipitation buffer and air-dried. The resultant pellet was resuspended in 50 μL of resolubilization buffer containing 8 M urea and 50 mM Tris pH 8.0, and then diluted with 400 μL 50 mM Tris pH 8.0 and digested by 1 μg trypsin overnight at 37 ℃.

Nano LC/MS/MS and data Analysis of Dph3 SILAC interactome sample. The SILAC tryptic digests were reconstituted in 50 μL of 0.5% formic acid (FA) estimated at 0.1 μg/μL for nanoLC-ESI-MS/MS analysis, which was carried out on an Orbitrap Elite mass spectrometer (Thermo-Fisher Scientific, San Jose, CA) equipped with a "CorConneX" nano ion source device (CorSolutions LLC, Ithaca, NY). The Orbitrap was interfaced with a Dionex UltiMate3000RSLCnano system (Thermo, Sunnyvale, CA). Each SILAC peptide sample (5 μL) was injected under "User Defined Program" onto a PepMap C18 trap column-nano Viper (5 μm, 100 μm × 2 cm, Thermo) at 20 μL/min flow rate and then separated on a PepMap C18 RP nano

column (3 µm, 75 µm x 25 cm, Thermo) which was installed in the nano device with a 10-µm spray emitter (NewObjective, Woburn, MA). The peptides were eluted with a 120 minutes gradient of 5% to 38% acetonitrile (ACN) in 0.1% formic acid at a flow rate of 300 nL/min, followed by a 7-min ramping to 95% ACN-0.1% FA and a 8-min hold at 95% ACN-0.1% FA. The column was re-equilibrated with 2% ACN-0.1% FA for 25 minutes prior to the next run. The Orbitrap Elite was operated in positive ion mode with nano spray voltage set at 1.6 kV and source temperature at 250 ℃ with external calibration for FT mass analyzer being performed. The instrument was operated in parallel data-dependent acquisition (DDA) under FT-IT mode using FT mass analyzer for one MS survey scan from m/z 375 to 1800 with a resolving power of 120,000 (FWHM at m/z 400) followed by MS/MS scans on top 20 most intensive peaks with multiple charged ions above a threshold ion count of 10,000 in FT mass analyzer. Dynamic exclusion parameters were set at repeat count 1 with a 30 s repeat duration, an exclusion list size of 500, 60 s exclusion duration with ±10 ppm exclusion mass width. Collision induced dissociation (CID) parameters were set at the following values: isolation width 2.0 m/z, normalized collision energy at 35 %, activation Q at 0.25, and activation time 10 ms. All data were acquired under Xcalibur 2.2 operation software (Thermo). All MS and MS/MS raw spectra were processed and searched using Sequest HT software within the Proteome Discoverer 1.4.1.14 (PD 1.4, Thermo Scientific). The Saccharomyces cerevisiae RefSeq sequence database (5,847 entries, downloaded on 5/17/2015 from NCBInr) was used for database searches. The database search was performed under a search workflow with the "Precursor Ions Quantifier" node for SILAC 2plex (Arg10, Lys8) quantitation. The default settings for protein identification in Sequest node were: two mis-cleavages for full trypsin with fixed carbamidomethyl modification of cysteine, variable modifications of 10.008 Da on Arginine and 8.014 Da on lysine, N-terminal acetylation, methionine oxidation and deamidation of asparagine and glutamine residues. The peptide mass tolerance and fragment mass tolerance values were 15 ppm and 0.8 Da, respectively. Only high confidence peptides defined by Sequest HT with a 1% FDR by Percolator were

considered for the peptide identification. The mass precision for expected standard deviation of the detected mass used to create extracted ion chromatograms was set to 3 ppm. The SILAC 2-plex quantification method within PD 1.4 was used to calculate the heavy/light ratios of all identified proteins. Only unique peptides were used for quantification. The final protein list was filtered by proteins with at least two peptides identified. 500 were set as the maximum H/L ratio to make it mathematically meaningful for peptides essentially not present in the light sample. Table in Figure 1b lists protein with H/L ratio greater than 10.

Cloning, expression and purification of Cbr1, Mcr1, Pga3, and Ncp1. Genomic DNA was extracted from *Saccharomyces cerevisiae* BY4741 strain using Pierce Yeast DNA Extraction Kit. The DNA sequence encoding for Cbr1 with an N-terminal truncation of 27 amino acids was amplified by PCR with primers ZL224 and ZL222 (Supplementary Table 2) from the genomic DNA. The amplified gene fragment was inserted into the pET28a vector and transformed into the *Escherichia coli* expression strain BL21 pRARE2. A single colony was used to inoculate an overnight starter culture, which was used to inoculate 2 liters of lysogeny broth (LB) containing 50 μg/mL kanamycin and 20 μg/mL chloramphenicol. Cells were grown at 37 ℃ to A_{600} of approximately 0.6 and cooled to 16 ℃. Expression was induced with 0.5 mM isopropyl β-D-1-thiogalactopyranoside (IPTG) and 50 μM riboflavin, and grown overnight at 16 ℃. Cells were harvested by centrifugation and lysed using the EmulsiFlex-C3 cell disruptor (Avestin, Inc., Canada). The protein was purified on BioLogic DuoFlow 10 System (Bio-Rad, Hercules, CA). The purification was performed on HisTrap HP column (GE Healthcare, Piscataway, NJ) with a linear gradient from 30 mM imidazole to 500 mM imidazole in 30 minutes. The yellow protein fractions were collected and dialyzed against 25 mM Tris-HCl buffer (pH 8.0) containing 150 mM NaCl. Protein concentration was determined by standard Bradford assay.

The DNA sequence encoding for Pga3 with an N-terminal truncation of 61 amino acids was amplified by PCR with primers ZL234 and ZL235 (Supplementary Table 2) from the genomic

DNA. The DNA sequence encoding Ncp1 with an N-terminal truncation of 33 amino acids was amplified by PCR with primers ZL316 and ZL318 from the genomic DNA. Yeast complementary DNA was used as template for amplification of the *MCR1* gene. Yeast RNA was purified using the TRIzol® reagent (Thermo Fisher Scientific). DNA was removed from the purified RNA using DNase I (New England Biolabs). The RNA was extracted with phenol/chloroform to inactivate DNase I. Total cDNA was synthesized from the purified RNA using SuperScript® III Reverse Transcriptase (Thermo Fisher Scientific). The DNA sequence encoding for Mcr1 with an N-terminal truncation of 31 amino acids was amplified by PCR with primers ZL240 and ZL241 (Supplementary Table 2) from the synthesized cDNA. Subsequent cloning and expression of recombinant Pga3, Ncp1, and Mcr1 were similar to that of Cbr1.

Ultraviolet–visible spectroscopy to monitor reduction of Dph3. Recombinant yeast Dph3 was purified as previously described.[9] The reaction was monitored on a Cary 50 Bio UV-Vis spectrophotometer (Varian) at 488 nm. Cbr1 (0.5 μM) was mixed with 100 μM of Dph3 in a cuvette. The reaction was initiated by addition of NADH or NADPH at a final concentration of 0.2 mM or as indicated. Reduction of Dph3 by Mcr1 or Pga3 was monitored at the same conditions as that of Cbr1.

Anaerobic reconstitution of the first step of yeast diphthamide biosynthesis. The Dph3 protein, Dph1-Dph2 complex and eEF2 proteins from BY4741 *DPH2* deletion strain were expressed and purified as previously described.[9] The reaction mixture was assembled in the anaerobic chamber under strictly anaerobic conditions. Aerobically purified Dph3, Cbr1 and eEF2 were degassed by a schlenk line. The reconstitution reactions were set up in an anaerobic chamber. Dph1-Dph2 (5 μM), Dph3 (10 μM), eEF2 (2 μM), Cbr1 or Mcr1 or Ncp1 (5 μM), and NADH or NADPH (200 μM) were added to a buffer containing 150 mM NaCl and 200 mM Tris-HCl at pH 7.4. Reactions without NADH or without reductases were also carried out as negative control. The reaction vials were sealed before being taken out of the anaerobic chamber.

^{14}C-SAM (ARC 0343-50, 18 μM) was injected into each reaction vial to initiate the reaction. The reaction mixtures were mixed by brief vortexing and incubated at 30 ℃ for 60 minutes. The reactions were stopped by adding protein loading dye and subsequently heating at 95 ℃ for 5 minutes, and then resolved by 12% SDS–polyacrylamide gel electrophoresis. The dried gel was exposed to a Phosphor Imaging screen and scanned using a Typhoon FLA 7000 (GE Healthcare Life Sciences).

Purification of eEF2 and its *in vitro* ADP-ribosylation by DT. Cells transformed with p423Met25-eEF2 (allow over-expression of eEF2 with a 8 His C-terminal tag) were cultured in synthetic complete media with histidine dropout at 30 ℃ with an initial A_{600} of 0.02 until the A_{600} reached approximately 1.0. Cells harvested were lysed and eEF2 was purified as previously described.[7] Purified eEF2 (1 μM) and Rh-NAD (25 μM) were incubated with DT (1 μM) at 30 ℃ in 50 mM NaCl, 30 mM dithiothreitol (DTT), 2 mM ethylenediaminetetraacetic acid (EDTA), and 25 mM Tris-HCl at pH 8.0 for 15 minutes as previously described.[6]

DT and γ-toxin sensitivity assays. For DT sensitivity assays, cells were transformed with plasmid pHL1015, which allows for galactose-inducible, glucose-repressible expression of diphtheria toxin as previously described.[6] Transformed cells were cultured in synthetic complete media with uracil dropout at 30 ℃ overnight, adjusted to A_{600} of 0.2 with autoclaved water, and then diluted serially in 4-fold increments. Aliquots of each dilution were spotted on glucose-containing or galactose-containing agar plates using a replica plater. Plates were incubated at 30 ℃. Cell growth was recorded 2-3 days after plating. DT sensitivity assay for cells co-transformed with p423Met25-eEF2 and pHL1015 were performed similarly and plated onto galactose-containing or glucose-containing synthetic complete with histidine and uracil dropout agar plates. For γ-toxin sensitivity assays, cells were transformed with plasmid pLF16 which allows for galactose-inducible, glucose-repressible expression of γ-toxin as previously

described.[24] Cultures were grown in synthetic complete media with leucine dropout at 30 ℃. Plating of cells on agar plates was performed similar to that of DT assays.

Cloning, expression and purification of γ-toxin. The DNA sequence encoding for γ-toxin with an N-terminal truncation of 19 amino acids was amplified by PCR with primers ZL436 and ZL437 (Supplementary Table 2) from pLF16. The amplified gene fragment was inserted into the pET28a vector and transformed into the *Escherichia coli* expression strain BL21 pRARE2. A single colony was used to inoculate an overnight starter culture, which was used to inoculate 2 liters of LB containing 50 μg/mL kanamycin and 20 μg/mL chloramphenicol. Cells were grown at 37 ℃ to A_{600} of approximately 0.6 and cooled to 16 ℃. Expression was induced with 0.5 mM IPTG and grown overnight at 16 ℃. Subsequent protein purification was performed similar to that of Cbr1.

Bulk tRNA isolation and in vitro γ-toxin treatment. Yeast cells were cultured in 2 liters YPD from initial A_{600} of 0.02 till A_{600} reached approximately 0.5. Cells were harvested and bulk tRNA was purified as previously described.[27] The total tRNAs (5μg) were incubated withγ-toxin (5 μM) in 10 mM NaCl, 10 mM $MgCl_2$, 1 mM DTT and 10 mM Tris-HCl at pH 7.4 for 2 hours at 30 ℃. The samples were separated on 12% polyacrylamide, 8M urea gels, and transferred to nylon membrane (GE Health, rpn119b) for northern blot. The oligonucleotide used to detect 5' of glu-tRNA was ordered from IDT (/5AmMC6/GTGATAGCCGTTACACTATATCGGA) and conjugated to Alexa Fluor® 680 (ThermoFisher, A37567). Northern blots were visualized by Odyssey® CLx imaging system (LI-COR).

Table1. Yeast strains used

Strain	*Genotype*	*Source*
HL813Y	*MAT***a** *his3Δ1 leu2Δ0 met15Δ0 ura3Δ0*	Open Biosystems (YSC1048)
HL1352Y	*MAT***a** *his3Δ1 leu2Δ0 met15Δ0 ura3Δ0 dph3-6xGLY-3xFLAG::HIS3*	This study
HL815Y	*MAT***a** *his3Δ1 leu2Δ0 met15Δ0 ura3Δ0 dph2::KAN*	Open Biosystems (YSC1021-553846)
HL1429Y	*MAT***a** *his3Δ1 leu2Δ0 lys2Δ0 ura3Δ0 dph3::KAN*	Open Biosystems (YSC6273-201938235)
HL1355Y	*MAT***a** *his3Δ1 leu2Δ0 met15Δ0 ura3Δ0 cbr1::KAN*	Open Biosystems (YSC6273-201920517)
HL1396Y	*MAT***a** *his3Δ1 leu2Δ0 met15Δ0 ura3Δ0 mcr1::KAN*	Open Biosystems (YSC6273-201936518)
HL1439Y	*MAT***a** *his3Δ1 leu2Δ0 met15Δ0 ura3Δ0 cbr1::KAN mcr1Δ::NAT*	This study
HL1400Y	*MAT***a** *his3Δ1 leu2Δ0 met15Δ0 ura3Δ0 cbr1::KAN mcr1Δ::NAT aim33::HIS3*	This study
HL1433Y	*MAT***a** *his3Δ1 leu2Δ0 met15Δ0 ura3Δ0 elp3::KAN*	Open Biosystems (YSC6273-201929585)
HL1401Y	HL813Y [pLF16, *CEN LEU2 UASGAL-γ-toxin*]	This study
HL1402Y	HL815Y [pLF16, *CEN LEU2 UASGAL-γ-toxin*]	This study
HL1403Y	HL1429Y [pLF16, *CEN LEU2 UASGAL-γ-toxin*]	This study
HL1405Y	HL1355Y [pLF16, *CEN LEU2 UASGAL-γ-toxin*]	This study
HL1406Y	HL1396Y [pLF16, *CEN LEU2 UASGAL-γ-toxin*]	This study
HL1407Y	HL1439Y [pLF16, *CEN LEU2 UASGAL-γ-toxin*]	This study
HL1442Y	HL1433Y [pLF16, *CEN LEU2 UASGAL-γ-toxin*]	This study
HL1416Y	HL813Y [pHL1025, p416 GALS DT-F2 (N45D)]	This study
HL1417Y	HL815Y [pHL1025, p416 GALS DT-F2 (N45D)]	This study
HL1418Y	HL1429Y [pHL1025, p416 GALS DT-F2 (N45D)]	This study

Table1. Continued

Strain	Genotype	Source
HL1419Y	HL1355Y [pHL1025, p416 GALS DT-F2 (N45D)]	This study
HL1420Y	HL1396Y [pHL1025, p416 GALS DT-F2 (N45D)]	This study
HL1440Y	HL1439Y [pHL1025, p416 GALS DT-F2 (N45D)]	This study
HL1441Y	HL1400Y [pHL1025, p416 GALS DT-F2 (N45D)]	This study
HL1443Y	HL813Y [pHL610E, p423 met25 eEF2 C-His]	This Study
HL1444Y	HL1429Y [pHL610E, p423 met25 eEF2 C-His]	This Study
HL1445Y	HL1355Y [pHL610E, p423 met25 eEF2 C-His]	This Study
HL1446Y	HL1396Y [pHL610E, p423 met25 eEF2 C-His]	This Study
HL1447Y	HL1439Y [pHL610E, p423 met25 eEF2 C-His]	This Study
HL1448Y	HL813Y [pHL610E, p423 met25 eEF2 C-His; pHL1025, p416 GALS DT-F2 (N45D)]	This Study
HL1449Y	HL1429Y [pHL610E, p423 met25 eEF2 C-His; pHL1025, p416 GALS DT-F2 (N45D)]	This Study
HL1450Y	HL1355Y [pHL610E, p423 met25 eEF2 C-His; pHL1025, p416 GALS DT-F2 (N45D)]	This Study
HL1451Y	HL1396Y [pHL610E, p423 met25 eEF2 C-His; pHL1025, p416 GALS DT-F2 (N45D)]	This Study
HL1452Y	HL1439Y [pHL610E, p423 met25 eEF2 C-His; pHL1025, p416 GALS DT-F2 (N45D)]	This Study

Table 2. List of primers

Primers for constructing endogenous Dph3 FLAG tag

ZL210

GCAGGCATCCACCCCCCTGAGCCTATTGCCGCTGCTGCCcggatccccgggttaattaa

ZL211

CTTTATTTCTATTTGTATTCTCGATCTAGCCTCTCATCTgaattcgagctcgtttaaac

Primers for deletion of *MCR1* gene

ZL244

ATAACGTATATAGGTTAAAATAATATTCCAAGTCAAAAACcggatccccgggttaattaa

ZL245

ATCCGAAATTAAAAAAAATATCAATTACTTTCCTCCATGCgaattcgagctcgtttaaac

Primers for verification of *MCR1* deletion

ZL354 ATAACGTATATAGGTTAAAATAATATTCC

ZL307 CAATTACTTTCCTCCATGC

Primers for deletion of *AIM33* gene

ZL242

TATCACATTTTTTCTTTGTAAAAAGCAACCATTCGCAACAcggatccccgggttaattaa

ZL243

TGCTTATTTACATGAAAAATCATCAATCGTAAACAGTTGAgaattcgagctcgtttaaac

Primers for verification of *AIM33* deletion

ZL250 GTATGTTTAGTATTAACTCATATCAC

ZL251 AAATACGAATATATATCTAAATATAATTAATGC

Primers for the *CBR1* gene

ZL224 CAGAGTGAATTCAAGACCAAGCCTGTGCT

ZL222 AGTCAGCTCGAGTTAAAACACAAACACCTGGT

Primers for the *PGA3* gene

ZL234 AGTCAGGGATCCAAAAGAAGAAGATCACTGTA

ZL235 AGTCAGCTCGAGTTAAAAGACGAAGACTTGAT

Primers for the *MCR1* gene

ZL240 CAGAGTGAATTCAACCGTAACCAACATTCC

ZL241 AGTCAGCTCGAGTTAAAATTTGAAAACTTGGT

Primers for the *NCP1* gene

ZL316

AGTCAGCCATGGGCCATCATCATCATCATCATATGTCCGATGACGGAGATAT

ZL318 AGTCAGCTCGAGTTACCAGACATCTTCTTGGTAT

Primers for the γ-toxin

ZL436

AGTCAGCCATGGGCCATCATCATCATCATCATCATCATGCAGCTACTACTGCGA

GA

ZL437 AGTCAGCTCGAGTTATACACATTTTCCATTCTGTAG

REFERENCES

1 Johansson, M. J., Esberg, A., Huang, B., Bjork, G. R. & Bystrom, A. S. *Mol Cell Biol* **28**, 3301-3312 (2008).

2 Liu, S. *et al. Proc Natl Acad Sci U S A* **109**, 13817-13822 (2012).

3 Honjo, T., Nishizuka, Y. & Hayaishi, O. *J Biol Chem* **243**, 3553-3555 (1968).

4 Lu, J., Huang, B., Esberg, A., Johansson, M. J. & Bystrom, A. S. *RNA* **11**, 1648-1654 (2005).

5 Liu, S., Milne, G. T., Kuremsky, J. G., Fink, G. R. & Leppla, S. H. *Mol Cell Biol* **24**, 9487-9497 (2004).

6 Su, X. *et al. Proc Natl Acad Sci U S A* **109**, 19983-19987 (2012).

7 Lin, Z. *et al. J Am Chem Soc* **136**, 6179-6182 (2014).

8 Zhang, Y. *et al. Nature* **465**, 891-896 (2010).

9 Dong, M. *et al. J Am Chem Soc* **136**, 1754-1757 (2014).

10 Mattheakis, L. C., Shen, W. H. & Collier, R. J. *Mol Cell Biol* **12**, 4026-4037 (1992).

11 Huang, B., Johansson, M. J. & Bystrom, A. S. *RNA* **11**, 424-436 (2005).

12 Jablonowski, D. *et al. Genetics* **159**, 1479-1489 (2001).

13 Selvadurai, K., Wang, P., Seimetz, J. & Huang, R. H. *Nat Chem Biol* **10**, 810-812 (2014).

14 Karlsborn, T. *et al. RNA Biol* **11**, 1519-1528 (2014).

15 Bianchi, V. *et al. Biochem Biophys Res Commun* **197**, 792-797 (1993).

16 Bar, C., Zabel, R., Liu, S., Stark, M. J. & Schaffrath, R. *Mol Microbiol* **69**, 1221-1233 (2008).

17 Kolaj-Robin, O., McEwen, A. G., Cavarelli, J. & Seraphin, B. *FEBS J* **282**, 819-833 (2015).

18 Glatt, S. *et al. Structure* **23**, 149-160 (2015).

19 Du, M., Shirabe, K. & Takeshita, M. *Biochem Biophys Res Commun* **235**, 779-783 (1997).

20 Chen, J. Y., Bodley, J. W. & Livingston, D. M. *Mol Cell Biol* **5**, 3357-3360 (1985).

21 Lamb, D. C., Kelly, D. E., Manning, N. J., Kaderbhai, M. A. & Kelly, S. L. *FEBS Lett* **462**, 283-288 (1999).

22 Belle, A., Tanay, A., Bitincka, L., Shamir, R. & O'Shea, E. K. *Proc Natl Acad Sci U S A* **103**, 13004-13009 (2006).

23 Frohloff, F., Fichtner, L., Jablonowski, D., Breunig, K. D. & Schaffrath, R. *EMBO J* **20**, 1993-2003, (2001).

24 Keppetipola, N., Jain, R., Meineke, B., Diver, M. & Shuman, S. *RNA* **15**, 1036-1044 (2009).

25 Funakoshi, M. & Hochstrasser, M. *Yeast* **26**, 185-192 (2009).

26 Longtine, M. S. *et al. Yeast* **14**, 953-961 (1998).

27 de Crecy-Lagard, V. *et al. Mol Biol Evol* **27**, 2062-2077 (2010).

CHAPTER 4

THE ROLE OF KTI13 IN DIPHTHAMIDE BIOSYNTHESIS PATHWAY AND tRNA WOBBLE URIDINE MODIFICATIONS

Abstract

Similar to Dph3 (also known as Kti11), the *Kluveromyces lactis* Toxin Insensitive 13 (Kti13) is also a protein involved in both the diphthamide biosynthesis and tRNA wobble uridine modifications. Interestingly, Dph3 and Kti13 form a stable heterodimer and this complex formation seems to be important for both modifications. However, the exact role of Kti13 in both modification reactions is unclear. Here, we present initial evidence for Kti13's role in lowering the reduction potential of Dph3 upon complex formation which presumably leads to more efficient electron transfer from Dph3 to Dph1-Dph2 and Elp3. Residues on Kti13 that are potentially important for this role are identified.

Introduction

Formation of the unique diphthamide modification in eukaryotes takes four steps, requiring at least seven proteins (Dph1-Dph7).[1-3] The first step requires a unconventional radical SAM enzyme as the catalytic subunit, the Dph1-Dph2 heterodimer. Dph1-Dph2 contains [4Fe-4S] clusters and relies on Dph3 as an electron donor to keep the [4Fe-4S] clusters in the active and reduced state.[4,5]

In eukaryotes, approximately 25% of cytoplasmic tRNA have the wobble uridine modified to 5-methoxycarbonylmethyluridine (mcm^5U), 5-carbamoylmethyl-2'-O-methyluridine (ncm^5U) or mcm^5s^2U. Synthesis of a common intermediate, 5-carboxymethyluridine (cm^5U), requires the eukaryotic elongator complex consisting of six subunits (Elp1-Elp6) and seven other associated proteins (Kti11-Kti14, Sit4, Sap185 and Sap190) in eukaryotes.[6,7] Elp3, a radical SAM enzyme, is the catalytic subunit for this step.

Both diphthamide biosynthesis and the tRNA wobble uridine modifications require Dph3 (also known as Kti11) as the electron donor for the iron-sulfur clusters in their biosynthetic enzymes. Therefore, deletion of the *DPH3* gene abolishes formation of both diphthamide and the tRNA wobble uridine modifications in the cells.

The *Kluveromyces lactis* Toxin Insensitive 13 (*KTI13*) was first shown to be important for formation of the tRNA wobble uridine modifications based on the resistance of *KTI13* deletion strain to the killer toxin.[8] Interestingly, while yeast cells with *DPH3* deletion have no tRNA wobble uridine modifications, yeast cells with *KTI13* deleted still maintain about 16%-18% tRNA wobble uridine modifications compared to that of wild type cells.[6] These

results suggest an important but subsidiary role of Kti13 in forming the tRNA wobble uridine modifications.

Recently, Kti13 was also reported to be important for diphthamide biosynthesis based on the fact that Kti13 deletion yeast cells are resistant to diphtheria toxin.[9] Dph3 and Kti13 form a stable heterodimer and this complex formation seems to be important for both modifications.[9,10] Surprisingly, the reported structure of the Dph3/Kti13 complex suggests that Kti13 blocks the redox active iron atom in Dph3.[10] Consistent with this, Kti13 was found to inhibit Dph3's electron acceptor/transfer activity by the non-physiological bacterial reductase NorW.[10] The impact of this inhibition by Kti13 *in vivo* and the exact role of Kti13 in helping to form both diphthamide and tRNA wobble uridine modificaitons are still unclear.

Here, we present initial evidence for Kti13's role in lowering the reduction potential of Dph3 which presumably leads to more efficient electron transfer to Dph1-Dph2 and Elp3. A few residues that are potentially important for this functional role are also identified.

Results and discussion

Kti13 knockout decreases but not completely abolishes diphthamide formation

Since yeast cells with *KTI13* deleted still maintains about 16%-18% tRNA wobble uridine modifications, we tested if Kti13 is also playing a similarly subsidiary role for the formation of diphthamide biosynthesis. We compared the level of diphthamide modification in WT or *kti13*Δ cells using the labeling method with DT and a fluorescently conjugated NAD analogue as previously described.[11] No fluorescence label on eEF2 was observed in *dph2*Δ or *dph7*Δ cells, indicating no diphthamide formation in these cells (Figure 4.1). Interestingly, *kti13*Δ

cells were found to retain some diphthamide formation (Figure 4.1). This is consistent with the previous finding that *KTI13* deletion does not fully abolish tRNA wobble uridine modifications[6], suggesting that Kti13 plays a similar and subsidiary role in both modification reactions.

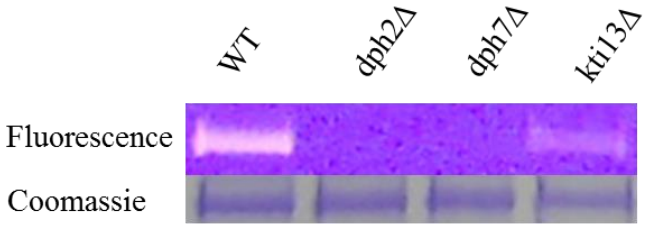

Figure 4.1. *In vitro* ADP-ribosylation using Rh-NAD. The lower panel was Coomassie blue-stained SDS-PAGE gel showing the eEF2 proteins and the upper panel shows the corresponding fluorescence labeling. The source strains for the total cell lysates were labeled above.

Kti13 inhibits the reduction of Dph3 by Cbr1 *in vitro*

Cbr1 is the physiological reductase of Dph3, as previously described in chapter 3. We next tested if this reduction by Cbr1 is affected in the presence of Kti13. We allowed Kti13 and Dph3 to form a heterodimer by pre-incubation of equal molar amounts of Dph3 and Kti13 proteins and then initiated the reduction of Dph3 by Cbr1 and NADH. We found that Dph3 reduction by Cbr1 is significantly inhibited by Kti13 (Figure 4.2b), consistent with the finding by Kolaj-Robin, et al. that Kti13 blocks the redox active iron atom in Dph3 in the complex.[10] However, this inhibition of Dph3's reduction is seemingly opposite to the Kti13's role in helping to form diphthamide or tRNA wobble uridine modifications.

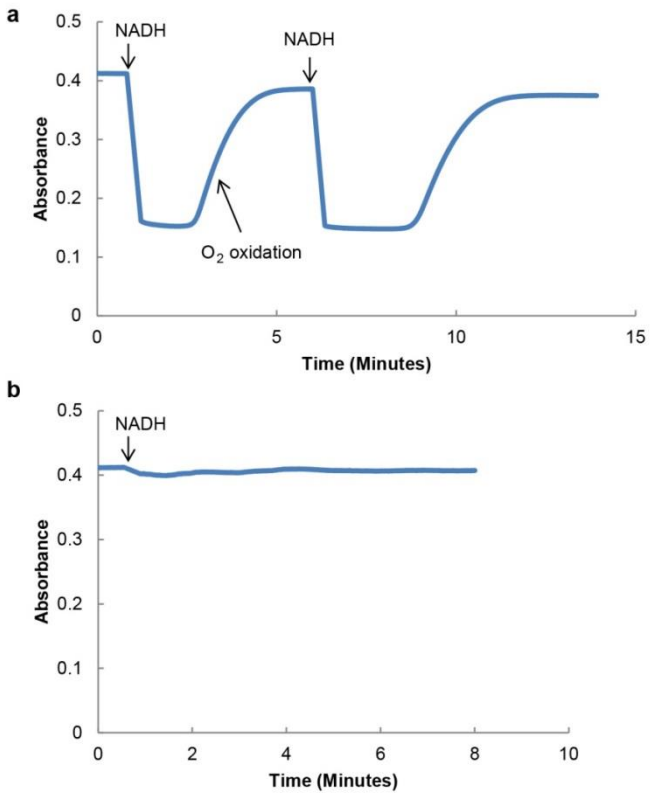

Figure 4.2. Kti13 inhibits Dph3 reduction. (A) Reduction of Dph3 by Cbr1 monitored using the 488 nm absorbance of oxidized Dph3. (B) Reduction of Dph3/Kti13 heterodimer by Cbr1 monitored using the 488 nm absorbance of oxidized Dph3.

Kti13 binding facilitates oxidation of Dph3 by oxygen

To test if the binding by Kti13 also blocks the oxidation process of Dph3, we compared the rate of oxidation in air between reduced Dph3 and reduced Dph3 in complex with Kti13. Dph3 or the Dph3/Kti13 complex was first reduced by dithionite in a glove box and the excess dithionite was removed. Oxidation of Dph3 by air was then monitored by 488 nm absorbance outside the glove box. Surprisingly, we found that the oxidation of reduced Dph3 in the presence of kti13 is faster compared to that of reduced Dph3 alone (Figure 4.3). This result suggests that Kti13 binding to Dph3 does not block electron transfer from Dph3 to oxygen. In contrary, it promotes the oxidation of reduced Dph3 by oxygen.

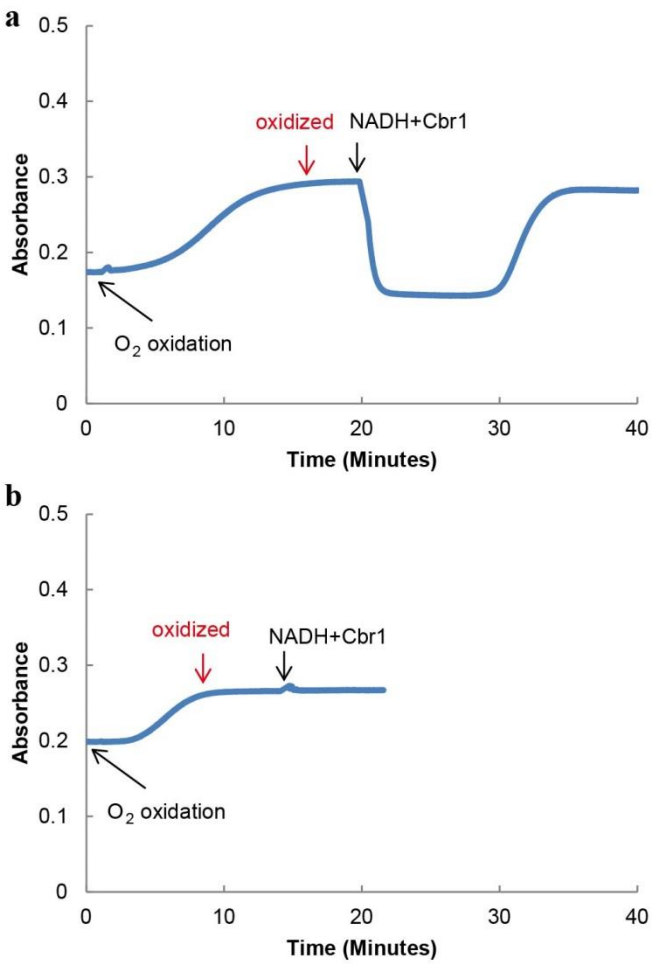

Figure 4.3. Kti13 promotes Dph3 oxidation by O_2. (A) Oxidation of reduced Dph3 monitored using the 488 nm absorbance of oxidized Dph3. Red arrow indicates the time point for oxidized Dph3. (B) Oxidation of reduced Dph3/Kti13 complex monitored using the 488 nm absorbance of oxidized Dph3. Red arrow indicates the time point for oxidized Dph3.

Kti13 reduces the reduction potential of Dph3 in Dph3/Kti13 complex

Although the binding of Kti13 to Dph3 inhibits the reduction of Dph3, it also promotes the oxidation of reduced Dph3. Thus, electron transfer from the iron in Dph3 is not blocked by binding to Kti13. Instead, it is possible that binding of Kti13 to Dph3 lowers the reduction potential of Dph3 by favoring the binding of Kti13 to oxidized form Dph3 compared to that of the reduced form of Dph3. As a result, Dph3 in complex with Kti13 is more easily oxidized but harder to be reduced.

To test this hypothesis, we measured the reduction potential of Dph3 or Dph3/Kti13 complex using a UV-Vis spectrophotometer method previously reported.[12] In these measurements, Nile blue, a redox-active dye with known reduction potential, was used as a reference. Xanthine/Xanthine oxidase was used as the electron source to slowly decrease the electron potential of the whole solution over time. The concentrations of the reduced or oxidized Dph3 and reference dye can be obtained from their corresponding absorbance at 490 nm and 640 nm in the UV-Vis spectra (Figure 4.4a and 4.4b). Since equilibrium is quickly reached for electrons exchanged in bulk solution, the reduction potential of Dph3 can then be calculated from the reference dye's reduction potential using the Nernst equation.

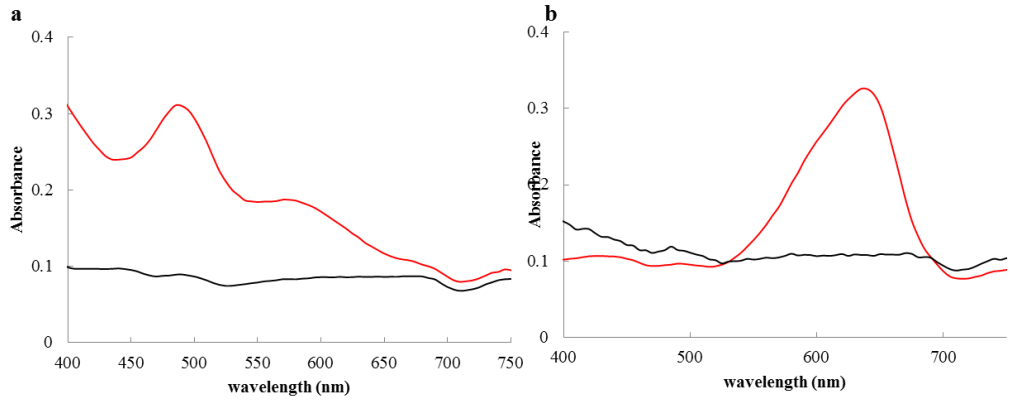

Figure 4.4. Absorbance spectra of Dph3 and Nile blue. (A) Red: oxidized Dph3; Black: reduced Dph3. (B) Red: oxidized Nile blue; black: reduced Nile blue.

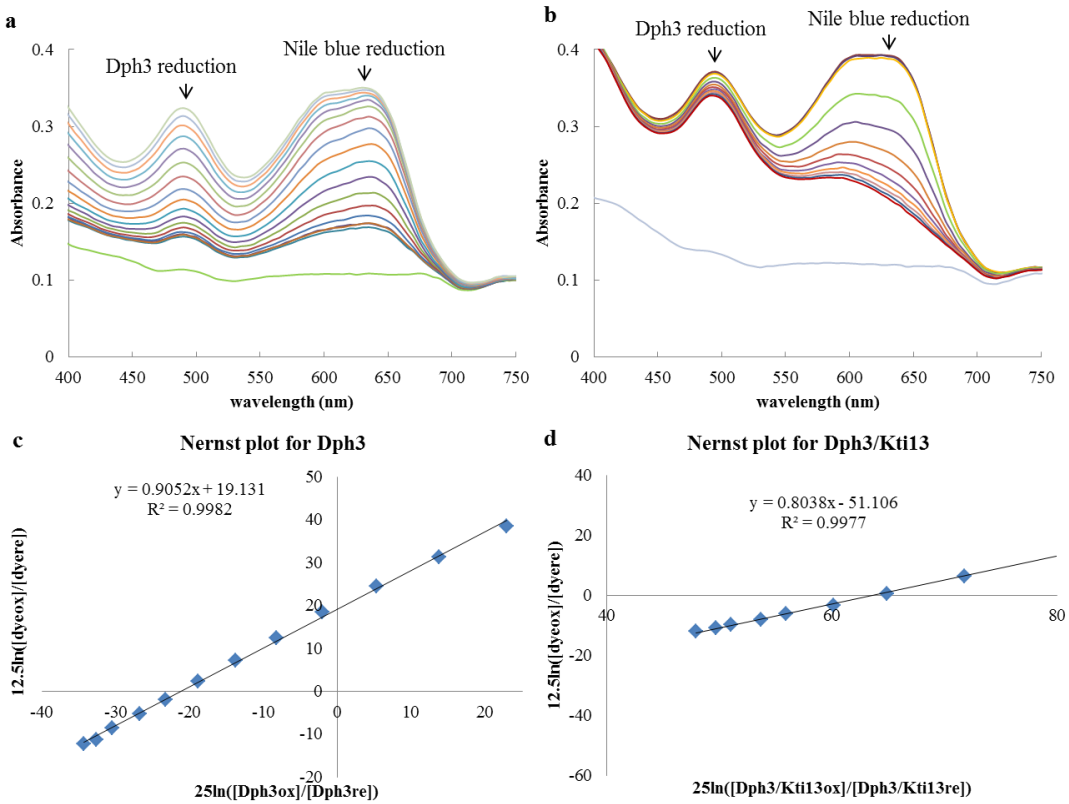

Figure 4.5. Measurement of reduction potential for Dph3 and Dph3/Kti13 complex at pH 7.4 at RT. (A) Spectra of Dph3 and Nile blue at different time point (electron potential). (B) Spectra of Dph3/Kti13 complex and Nile blue at different time point (electron potential). (C) Nernst plot for Dph3 reduction potential. The sum of y-intersection (19 mV) and reduction potential of Nile blue (-116) equals reduction potential of Dph3 (-96mV). (C) Nernst plot for Dph3/Kti13 reduction potential. The sum of y-intersection (-51 mV) and reduction potential of Nile blue (-116) equals reduction potential of Dph3 (-167mV).

After initiation of xanthine oxidase to decrease the overall electron potential of the whole solution, the UV-Vis spectra at different time points were taken. Notably, in the Dph3 measurement, the Dph3 reduction as indicated by absorbance at 490 nm is slightly faster than that of Nile blue at 640 nm (Figure 4.5a). However, in the Dph3/Kti13 measurement, the Dph3 reduction is considerably slower than that of Nile blue (Figure 4.5b). These spectra patterns already suggested that the reduction potential of Dph3/Kti13 is much lower than that of Dph3 alone so that Dph3 is much harder to be reduced when it is in complex with Kti13. A

more quantitative analysis using the Nernst plot[12] showed that the reduction potential for Dph3 is -96 mV while that of Dph3/Kti13 is -167 mV (Figure 4.5c and 4.5d).

However, the measurement of the reduction potential by this method is most accurate when the reduction potential of the measured target is close to that of the reference dye. Since the reduction potential of Dph3/Kti13 is considerably lower than that of Nile blue, the measurement for it is not very accurate. The actual reduction potential value for Dph3/Kti13 is likely lower than -167mV. Other reference dyes with a comparable reduction potential to Dph3/Kti13 would be needed for more accurate measurement in the future. Alternatively, electrochemical measurement or other methods might be employed to determine the reduction potential more accurately in the future.

Nonetheless, these preliminary measurement results clearly revealed that the binding of Kti13 to Dph3 decreases the reduction potential of Dph3 significantly. This immediately raises the hypothesis that Kti13's subsidiary role in both diphthamide biosynthesis pathway and tRNA wobble uridine modifications is to reduce the electron potential of Dph3 so that Dph3 can donate electrons to Dph1-Dph2 or Elp3 more efficiently. Although the exact reduction potentials of Dph1-Dph2 or Elp3 are not reported, the reduction potential for radical SAM enzymes falls in the range of -400 mV to -600 mV.[13] Thus, reducing the electron potential of the electron donor Dph3 could significantly facilitate the electron transfer to the radical SAM enzymes Dph1-Dph2 and Elp3.

Potential residues in Kti13 important for lowering the reduction potential of Dph3

The structure of the Dph3/Kti13 heterodimer was recently reported.[9,10] Based on the structure, there are a few negatively charged residues from Kti13 surrounding the iron in Dph3 (Figure 4.6a). Furthermore, these residues are conserved among the Kti13 orthologs from different species (Figure 4.6b). Thus, it is possible that these residues are important to lower the reduction potential of Dph3 upon binding.

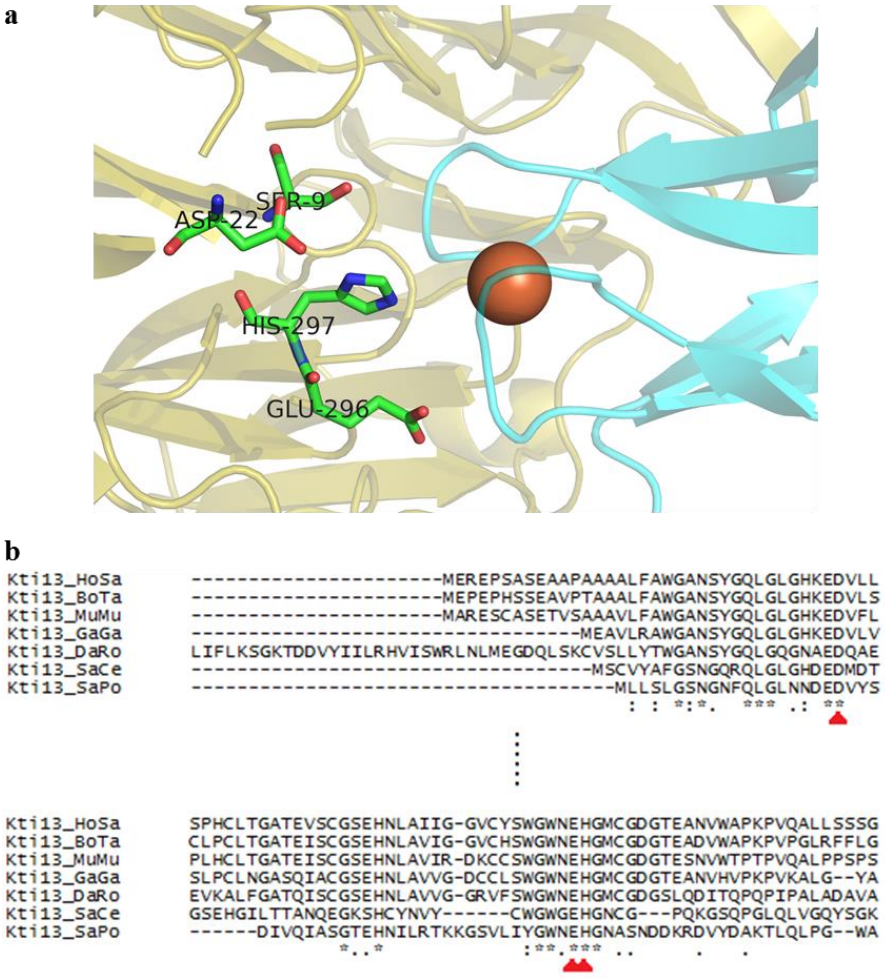

Figure 4.6. Potentially important residues in Kti13 for reducing Dph3's reduction potential. (A) Ser9, Asp22 and Glu296 are three negatively charged residues close to the iron in Dph3. His297 is the residue closest to the iron. (B) Asp22, Glu296 and His297 are conserved among the Kti13 orthologs.

We next tested if these mutations affect the function of Kti13 *in vivo*. We re-introduced either WT Kti13 or mutant Kti13 into yeast cells with Kti13 deleted and examined the diphthamide or tRNA wobble uridine modification formation by the DT or Killer toxin assay. Interestingly, consistent with the previous finding that the H297 in Kti13 is important for Kti13's activity[9], we found that cells transformed with H297A mutant had resistance to DT or killer toxin comparable to that of empty vector control (Figure 4.7a and 4.7b). These results suggest that H297A completely abolish the function of Kti13 in both diphthamide and tRNA modification reaction. Given that H297A was shown to increase the binding affinity of Kti13 and Dph3[9,10], the loss of function in H297A Kti13 is not due to ineffective complex formation of Kti13 and Dph3. On the contrary, it is possible that Kti13 utilizes some of the binding energy to lower the reduction potential of Dph3 while the H297A mutant gains more binding energy because no binding energy is used to lower the reduction potential of Dph3. Another possibility is that H297 also plays a crucial role in mediating the electron transfer between the iron in Dph3 and its electron acceptor.

We also found that the D22A and E296A mutants both partially affect the formation of the tRNA wobble uridine formation. Furthermore, their effects are additive (Figure 4.7a), suggesting that these negatively charged residues also play a role in lowering the reduction potential of Dph3. Interestingly, D22A and E296A single mutants did not display any resistance to DT, indicating that formation of diphthamide is not affected by these mutations in Kti13. This is consistent with our previous finding that diphthamide formation needs less electrons compared to the tRNA wobble uridine modifications due to its lower abundance (Chapter 3). Thus, although the D22A and E296A single mutant both showed a phenotype in

the killer toxin assay, the decrease in Kti13 activity due to these mutations is not strong enough to show a phenotype in the DT assay. In the future, the DT resistance of D22A and E296A double mutant should be tested to see if the combined effects of the two mutations are sufficient to affect diphthamide biosynthesis.

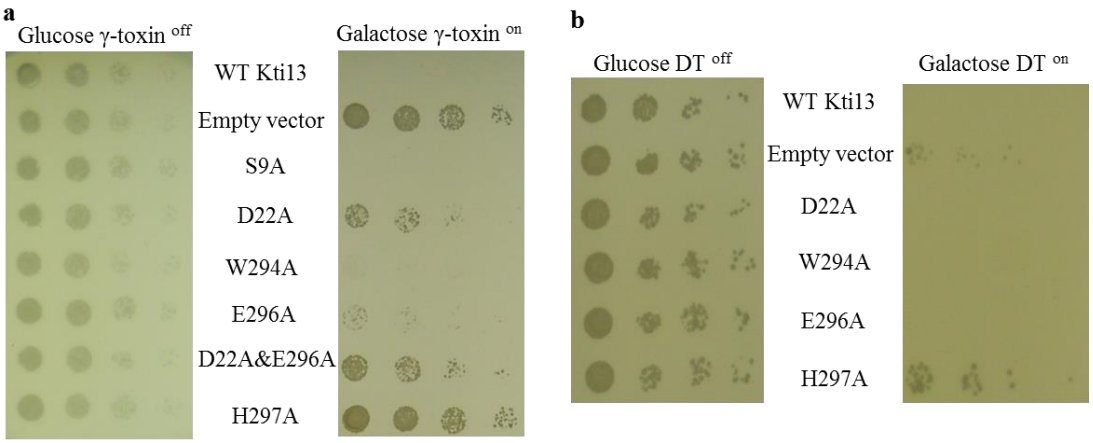

Figure 4.7. Phenotypic characterization of Kti13 mutants. (A) The killer toxin (γ-toxin) assay for Kti13 mutants. (B) The diphtheria toxin (DT) assay for Kti13 mutants.

Discussion

The function of Kti13 in both diphthamide biosynthesis and tRNA wobble uridine modifictions is still poorly understood. Here, our preliminary results show that Kti13 is playing a subsidiary role in both modifications and its likely role is to facilitate electron transfer from Dph3 to the iron-sulfur clusters in Dph1-Dph2 or Elp3. Specifically, the binding of Kti13 to Dph3 lowers the reduction potential of Dph3, making it a better electron donor to its electron acceptors. We also identified a few potential residues that are important for Kti13 to lower the reduction potential of Dph3. However, more vigorous measurements of the reduction potential of Dph3 upon binding of different Kti13 mutants are needed in the future to analyze the exact contribution of each residue.

Methods

***In vitro* ADP-ribosylation of endogenous eEF2 with total cell lysates.** The yeast cell lysates were prepared as described previously.[11,14] The concentration of the lysates were determined by Bradford assay. Yeast total cell lysates (20ug) and Rh-NAD (50 μM) were incubated with DT (0.1 μM) at 30 ℃ for 15 minutes in 25 mM Tris-HCl (pH 8.0), 50 mM NaCl, 30 mM dithiothreitol (DTT) and 2 mM ethylenediaminetetraacetic acid (EDTA). The reaction mixture was resolved by SDS-PAGE. Rhodamine fluorescence signal from protein gel was visualized on a Fisher Scientific Ultraviolet Transilluminators.

Cloning, expression and purification of Kti13. Genomic DNA was extracted from *Saccharomyces cerevisiae* BY4741 strain using Pierce Yeast DNA Extraction Kit. The DNA sequence encoding for Kti13 was amplified by PCR with primers ZL191 and ZL190 (Table 1) from the genomic DNA. The amplified gene fragment was inserted into the pET28a vector and transformed into the *Escherichia coli* expression strain BL21 pRARE2. A single colony was used to inoculate an overnight starter culture, which was used to inoculate 2 liters of LB containing 50 μg/mL kanamycin and 20 μg/mL chloramphenicol. Cells were grown at 37 ℃ to A_{600} of approximately 0.6 and cooled to 16 ℃. Expression was induced with 0.5 mM isopropyl β-D-1-thiogalactopyranoside (IPTG), and grown overnight at 16 ℃. Cells were harvested by centrifugation and lysed using the EmulsiFlex-C3 cell disruptor (Avestin, Inc., Canada). The protein was purified on BioLogic DuoFlow 10 System (Bio-Rad, Hercules, CA). The purification was performed on HisTrap HP column (GE Healthcare, Piscataway, NJ) with a linear gradient from 30 mM imidazole to 500 mM imidazole in 30 minutes. The protein

fractions were collected and dialyzed against 25 mM Tris-HCl buffer (pH 8.0) containing 150 mM NaCl. Protein concentration was determined by standard Bradford assay.

Ultraviolet–visible spectroscopy to monitor the reduction of Dph3. Recombinant yeast Dph3 was purified as previously described.[5] The reaction was monitored on a Cary 50 Bio UV-Vis spectrophotometer (Varian) at 488 nm. Cbr1 (0.5 μM) was mixed with Dph3 (50 μM) with or without Kti13 (50 μM) in a cuvette. The reaction was initiated by addition of NADH at a final concentration of 0.2 mM.

Ultraviolet–visible spectroscopy to minitor the oxidation of Dph3

Aerobically purified Dph3 and Kti13 were degassed by a schlenk line. Dph3 (50 μM) and Dph3/Kti13 (1:1 at 50 μM) were reduced by sodium dithionite (500 μM) in the glove box. Excess dithionite were removed by passing the protein solution through two freshly pre-equilibrated micro bio-spin columns (Bio-rad 7326221). 100 μL of reduced Dph3 or reduced Dph3/Kti13 was transferred into the UV-vis cuvettes and sealed with black taps in the glove box. UV-vis cuvettes were taken out of the glove box and the oxidation of Dph3 in air was monitored at 488 nm after removing the seal.

Measurement of the reduction potentials of Dph3 and Dph3/Kti13

The measurement was performed according to a previously reported method.[12] Reduction potentials were determined using a buffered solution (200 μL total volume, 50 mM Tris pH7.4 and 150mM NaCl) containing the following constituents: xanthine (300 μM) as a source of electrons (30 mM stock solution made in 0.1 M NaOH); Dph3 (50 μM) or Dph3/Kti13 (1:1, 50 μM); Nile blue (10 μM); catalase (5 μg/mL); glucose (5 mM); glucose

oxidase (50 μg/mL), and xanthine oxidase (50 nM). Xanthine was first added to buffered solution before adding other components to prevent denaturation of proteins. Glucose, glucose oxidase, catalase and Kti13 (if included) were then added to reaction buffer and incubated at room temperature for 5 minutes to get rid of dissolved oxygen in solution. Dph3 and Nile blue were then added to reaction mixture and incubated for another 5mins. Finally, xanthine oxidase was added with careful pipetting to initiate the reaction and the spectrum was immediately recorded.

Subsequent spectra were collected every 30 seconds over a period after the addition of xanthine oxidase. When the spectra remained constant, sodium dithionite (5 mM) was added at the end of the reaction to obtain an absorbance reading for the fully reduced protein. Data were fitted to a Nernst plot to obtain the reduction potential for Dph3 or Dph3/Kti13 as previously described.[12] All potentials are given versus a normal hydrogen electrode (NHE).

Cloning of Kti13 mutants for toxin sensitivity assay. Mutagenesis of kti13 was done using the overlap PCR method. For the H297A Kti13 mutant, the plasmid containing the WT Kti13 gene sequence was used as a template to amplify two overlapped fragments containing the desired mutation with two sets of primers (ZL191 and ZL269, ZL190 and Zl268, Table 2). The PCR products were used as templates for another round of PCR with the primers ZL329 and ZL190 (Table 2). The amplified gene fragment was inserted into the p413 Gals vector. Cloning of other Kti13 mutants were performed similarly to that of H297A mutant.

DT and γ-toxin sensitivity assays for Kti13 mutants. For DT sensitivity assays, *kti13*Δ cells were co-transformed with p413Gals-Kti13/mutants and p416Gals-DT (N45D). Transformed

cells were cultured in synthetic complete media with histidine and uracil dropout at 30 ℃ overnight, adjusted to A_{600} of 0.2 with autoclaved water, and then diluted serially in 4-fold increments. Aliquots of each dilution were spotted on glucose-containing or galactose-containing synthetic complete media with histidine and uracil dropout agar plates using a replica plater. Plates were incubated at 30 ℃. Cell growth was recorded 2-3 days after plating. For γ-toxin sensitivity assays, cells were co-transformed with p413Gals-Kti13/mutants and pLF16 which allows for galactose-inducible, glucose-repressible expression of γ-toxin (killer toxin) as previously described.[15] Cultures were grown in synthetic complete media with leucine and histidine dropout at 30 ℃. Plating of cells on agar plates was performed similar to that of DT assays.

Table 1. List of primers used.

Primers for the KTI13 gene

ZL191 AGTCAGGGATCCATGAGTTGTGTGTATGCGTT

ZL190 AGTCAGCTCGAGCTAGAGCACGATCCACGTGG

Primers for kti13 H297A mutagenesis

ZL268 TGGGGCTGGGGAGAGGCTGGCAACTGCGGCCCG

ZL269 CTCTCCCCAGCCCCAGCAGTATACATTGTA

ZL329 AGTCAGACTAGTATGAGTTGTGTGTATGCGTT

Primers for kti13 D22A mutagenesis

ZL348 CTGGGGCACGATGAGGCTATGGATACCCCACAG

ZL349 CTGTGGGGTATCCATAGCCTCATCGTGCCCCAG

Primers for kti13 E296A mutagenesis

ZL363 GCTGGGGCTGGGGAGCGCATGGCAACTGCGG

ZL364 CCGCAGTTGCCATGCGCTCCCCAGCCCCAGC

Primers for kti13 W294A mutagenesis

ZL266 GTATACTGCTGGGGCGCGGGAGAGCATGGCAAC

ZL267 GCCCCAGCAGTATACATTGTAACAGTGAGA

Primers for kti13 S9A mutagenesis

ZL361 GTGTATGCGTTTGGGGCTAATGGGCAAAGGC

ZL362 GCCTTTGCCCATTAGCCCCAAACGCATACAC

Primers for kti13 E21A mutagenesis

ZL352 GGACTGGGGCACGATGCGGATATGGATACCCCA

ZL353 TGGGGTATCCATATCCGCATCGTGCCCCAGTCC

REFERENCES

1 Liu, S., Milne, G. T., Kuremsky, J. G., Fink, G. R. & Leppla, S. H. Identification of the proteins required for biosynthesis of diphthamide, the target of bacterial ADP-ribosylating toxins on translation elongation factor 2. *Mol Cell Biol* **24**, 9487-9497, doi:10.1128/MCB.24.21.9487-9497.2004 (2004).

2 Su, X. *et al.* Chemogenomic approach identified yeast YLR143W as diphthamide synthetase. *Proc Natl Acad Sci U S A* **109**, 19983-19987, doi:10.1073/pnas.1214346109 (2012).

3 Lin, Z. *et al.* Dph7 catalyzes a previously unknown demethylation step in diphthamide biosynthesis. *J Am Chem Soc* **136**, 6179-6182, doi:10.1021/ja5009272 (2014).

4 Zhang, Y. *et al.* Diphthamide biosynthesis requires an organic radical generated by an iron-sulphur enzyme. *Nature* **465**, 891-896, doi:10.1038/nature09138 (2010).

5 Dong, M. *et al.* Dph3 is an electron donor for Dph1-Dph2 in the first step of eukaryotic diphthamide biosynthesis. *J Am Chem Soc* **136**, 1754-1757, doi:10.1021/ja4118957 (2014).

6 Huang, B., Johansson, M. J. & Bystrom, A. S. An early step in wobble uridine tRNA modification requires the Elongator complex. *RNA* **11**, 424-436, doi:10.1261/rna.7247705 (2005).

7 Jablonowski, D. *et al.* Sit4p protein phosphatase is required for sensitivity of Saccharomyces cerevisiae to Kluyveromyces lactis zymocin. *Genetics* **159**, 1479-1489 (2001).

8 Fichtner, L. & Schaffrath, R. KTI11 and KTI13, Saccharomyces cerevisiae genes controlling sensitivity to G1 arrest induced by Kluyveromyces lactis zymocin. *Mol Microbiol* **44**, 865-875, doi:2928 [pii] (2002).

9 Glatt, S. *et al.* Structure of the Kti11/Kti13 heterodimer and its double role in modifications of tRNA and eukaryotic elongation factor 2. *Structure* **23**, 149-160, doi:10.1016/j.str.2014.11.008 (2015).

10 Kolaj-Robin, O., McEwen, A. G., Cavarelli, J. & Seraphin, B. Structure of the Elongator cofactor complex Kti11/Kti13 provides insight into the role of Kti13 in Elongator-dependent tRNA modification. *FEBS J* **282**, 819-833, doi:10.1111/febs.13199 (2015).

11 Su, X. *et al.* YBR246W is required for the third step of diphthamide biosynthesis. *J Am Chem Soc* **134**, 773-776, doi:10.1021/ja208870a (2012).

12 Efimov, I. *et al.* A simple method for the determination of reduction potentials in heme proteins. *FEBS Lett* **588**, 701-704, doi:10.1016/j.febslet.2013.12.030 (2014).

13 Broderick, J. B., Duffus, B. R., Duschene, K. S. & Shepard, E. M. Radical S-adenosylmethionine enzymes. *Chem Rev* **114**, 4229-4317, doi:10.1021/cr4004709 (2014).

14 Du, J., Jiang, H. & Lin, H. Investigating the ADP-ribosyltransferase activity of sirtuins with NAD analogues and 32P-NAD. *Biochemistry* **48**, 2878-2890, doi:10.1021/bi802093g 10.1021/bi802093g [pii] (2009).

15 Keppetipola, N., Jain, R., Meineke, B., Diver, M. & Shuman, S. Structure-activity relationships in Kluyveromyces lactis gamma-toxin, a eukaryal tRNA anticodon nuclease. *RNA* **15**, 1036-1044, doi:10.1261/rna.1637809 (2009).

CHAPTER 5

THE BIOLOGICAL FUNCTION OF DIPHTHAMIDE: AN EXPLORATARY STUDY

Abstract

Uniquely present on archaeal and eukaryotic elongation factor 2 (eEF2), diphthamide represents one of the most intriguing post-translational modifications on proteins. This exceptional modification is targeted by the pathogenic bacterium, Corynebacterium Diphtheria, which causes the infectious disease diphtheria in humans. Diphtheria toxin (DT) produced by this bacterium catalyzes the ADP-ribosylation of the diphthamide residue of eEF2 which inactivates the eEF2. Although the pathological relevance of diphthamide is well studied, the physiological function of diphthamide is still poorly understood. Diphthamide is recently reported to be important for preventing -1 translational frame shift in yeast and mammalian cells. Here, we summarize our efforts to identify the potential "frameshifted proteome" using ribosomal profiling. We also found that diphthamide deficient cells are hypersensitive to rapamycin treatment, implicating a role of diphthamide in stress response.

Introduction

Diphthamide is a post-translationally modified histidine residue uniquely found in eukaryotic and archaeal elongation factor 2 (eEF2). During certain bacterial infections, it is the target of bacterial toxins, Diphtheria toxin (DT), Pseudomonas exotoxin A (ETA) and Cholix toxin, which catalyze the ADP-ribosylation reaction on the diphthamide residue of EF2 using NAD as the ADP-ribosyl donor.[1]

Unlike the well-defined pathological relevance of diphthamide, the biological function of diphthamide is still enigmatic. Diphthamide modification makes cells susceptible to bacterial toxins, yet it is highly conserved among archaea and eukaryotes. Moreover, the formation of diphthamide involves a sophisticated group of proteins performing multiple reaction steps.[2-5] It is hard to believe that such a system exists only to be exploited by bacterial toxins. The evolutionary conservation and complexity of diphthamide modification suggest an important biological function of diphthamide.

Diphthamide is uniquely present on the eEF2 which is essential for the translocation of ribosome along the mRNA during translation. Crystal structure of yeast eEF2 revealed that this modification on His699 is located at the tip of domain IV of the protein.[6] The cryo-electron microscopic reconstruction of the yeast ribosome with eEF2 stabilized by sordarin showed that the tip of domain IV of eEF2 is in close proximity with the tRNA in the P-site.[7] It was then speculated that the tip of domain IV on eEF2 is important to ensure that the mRNA follows the movement of the tRNAs to prevent frameshifts during translation.[7]

Consistent with this proposed role of diphthamide in maintaining translation fidelity, the lack of diphthamide was shown to result in elevated -1 frameshift in protein synthesis using artificial reporter systems with a "slippery sequence" prone to translational frameshift.[8,9] It was proposed that the positive charge incurred by diphthamide modification helps eEF2 to maintain conformational integrity.[9] However, it is unclear if the observation of elevated translational -1 frameshift in diphthamide deficient cells using an artificial reporter system is physiologically relevant.

Here, we attempted to use the ribosome profiling method based on the deep sequencing of ribosome-protected mRNA fragments[10] to compare the translational profiles of wild type yeast cells and diphthamide deficient cells. Since the ribosome profiling method enables genome-wide investigation of translation of mRNAs with subcodon resolution, the potential "frameshifted proteome" in diphthamide deficient cells may be identified by looking at mRNAs with shifted reading frame in cells lacking diphthamide.

Results and discussion

Luciferase reporter shows increased -1 frameshift in *dph6*Δ and *dph7*Δ cells

Dph6 and Dph7 are involved in the third or fourth step of the biosynthesis pathway. Their deletion strains contain intermediates (methylated diphthine or diphthine) with higher structural resemblance to diphthamide. Therefore, we first tested if the increase in -1 frameshift reported in *dph2*Δ and *dph5*Δ cells would also be observed in *dph7*Δ and *dph6*Δ cells using the dual luciferase reporter system.[11]

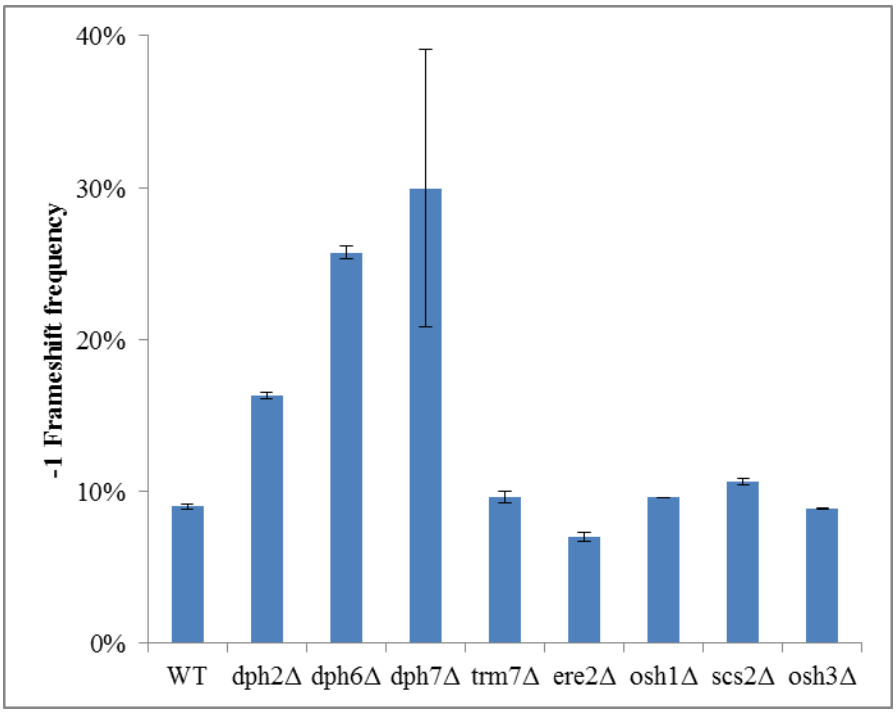

Figure 5.1. *dph6*Δ and *dph7*Δ cells have increased -1 frameshift. Dual luciferase reporter system: firefly luciferase is translated only when a −1 frameshift occurs and the ratio of firefly luciferase activity to renilla luciferase activity reflects -1 frameshift frequency in the cells.

Consistent with the previous reports[8,9], we found that -1 frameshift frequency was significantly increased in *dph2*Δ cells compared to that of the WT (Figure 5.1). Deletion of other genes that are not involved in diphthamide biosynthesis, such as *ERE2*, *OSH1* and *OSH3*, did not lead to increase in the -1 frameshift frequency (Figure 5.1). Most importantly, we found that *dph7*Δ and *dph6*Δ cells also have elevated -1 frameshift frequency. Interestingly, the increases in -1 frameshift frequency in these two strains were even more drastic compared to the increase in *dph2*Δ cells (Figure 5.1). These results confirmed the observed increase in -1 frameshift frequency in diphthamide deficient cells.

However, the dual luciferase reporter system incorporates a “slippery sequence” prone to translational frameshift to promote the basal level of frameshift. It is unclear if the

observation of elevated translational -1 frameshift in diphthamide deficient cells using such an artificial reporter system is physiologically relevant.

Ribosome profiling to identify potential frameshifted proteins

In an attempt to verify the physiological relevance of diphthamide's role in preventing translational -1 frameshift and identify the potential "frameshifted proteome", we performed ribosome profiling in WT, *dph2*Δ, *dph5*Δ and *dph7*Δ cells. Briefly, the polysomes isolated from the total cell lysates were treated with RNAase to digest the unprotected mRNA fragments. The ribosome protected fragments (RPFs) were then purified, deep sequenced and aligned to the genome. This technique allows mapping of the locations of translating ribosomes on mRNAs with subcodon precision. When RPFs are aligned to mRNA, a characteristic triplet periodicity pattern is observed.[12] The triplet periodicity of RPFs was used to develop a computational method for detecting transitions between reading frames.[12]

Therefore, with the help of Dr. Shu-Bing Qian and Dr. Ji Wan, we utilized this developed computational method to analyze our ribosome profiling data in order to identify proteins with increased frameshift events in diphthamide deficient cells. Specifically, the periodicity transition score (PTS) was used as an indicator of the likelihood of a frame transition in an mRNA during translation.[12] Therefore, we searched for proteins with significantly increased PTS in *dph2*Δ and *dph5*Δ cells compared to that of WT. As shown in Figure 5.2, a few proteins were found to have consistently higher PTS in both *dph2*Δ and *dph5*Δ cells.

Gene	WT PTS	*dph2*Δ PTS	*dph5*ΔPTS	Protein function
YNL038W	0.056864	18.73961	16.72405	involved in the synthesis of glycosylphosphatidylinositol
YOR189W	-1.4567	14.84072	4.491452	Component of the INO80 chromatin remodeling complex
YDR288W	-5.45845	22.00716	11.26602	Component of the SMC5-SMC6 complex; abundance increases in response to DNA replication stress
YOL159C-A	1.347036	18.82798	25.1157	Protein of unknown function
YPL064C	0.123308	8.286659	11.59895	putatively involved in pre-mRNA splicing; protein abundance increases in response to DNA replication stress

Figure 5.2. List of proteins with increased PTS in diphthamide deficient cells. Only proteins consistently showed a significant increase of PTS (>5) were included.

Validation of frameshifted protein targets

To test if the protein targets identified by ribosome profiling indeed had higher frameshift events in cells lacking diphthamide, we cloned and expressed these targets with N-terminal flag tags in WT and *dph2*Δ cells. Since a frameshift during translation will lead to pre-mature translational termination, smaller protein fragments will be produced when the frameshift occurs. Therefore, we used anti-Flag western blot to detect flag signals with molecular size smaller than that of the target proteins. We expected to see higher levels of these smaller fragments in the *dph2*Δ cells compared to those of the WT cells.

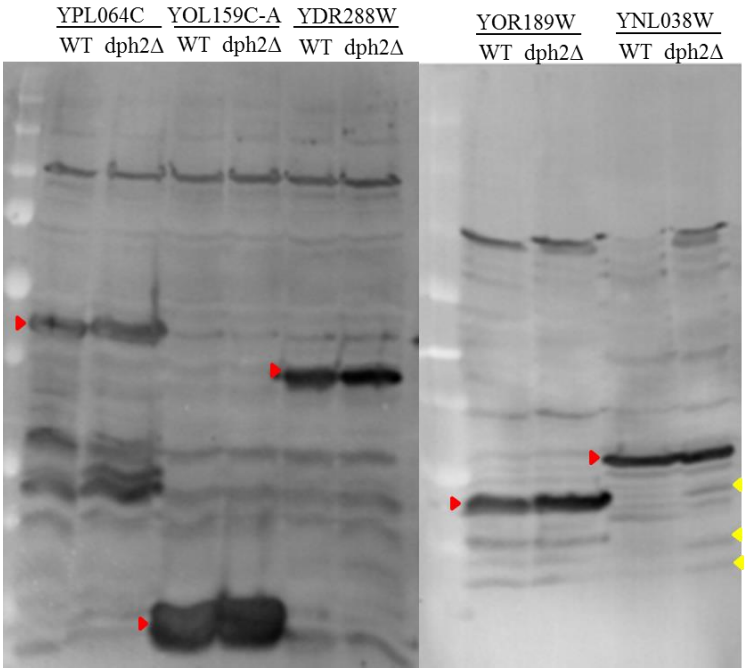

Figure 5.3. Anti-Flag western blot to detect frameshifted protein fragments. Red arrows indicate the bands corresponding to protein targets. Yellow arrows point to potential frameshifted fragments present only in dph2 deletion cells.

We found that the target protein levels were similar in WT and *dph2*Δ cells, suggesting no significant differences in the frameshift frequency (Figure 5.3). In *dph2*Δ cells over-expressing YNL038W protein, we found a few unique flag signals with protein size smaller than that of the target proteins. These bands were not present in the corresponding WT sample (Figure 5.3). However, the intensity of these bands were still much weaker compared to that of the intact protein targets. Furthermore, it is unclear if these bands were indeed frameshifted fragments or degraded fragments of target proteins.

Since only a few candidates were identified from the ribosome profiling analysis and the protein levels of these identified candidates were mostly unaffected by diphthamide, the observed increase in -1 frameshift from the luciferase reporter was probably not physiologically significant.

Hypersensitivity of diphthamide deficient cells to rapamycin

The elusive biological function of diphthamide prompted us to look for growth phenotypes of diphthamide deficient cells under different conditions. In *Saccharomyces cerevisiae*, a systematic profiling of the growth fitness of ~5000 homozygous gene deletion strains has been performed.[13,14] The growth responses to ~400 small molecules and environmental stresses were scored. We then looked for top sensitivity-inducing conditions for the DPH gene deletion strains in the database. Interestingly, we found that *dph2*Δ**,** *dph4*Δ**,** *dph5*Δ, *dph6*Δ and *dph7*Δ consistently showed higher sensitivity to rapamycin (Figure 5.4). Dph3 was not included in the original deletion strain collections.

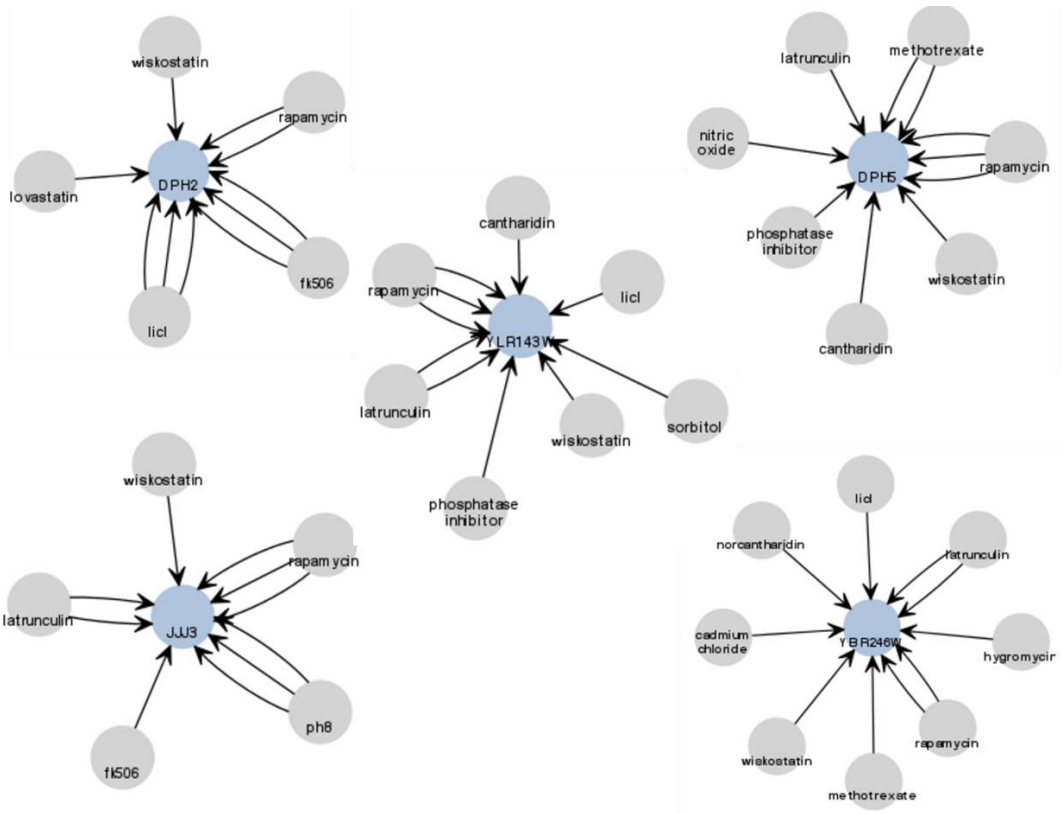

Figure 5.4. Top sensitivity-inducing conditions for the DPH gene deletion strains. The arrows indicate inhibition of the drug on the gene deletion strain. The number of arrows indicates how many times the drug was tested. Drug interaction maps for *DPH2*, *DPH4* (*JJJ3*), *DPH5*, *DPH6* (*YLR143W*) and *DPH7* (*YBR246W*) were shown.

To confirm the sensitivity of diphthamide deficient cells to rapamycin, we performed a grow assay for WT or DPH deletion yeast cells treated with rapamycin. Indeed, we found that all the DPH deletion strains showed some growth defect compared to WT, suggesting that diphthamide deficient cells are hypersensitive to rapamycin (Figure 5.5).

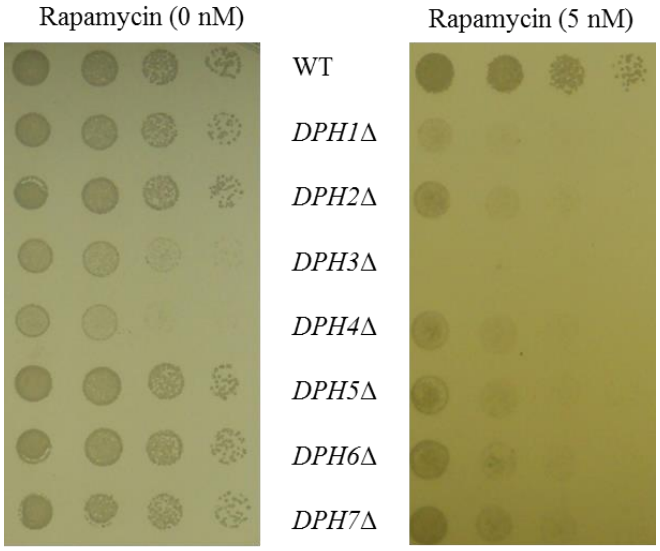

Figure 5.5. DPH deletion strains are hypersensitive to rapamycin. Cells were plated with a serial dilution onto YPD plates containing 0 nM or 5 nM rapamycin.

Rapamycin inhibits TOR (Target of Rapamycin) which is important for cap-dependent translation initiation.[15] Together with the hypersensitivity of diphthamide deficient cells to rapamycin, it is possible that diphthamide is important for cell growth under stress conditions when TOR is inhibited. Consistent with this idea, diphthamide was reported to be essential for the translation of viral mRNA containing the Cricket Paralysis Virus Internal Ribosomal Entry Site (CrPV-IRES) *in vitro*.[16] Therefore, it is likely that diphthamide is important for cap-independent translation that is crucial for cell survival under stress conditions when the cap-dependent translation is inhibited. To test this hypothesis in the future, proteomic studies comparing the protein expression profiles between WT and DPH deletion cells upon

rapamycin treatment can be conducted to identify the proteins relying on IRES cap-independent translation.

Methods

Dual luciferase reporter assay for -1 frameshit in cells. Cells were transformed with either PJD375 (control plasmid with no slippery sequence to provide basal ratio of renilla luciferase and firefly luciferase activity) or PJD378 (HIV -1 frameshift slippery sequence before luciferase acivity). Transformed cells were culture in glucose synthetic complete with uracil dropout media till stationary phase. Cells were harvested by centrifugation. ~ 1.5 x 10^8 cells were mixed with 0.3 g glass beads and 0.25 mL Phosphate-buffered saline. The mixture was vortexed for five 1 min-intervals with cooling on ice in between each interval. The lysed cells were centrifuged to collect the supernatant. Then 5 μg of cell lysate was used for the dual luciferase activity assay using a commercial kit (Promega E1910). The renilla luciferase and firefly luciferase readings from cells transformed with PJD378 were normalized by the reading from cells transformed with PJD375. The normalized renilla luciferase and firefly luciferase readings were used to obtain the -1 frameshift frequency in the cells.

Cell culture and lysis for ribosome profiling. Yeast cells were cultured in 300 mL YPD media until A_{600} of approximately 0.5 was reached. The cells were treated with cycloheximide (0.1 g/L) for 3 minutes to stop translation. Cells were immediately centrifuged at 4,000 g for 4 minutes and the cell pellets were solubilized in 1 mL lysis buffer (10 mM Hepes, pH 7.4, 100 mM KCl, 5 mM $MgCl_2$, 100 μg/ml CHX, 5 mM DTT, 20 U/ml SUPERase_In, and 2% (vol/vol) Triton X-100) were quickly frozen in liquid N_2. Frozen cells were grinded into power to lyse the cells. Lysed cells were centrifuged at 17,000 g to collect the supernatant.

Polysome profiling and cDNA library construction of RPF. Sucrose solutions were prepared in polysome gradient buffer (10 mM Hepes, pH 7.4, 100 mM KCl, 5 mM $MgCl_2$,

100 μg/ml CHX, 5 mM DTT, and 20 U/ml SUPERase_In (Ambion)). Sucrose density gradients (15% - 45% (wt/vol)) were freshly made in SW41 ultracentrifuge tubes (Fisher) using a BioComp Gradient Master (BioComp) according to the manufacturer's instructions. Approximately 650 μl supernatant was loaded onto sucrose gradients, followed by centrifugation for 100 min at 38 000 rpm, 4 ℃, in an SW41 rotor. Separated samples were fractionated at 0.375 ml/min using a fractionation system (Isco) that continually monitored OD_{254} values. Fractions were collected into tubes at 1-min intervals. To convert the polysome into monosome, *E. coli* RNase I (Ambion) was added into the pooled polysome samples (750 U per 100 A260 units) and incubated at 4 ℃ for 1 h. Total RNA extraction was performed using TRIzol reagent. Subsequent cDNA library construction of ribosome protected fragments was performed as previously described.[17]

Sequencing and data analysis. Deep sequencing on PRF library constructed was performed by the Cornell Illumina Sequencing facility using HiSeq instrument. Data analysis as performed according to the method developed by Michel et .al.[12]

Validation of potential frameshifted targets. Yeast complementary DNA was used as template for amplification of the target genes. Yeast RNA was purified using the TRIzol® reagent (Thermo Fisher Scientific). DNA was removed from the purified RNA using DNase I (New England Biolabs). The RNA was extracted with phenol/chloroform to inactivate DNase I. Total cDNA was synthesized from the purified RNA using SuperScript® III Reverse Transcriptase (Thermo Fisher Scientific). The DNA sequence encoding for YNL038W was amplified by PCR with primers ZL181 and ZL179. The amplified fragment was inserted into p423Gal1 vector. Cells transformed with p423Gal1-YNL038W were cultured in galactose

synthetic complete with histidine drop out. ~ 6 x 10^8 cells were lysed with 0.3 g glass beads and 0.4 mL lysis buffer (25 mM Tris pH8.0, 150 mM NaCl, 1X protease inhibitior cocktail). Then 20 µg of cell lysate was used for subsequent anti-Flag western blot analysis. The cloning and validation of other targets were performed similarly to that of YNL038W. The primers used are listed in table 1.

Growth assay for cells treated with rapamycin. Yeast cells were cultured in YPD media at 30 ℃ overnight, adjusted to OD_{600} of 0.2 with autoclaved water, and then diluted serially in 4-fold increments. Aliquots of each dilution were spotted on YPD agar plates containing no rapamycin or 5 nM rapamycin using a replica plater. Plates were incubated at 30 ℃. Cell growth was recorded 1-2 days after plating.

Table 1. List of primers used.

Primers for the YNL038W gene

ZL181 agtcagGGATCCATGGGAgactacaaggacgacgatgacaagATGATTAGTAAAGAGTAT

ZL179 agtcagCTCGAGTCAATCTTTTGGTCTGCTCA

Primers for the YOR189W gene

ZL180 agtcagACTAGTATGGGAgactacaaggacgacgatgacaagATGTCCCAAGAAAGTAGT

ZL177 agtcagCTCGAGTTATGAGTCCAGTCCATCCT

Primers for the YDR288W gene

ZL183 agtcagGGATCCATGGGAgactacaaggacgacgatgacaagATGAGTTCTATAGATAAT

ZL184 agtcagCTCGAGCTATATAGAATATGAATC

Primers for the YOL159C-A gene

ZL185 agtcagGGATCCATGGGAgactacaaggacgacgatgacaagATGCAATACTGTGAACTC

ZL186 agtcagCTCGAGTTACTGTCGAGGGTTCCA

Primers for the YPL064C gene

ZL187 agtcagGGATCCATGGGAgactacaaggacgacgatgacaagATGTCCAGTAATATAGAA

ZL188 agtcagCTCGAGTCACTTTAGAATATTCTT

REFERENCES

1 Honjo, T., Nishizuka, Y. & Hayaishi, O. Diphtheria toxin-dependent adenosine diphosphate ribosylation of aminoacyl transferase II and inhibition of protein synthesis. *J Biol Chem* **243**, 3553-3555 (1968).

2 Liu, S., Milne, G. T., Kuremsky, J. G., Fink, G. R. & Leppla, S. H. Identification of the proteins required for biosynthesis of diphthamide, the target of bacterial ADP-ribosylating toxins on translation elongation factor 2. *Mol Cell Biol* **24**, 9487-9497, doi:10.1128/MCB.24.21.9487-9497.2004 (2004).

3 Carette, J. E. *et al.* Haploid genetic screens in human cells identify host factors used by pathogens. *Science* **326**, 1231-1235, doi:10.1126/science.1178955 (2009).

4 Su, X. *et al.* Chemogenomic approach identified yeast YLR143W as diphthamide synthetase. *Proc Natl Acad Sci U S A* **109**, 19983-19987, doi:10.1073/pnas.1214346109 (2012).

5 Lin, Z. *et al.* Dph7 catalyzes a previously unknown demethylation step in diphthamide biosynthesis. *J Am Chem Soc* **136**, 6179-6182, doi:10.1021/ja5009272 (2014).

6 Jorgensen, R. *et al.* Two crystal structures demonstrate large conformational changes in the eukaryotic ribosomal translocase. *Nat Struct Biol* **10**, 379-385, doi:10.1038/nsb923 (2003).

7 Spahn, C. M. *et al.* Domain movements of elongation factor eEF2 and the eukaryotic 80S ribosome facilitate tRNA translocation. *EMBO J* **23**, 1008-1019, doi:10.1038/sj.emboj.7600102

7600102 [pii] (2004).

8 Ortiz, P. A., Ulloque, R., Kihara, G. K., Zheng, H. & Kinzy, T. G. Translation elongation factor 2 anticodon mimicry domain mutants affect fidelity and diphtheria toxin resistance. *J. Biol. Chem.* **281**, 32639-32648 (2006).

9 Liu, S. *et al.* Diphthamide modification on eukaryotic elongation factor 2 is needed to assure fidelity of mRNA translation and mouse development. *Proc Natl Acad Sci U S A* **109**, 13817-13822, doi:10.1073/pnas.1206933109 (2012).

10 Ingolia, N. T., Ghaemmaghami, S., Newman, J. R. & Weissman, J. S. Genome-wide analysis in vivo of translation with nucleotide resolution using ribosome profiling. *Science* **324**, 218-223, doi:10.1126/science.1168978 (2009).

11 Harger, J. W. & Dinman, J. D. An in vivo dual-luciferase assay system for studying translational recoding in the yeast Saccharomyces cerevisiae. *RNA* **9**, 1019-1024 (2003).

12 Michel, A. M. *et al.* Observation of dually decoded regions of the human genome using ribosome profiling data. *Genome Res* **22**, 2219-2229, doi:10.1101/gr.133249.111 (2012).

13 Hillenmeyer, M. E. *et al.* The chemical genomic portrait of yeast: Uncovering a phenotype for all genes. *Science* **320**, 362-365, doi:10.1126/science.1150021 (2008).

14 Hillenmeyer, M. *et al.* Systematic analysis of genome-wide fitness data in yeast reveals novel gene function and drug action. *Genome Biol.* **11**, R30 (2010).

15 Ma, X. M. & Blenis, J. Molecular mechanisms of mTOR-mediated translational control. *Nat Rev Mol Cell Biol* **10**, 307-318, doi:10.1038/nrm2672 (2009).

16 Murray, J. *et al.* Structural characterization of ribosome recruitment and translocation by type IV IRES. *Elife* **5**, doi:10.7554/eLife.13567 (2016).

17 Ingolia, N. T., Brar, G. A., Rouskin, S., McGeachy, A. M. & Weissman, J. S. The ribosome profiling strategy for monitoring translation in vivo by deep sequencing of ribosome-protected mRNA fragments. *Nat Protoc* **7**, 1534-1550, doi:10.1038/nprot.2012.086 (2012).

CONLUSIONS AND FUTURE DIRECTIONS

Diphthamide is a post-translationally modified histidine residue uniquely found in eukaryotic and archaeal elongation factor 2 (eEF2), a protein involved in the elongation step of protein synthesis. It is the target of the bacterial toxins, Diphtheria toxin (DT) and Pseudomonas exotoxin A (ETA), which catalyze the ADP-ribosylation reaction on the diphthamide residue of eEF2. ADP-ribosylation on eEF2 inactivates eEF2, which in turn stops protein translation, leading to cell death. The diphthamide biosynthesis pathway in eukaryotes was initially proposed to involve three steps, requiring seven proteins, Dph1-Dph7. While the functional assignments of Dph1-Dph6 were well established, the role of Dph7 in the pathway was unclear.

Chapter 2 – Potential functional role of Dph7 as an isomerase

In Chapter 2, I showed that Dph7 catalyzes an additional demethylation step in the diphthamide biosynthesis pathway and identified a previously unknown intermediate, methylated diphthine, from yeast DPH7 deletion strain. I proposed a revisited four-steps diphthamide biosynthesis pathway. However, the functional implication of the additional methylation-demethylation step catalyzed by Dph7 is still unclear at this point. Interestingly, the recently reported crystal structure of eEF2 suggests that the chiral center of the third carbon has a R-configuration (D-diphthamide) [1] instead of an S- configuration (L-diphthamide) in the previously proposed structure. If this chirality assignment is reliable, it implies that there is a change in chirality during the diphthamide biosynthesis. Therefore, it is possible that the extra methylation on methylated diphthine is to neutralize the negative

charged on the carboxylate group which helps the subsequent inversion of chirality. It would be interesting to verify this isomerization reaction catalyzed by Dph7 in the future.

One possible experiment to demonstrate the change in chirality is to purify *dph*7Δ eEF2 and *dph*6Δ eEF2, hydrolyze the purified eEF2 into single amino acids by acid hydrolysis, and compare the resultant amino acid residues. The *dph*7Δ eEF2 contains L-methylated diphthine which would be converted to L-diphthine during the acid hydrolysis while *dph*6Δ eEF2 presumably yields D-diphthine. It may be possible to separate the L-diphthine and D-diphthine residues as they are stereoisomers. LC-MS may be used to detect and identify the diphthine peaks. However, if diphthine does not separate well from other amino acid residues, it may be necessary to radioactively label diphthine by starting with cells cultured with [β-^{3}H]histidine.[2] In this way, diphthine will only need to be separated from the unmodified histidine residues. Synthetic standards of L-diphthine and D-diphthine may also be needed to demosntrate the separation of L-diphthine and D-diphthine.

Chapter 3 – Validate potential correlation of NADH level with tRNA wobble uridine modificaitons

Both diphthamide and the tRNA wobble uridine modification reactions require Dph3 as an electron donor for the iron-sulfur clusters in their biosynthetic enzymes. In Chapter 3, using a proteomic approach, I identified cytochrome B5 reductase (Cbr1) as a NADH-dependent reductase for Dph3. The NADH- and Cbr1-dependent reduction of Dph3 may provide a regulatory linkage between cellular metabolic state and protein translation. It would therefore be interesting to validate the correlation between the NADH level and the tRNA wobble

uridine modificaitons in the furure.

It has been reported that over-expression of bacterial NADH oxidase can alter the concentration of cellular NAD^+/NADH ratio in mamalian cells.[3] One can test if the over-expression of the bacterial NADH oxidase will decrease the level of tRNA wobble uridine modificaitons. It may also be interesting to quantify tRNA modification levels at cellular states where NAD^+/NADH is elevated, e.g. oxidative stress.

Chapter 4 –Validate functional role of Kti13 to reduce reduction potential of Dph3

In chapter 4, I summarize my recent work on functional characterization of Kti13, the newly reported protein to be involved in diphthamide biosynthesis. Kti13 plays a subsidiary role in both diphthamide and tRNA wobble uridine modifications. My initial measurement of Dph3's reduction potential suggest that the presence of Kti13 decreases the reduction potential of Dph3, allowing more efficient electron transfer to Dph3's electron acceptors. Using toxin assays, mutations that affect Kti13's function in diphthamide and tRNA modifications were also identified.

In the future, more vigorous measurements of the reduction potential of Dph3 upon binding of different Kti13 mutants are needed in the future to attribute the exact contribution of each residue.

Chapter 5 –Explore the function of diphthamide modification in IRES dependent transaltion

The final part of my thesis describes my effort in elucidating the poorly understood biological function of diphthamide. Using ribosome profiling, I attempted to identify the potential

"frameshifted proteome" using ribosomal profiling but there was no apparent physiological substrate. I then showed that diphthamide deficient cells are hypersensitive to rapamycin treatment. Rapamycin inhibits TOR (Target of Rapamycin) which is important for cap-dependent translation initiation.[4] The hypersensitive of diphthamide deficient cells to rapamycin suggests that diphthamide is important for cell growth when cap-dependent translation is inhibited. Consistent with this idea, diphthamide was reported to be essential for the translation of viral mRNA containing the Cricket Paralysis Virus Internal Ribosomal Entry Site (CrPV-IRES) *in vitro*.[5] Therefore, it is likely that diphthamide is important for the cap-independent translation under stress conditions when the cap-dependent translation is inhibited.

To test this hypothesis in the future, proteomic studies comparing the protein expression profiles between WT and DPH deletion cells upon rapamycin treatment can be conducted to identify the proteins relying on IRES cap-independent translation. Candidate proteins may be verified in a few ways. Firstly, the protein and mRNA level of candidate genes in WT and DPH deletion cells can be checked to confirm that the translation of these candidate genes under stress conditions are affected in DPH deletion cells. Secondly, the 5' UTR region of these genes can be fused to a luciferase reporter (either with a 5' block[6] or inserted in-between two luciferase) to compare their IRES cap-independent translation efficiency. This result is important to confirm that the change in protein level is due to reduced IRES cap-independent translation. Finally, it would be important to establish phenotypes for diphthamide deficient cells related to the function of the protein target.

It has been reported that cap-independent translation is required for a set of genes important

for invasive growth in yeast.[6] Therefore, it will be interesting to test if translation of these genes is affected by diphthamide deficiency using the above mentioned methods.

REFERENCES

1 Jorgensen, R., Merrill, A. R. & Andersen, G. R. The life and death of translation elongation factor 2. *Biochem Soc Trans* **34**, 1-6, doi:10.1042/BST20060001 (2006).

2 Dunlop, P. C. & Bodley, J. W. Biosynthetic labeling of diphthamide in Saccharomyces cerevisiae. *J Biol Chem* **258**, 4754-4758 (1983).

3 Titov, D. V. *et al.* Complementation of mitochondrial electron transport chain by manipulation of the NAD+/NADH ratio. *Science* **352**, 231-235, doi:10.1126/science.aad4017 (2016).

4 Ma, X. M. & Blenis, J. Molecular mechanisms of mTOR-mediated translational control. *Nat Rev Mol Cell Biol* **10**, 307-318, doi:10.1038/nrm2672 (2009).

5 Murray, J. *et al.* Structural characterization of ribosome recruitment and translocation by type IV IRES. *Elife* **5**, doi:10.7554/eLife.13567 (2016).

6 Gilbert, W. V., Zhou, K., Butler, T. K. & Doudna, J. A. Cap-independent translation is required for starvation-induced differentiation in yeast. *Science* **317**, 1224-1227, doi:10.1126/science.1144467 (2007).